AD-A080 488 SRI INTERNATIONAL MENLO PARK CA F/G 1/2
INERTIALLY AUGMENTED APPROACH COUPLERS. (U)
JUN 79 D A TIEDEMAN, F B BENSON, L V MILLER DOT-FA75WA-3650
UNCLASSIFIED FAA-RD-79-118 NL

1 OF 2
AD-A080488

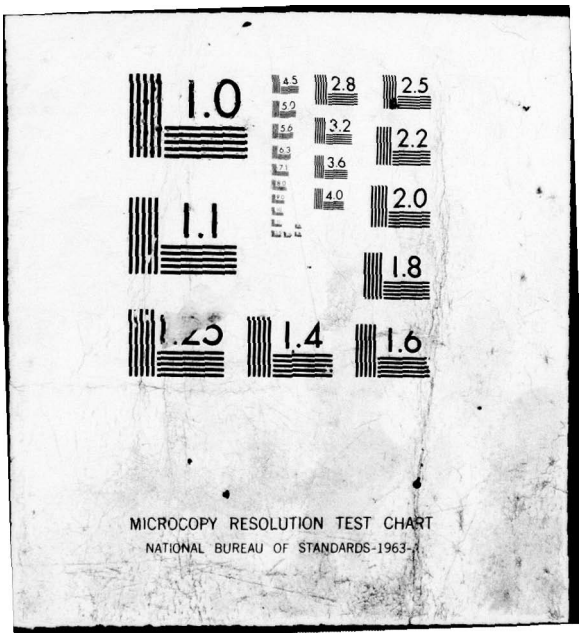
1.0
1.1
1.25
1.4
1.6
1.8
2.0
2.2
2.5
2.8
3.2
3.6
4.0
4.5
5.0
5.6
6.3
7.1
MICROCOPY RESOLUTION TEST CHART
NATIONAL BUREAU OF STANDARDS-1963-A

Report No. FAA-RD-79-118

(12)

LEVEL II

INERTIALLY AUGMENTED APPROACH COUPLERS

ALL-WEATHER LANDING SYSTEMS, ENGINEERING SERVICES
SUPPORT PROJECT, TASK 5

D.A. Tiedeman, F.B. Benson, L.V. Miller, R.J. Rudig,
T.J. Schuldt, C.P. Shih, E.D. Skelley

COLLINS GOVERNMENT AVIONICS DIVISION, ROCKWELL INTERNATIONAL, CEDAR RAPIDS, IOWA
SRI INTERNATIONAL, MENLO PARK, CALIFORNIA 94025

AD A080488

DDC
RECEIVED
FEB 12 1980
A

June 1979

Final Report

Document is available to the U.S. public through
the National Technical Information Service,
Springfield, Virginia 22161.

DDC FILE COPY

Prepared for

U.S. DEPARTMENT OF TRANSPORTATION
FEDERAL AVIATION ADMINISTRATION
Systems Research & Development Service
Washington, D.C. 20590

80 2 8 029

NOTICE

This document is disseminated under the sponsorship of the Department of Transportation in the interest of information exchange. The United States Government assumes no liability for its contents or use thereof.

DISCLAIMER NOTICE

THIS DOCUMENT IS BEST QUALITY PRACTICABLE. THE COPY FURNISHED TO DDC CONTAINED A SIGNIFICANT NUMBER OF PAGES WHICH DO NOT REPRODUCE LEGIBLY.

(12) 127

Technical Report Documentation Page

1. Report No. (19)	2. Government Accession No.	3. Recipient's Catalog No.
(18) FAA-RD-79-118		

4. Title and Subtitle
(6) INERTIALLY AUGMENTED APPROACH COUPLERS.

5. Report Date (11)
June 1979

6. Performing Organization Code

7. Author(s) (10)
D.A. Tiedeman, F.B. Benson, L.V. Miller, R.J. Rudig, T.J. Schuldt, C.P. Shih, E.D. Skelley

8. Performing Organization Report No.
SRI Project 4364

9. Performing Organization Name and Address
SRI International
333 Ravenswood Avenue
Menlo Park, California 94025

10. Work Unit No. (TRAIS)

11. Contract or Grant No. (15)
DOT-FA75WA-3650

13. Type of Report and Period Covered (9)
Final Report
June 1975 — June 1979

12. Sponsoring Agency Name and Address
U.S. Department of Transportation
Federal Aviation Administration
Systems Research and Development Service
Washington, D.C. 20590

14. Sponsoring Agency Code
FAA/ARD-740

15. Supplementary Notes
Prepared on ALL-WEATHER LANDING SYSTEMS, Engineering Services Support, Project 4364, Task 5. Work done by Collins Government Avionics Division, Rockwell International, and by Boeing Commerical Airplane Company.

16. Abstract
This final report collects and summarizes the results of a series of engineering design studies and tests of methods for acceleration augmentation of airplane control systems for approach and landing. Emphasis was on the use of body-mounted accelerometers, which are reasonably inexpensive. Control laws were developed for several aircraft (CV-880, DC-10, B-727) and tested by simulation with both automatic and human pilots; they included automatic landing systems, flight director with full ILS, and flight director for nonprecision approach. The modified flight director (MFD) control algorithms (pitch, roll and thrust) were also tested in large-scale piloted flight simulations under Task 2 of the AWLS project. The objectives were to achieve approach-and-landing performance on Category I and II ILS beams comparable to that with current systems on Category III beams, and to obtain improved performance over current systems in coping with low-level wind shear. The low-cost system designs met these objectives, and exhibited performance comparable to that attainable with an expensive full inertial navigation system. Collins supported tests of the methods in DC-10 and B-727 flight simulators. The MFD controls were implemented in a Gulfstream I test airplane for FAA tests.

17. Key Words	18. Distribution Statement
Acceleration Augmentation Automatic Landing Flight Director Wind Shear	Document is available to the U.S. public through the National Technical Information Service, Springfield, VA 22161

19. Security Classif. (of this report)	20. Security Classif. (of this page)	21. No. of Pages	22. Price
Unclassified	Unclassified	134	

Form DOT F 1700.7 (8-72) Reproduction of completed page authorized

410 281

JOB

METRIC CONVERSION FACTORS

Approximate Conversions to Metric Measures

Symbol	When You Know	Multiply by	To Find	Symbol
	LENGTH			
in	inches	*2.5	centimeters	cm
ft	feet	30	centimeters	cm
yd	yards	0.9	meters	m
mi	miles	1.6	kilometers	km
	AREA			
in^2	square inches	6.5	square centimeters	cm^2
ft^2	square feet	0.09	square meters	m^2
yd^2	square yards	0.8	square meters	m^2
mi^2	square miles	2.6	square kilometers	km^2
	acres	0.4	hectares	ha
	MASS (weight)			
oz	ounces	28	grams	g
lb	pounds	0.45	kilograms	kg
	short tons (2000 lb)	0.9	tonnes	t
	VOLUME			
tsp	teaspoons	5	milliliters	ml
Tbsp	tablespoons	15	milliliters	ml
fl oz	fluid ounces	30	milliliters	ml
c	cups	0.24	liters	l
pt	pints	0.47	liters	l
qt	quarts	0.95	liters	l
gal	gallons	3.8	liters	l
ft^3	cubic feet	0.03	cubic meters	m^3
yd^3	cubic yards	0.76	cubic meters	m^3
	TEMPERATURE (exact)			
°F	Fahrenheit *temperature*	5/9 (after *subtracting* 32)	Celsius temperature	°C

*1 in = 2.54 exactly. For other exact conversions and more detailed tables, see NBS Misc. Publ. 286, Units of Weights and Measures, Price $2.25, SD Catalog No. C13.10:286.

Approximate Conversions from Metric Measures

Symbol	When You Know	Multiply by	To Find	Symbol
	LENGTH			
mm	millimeters	0.04	inches	in
cm	centimeters	0.4	inches	in
m	meters	3.3	feet	ft
m	meters	1.1	yards	yd
km	kilometers	0.6	miles	mi
	AREA			
cm^2	square centimeters	0.16	square inches	in^2
m^2	square meters	1.2	square yards	yd^2
km^2	square kilometers	0.4	square miles	mi^2
ha	hectares (10,000 m^2)	2.5	acres	
	MASS (weight)			
g	grams	0.035	ounces	oz
kg	kilograms	2.2	pounds	lb
t	tonnes (1000 kg)	1.1	short tons	
	VOLUME			
ml	milliliters	0.03	fluid ounces	fl oz
l	liters	2.1	pints	pt
l	liters	1.06	quarts	qt
l	liters	0.26	gallons	gal
m^3	cubic meters	35	cubic feet	ft^3
m^3	cubic meters	1.3	cubic yards	yd^3
	TEMPERATURE (exact)			
°C	Celsius temperature	9/5 (then *add* 32)	Fahrenheit temperature	°F

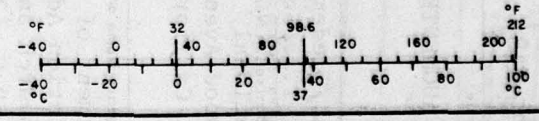

PREFACE

Task 5 of the All-Weather Landing Systems (AWLS) project determines the air/ground system requirements for systems using the least sophisticated source of acceleration or velocity information available or potentially available in air carrier cockpits for the safe conduct of Category III operations with varying conditions of windshear on Category I or II ground facilities. Work on this task was performed by Collins Government Avionics Division, Rockwell International, of the AWLS team. SRI monitored the effort.

The technical approach was based on the use of body-mounted accelerometers for augmentation of automatic landing systems and of flight directors for approach and landing. Candidate system algorithms or control laws were developed, analyzed, tested in analog computer simulations, and compared. The most promising algorithms were further tested in piloted flight simulators under Task 2.

This final report collects the various studies, summarizes their results, and gives the overall conclusions; W. H. Foy of SRI is the editor. The sponsoring organizations are the Wind Shear Program and the Approach and Landing Division (ARD-740) of the FAA Systems Research and Development Service; the Technical Monitor is W. J. Cox.

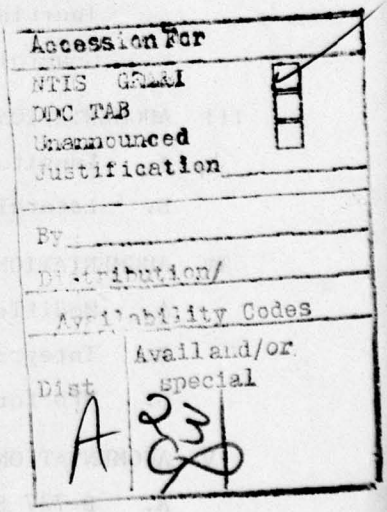

CONTENTS

PREFACE ii

METRIC CONVERSION FACTORS iii

LIST OF ILLUSTRATIONS v

LIST OF TABLES vi

I INTRODUCTION 1

A. Program, Objectives and Approach 1

B. Organization of Report 5

II BACKGROUND REVIEW 7

A. Conventional vs Inertially Augmented Approach and Landing Control Laws 7

B. Inertially Augmented Automatic Landing System: Autopilot Performance With Imperfect ILS Beams 13

C. Application of Inertial Navigation and Modern Control Theory to the All-Weather Landing Problem 16

D. Design, Development and Flight Evaluation of Inertially Augmented Automatic Landing Systems 22

E. General Results 24

III AUGMENTATION OF THE CV-880 AUTOLAND SYSTEM 27

A. Longitudinal Axis and Autothrottle 29

B. Lateral Axis Control 44

IV AUGMENTATION OF THE DC-10 FLIGHT CONTROL SYSTEM 57

A. Modified Flight Director (MFD) 58

B. Integration of Thrust Command in MFD 73

C. MFD for Nonprecision Approach 80

V AUGMENTATION OF THE B-727 FLIGHT DIRECTOR 89

A. B-727 Simulation 89

B. Modified Flight Director (MFD) for B-727 92

VI MFD IMPLEMENTATION IN GULFSTREAM I 107

VII CONCLUSIONS 109

APPENDICES

A WIND, TURBULENCE, BEAM NOISE AND BEAM DISTURBANCE MODELS . . . A-1

B COMPLEMENTARY FILTER TECHNIQUE B-1

ILLUSTRATIONS

1 Simplified Bank Commands 8

2 Damping Methods 11

3 Simulated Localizer Disturbances 17

4 Pitch Systems: "All-Causes" Footprint Performance 18

5 Roll Systems: "All-Causes" Footprint Performance 19

6 Illustrative Model of a Trajectory Control System 21

7 Simplified Autothrottle Model 30

8 Simplified CV-880 Pitch Loop 31

9 Conventional CV-880 Control Law 32

10 Glideslope Control Laws Functional Diagram 35

11 Comparison of Systems with Vertical Gusts 39

12 Altitude of 3σ Pitch Excursions in 4-s Beam Noise 40

13 Beam Outage Data: Vertical Rate vs Path Deviation at 50 ft . . 42

14 Roll Loop and Yaw Damper Block Diagram 47

15 Localizer Capture 48

16 Unaugmented System Localizer Track Law 50

17 Platform System Localizer Track Law 51

18 Accelerometer System Localizer Track Law 52

19 Longitudinal Inner Loop Block Diagram 59

20 Lateral Inner Loop Block Diagram 60

21 Simplified Longitudinal Control Law for Modified Flight Director 61

22 FAA Windshear Phase 2: Longitudinal Control Law 63

23	FAA Windshear Phase 2: Simulated Autothrottle	64
24	Gusts, Radio Noise, Thunderstorm Shear	67
25	FAA Windshear Phase 2: Simplified Lateral Control Law	68
26	FAA Windshear Phase 2: Lateral Control Law	70
27	Gust, Localizer Noise, Thunderstorm Shear	72
28	Simplified Speed Axis Control Law (With Groundspeed)	76
29	Simplified Speed Axis Control Law (Without Groundspeed Information)	79
30	Speed Control Law	81
31	Pseudoaltitude Error Calculations	83
32	Synthetic Glideslope Calculations	84
33	Nonprecision Approach Responses	86
34	Autothrottle and Engine Model	88
35	Simulated Pitch Pilot for B-727	93
36	Simulated Autothrottle for B-727	94
37	Longitudinal Track Law: Baseline Flight Director	96
38	Lateral Track Law: Baseline Flight Director	97
39	MFD Longitudinal Control Law for B-727	99
40	MFD Lateral Control Law for B-727	100
41	Baseline F/D - Combination	102
42	Modified F/D - Combination	103
B-1	Second-Order Complementary Filter	B-5

TABLES

1	Longitudinal Statistical Data	43
2	Lateral Statistical Results	55
3	Performance of Baseline and MFD Systems	105

I INTRODUCTION

A. Program, Objectives and Approach

The All-Weather Landing Systems (AWLS) project is developing the capability for all types of aircraft to operate in conditions of low visibility and/or low-level windshear. Task 5 applied inertial augmentation methods to approach and landing, both by an automatic landing system and manually with a flight director. The task used relatively inexpensive body-mounted accelerometers for inertial damping, radio beam noise-smoothing, and windshear protection. Although a full inertial navigation system (INS) can effectively detect winds, control the aircraft to a desired path in space, and coast it through beam disturbances or signal dropouts on an approach and landing supported by an instrument landing system (ILS), such a system is expensive.

The objectives of Task 5 were to realize at least some of the benefits of inertial augmentation with a system considerably cheaper, particularly in achieving the following:

- Landing operations at Category I or II ILS facilities with visibilities that are currently in effect.
- Improvement in the conduct of landing operations in low-level windshear.

In subtasks specified for the first phase of Task 5, prior development work was reviewed and a plan was prepared for evaluation of inertial augmentation on a government-furnished aircraft.

During the second phase, which was carried out after FAA approval, the landing system on the aircraft was updated, tests were supported, test data were analyzed, the performance was analyzed, and a final report was prepared. The effort included the development and analysis of candidate airplane control laws incorporating acceleration information, test of the control laws on fast-time analog computers, development and analysis of algorithms for inertially augmented flight director command signals, test of the modified flight director commands in piloted flight simulators, and implementation of the modified flight director commands in the FAA Grumman Gulfstream I test airplane.

The AWLS project is under the supervision of Mr. Dean F. Babcock and is led by Dr. Wade H. Foy, both of SRI's Aviation Systems Laboratory. The technical work on Task 5 was performed by Collins Government Avionics Division, Rockwell International, an AWLS team member, and was led by Mr. Jim L. Foster. Phase 1 started in June 1975. The review of

background work on inertial augmentation was completed on 17 March 1976. The evaluation plan was written by Collins, submitted to the FAA on 8 December 1975, and approved.

In carrying out the plan, the first job was to evaluate the capability of acceleration augmentation of an automatic control system, using body-mounted accelerometers, to improve landing performance with Category I and II ILS beams and with windshear. The FAA Convair 880 test airplane was selected for analysis. Longitudinal control laws and, separately, lateral control laws were developed, analyzed, and tested in fast-time hybrid analog-digital computers. Four systems were compared:

- Platform System (full INS)
  - Inertial platform data
  - Inertially referenced path damping
  - Inertially complemented radio filtering
- Accelerometer System (inertial augmentation)
  - Conventional sensor data (body-mounted accelerometers)
  - Inertially referenced path damping
  - Pitch-complemented path damping filter
  - Inertially complemented radio filtering
- Unaugmented System (certified Category III system)
  - Conventional sensor data (body-mounted accelerometers)
  - Inertially referenced path damping
  - Pitch-complemented path damping filter
- Conventional Systems (non-Category III, no inertial augmentation or damping)

The systems were tested in the computer against four wind models with shear and against ILS beam disturbances. The performance criteria corresponded to those prescribed in the applicable FAA advisory circulars.[1,2*] The windshear performance of the first three systems was significantly better than the conventional system. For instance, with a wind model of a thunderstorm cold air outflow, all three inertially damped systems maintained sufficient control of all flight parameters to complete successfully an automatic landing, whereas the conventional (non-Category III) system contacted the ground 2,000 ft prior to runway threshold at a descent rate of 21 ft/s.

The platform and accelerometer systems offer additional advantages when windshear and noisy beam conditions occur simultaneously. In

---

*References are listed at the end of this report.

general, the accelerometer system was considered better than the unaugmented system and was comparable to the inertial platform system. This subtask was completed 10 August 1976.

The next subtask required that the autopilot algorithms be modified for flight director use. Again, the CV-880 aircraft computer model was used for this work. Digital analysis and automatic and pilot-in-the loop analog simulation verified the refined algorithms. The aircraft model was then changed to a DC-10, using aerodynamic data supplied by Douglas Aircraft Company. An extensive set of data runs in both automatic and manual control modes showed that the refined algorithms exhibited good stability and performance characteristics on the DC-10. Frequency response analysis of the refined algorithms with a pilot model replacing the automatic attitude control loop showed acceptable gain and phase margins.

The algorithms thus defined were taken to Douglas, Long Beach, California for use on the Douglas DC-10 piloted flight simulator. The algorithms at Douglas were implemented in Fortran, using nonlinear, large disturbance, six-degree-of-freedom motion equations for the DC-10. Correlation of the system performance with that found at Collins was good. These algorithms for a "modified flight director" (MFD) were then tested by the AWLS team in experiment 3 of the phase 2 DC-10 flight simulation tests under Task 2 of the AWLS project; the test and results have been described in detail.[3]

Briefly, the results indicated that the modified (acceleration-augmented) algorithm produced a 40% improvement in glideslope tracking over the baseline (conventional DC-10) algorithm. Data also showed that the modified flight director had a significantly higher success rate in the windshear environments than the baseline flight director. Specifically, in the thunderstorm shear, the MFD success rate was approximately 80%, compared to about 45% for the baseline system. This work was completed 15 April 1977.

The DC-10 MFD algorithms applied to pitch and roll control. The acceleration-augmentation method showed potential for performance improvement, so the next two subtasks applied the technique to another airplane and coupled the DC-10 attitude control with thrust control. The B-727-200 airplane was selected for trial, and the Boeing Commercial Airplane Company was tasked by SRI to provide an approach-and-landing simulation model. Using aerodynamic data supplied by Boeing, the Collins engineers designed and analyzed pitch and roll MFD control signals for the B-727 flight director. The B-727 model and the MFD algorithms were installed in the Flight Simulator for Advanced Aircraft (FSAA) at Ames Research Center of the National Aeronautics and Space Administration. Windshear simulation tests were run by the AWLS team with seven subject pilots under AWLS project Task 2; the results again showed promise.

In a parallel effort, the DC-10 pitch and roll MFD algorithms were integrated with accelerometer-augmented thrust commands presented on

the flight director Fast/Slow (F/S) indicator. Collins designed two thrust-control algorithms: one without groundspeed (GNS) information and one that used GNS to compensate for a diminishing headwind. Both were analyzed, then taken to Long Beach and installed on the DC-10 flight simulator. They were tested as part of the phase 3 DC-10 simulation tests, conducted by the AWLS team, again under Task 2; a detailed description of the tests has been published.[4]

In summary, of the two thrust commands, the algorithm with GNS performed best; the integrated MFD system--consisting of acceleration-augmented pitch, roll and thrust commands for the flight director--was useful in coping with windshear. These tests were completed in March 1978.

The modified flight director algorithms had been developed for approach and landing supported by a full ILS--that is, for a precision approach. The next subtask was to design and analyze comparable control laws for a nonprecision approach, in which the glideslope beam was absent and only the localizer and marker beacons were available. It was assumed that GNS measurements would be available and that position could be initialized (for instance, by noting the point of passage of the center of the outer marker on approach); then the aircraft longitudinal position could be computed by integrating GNS with respect to time. With altitude above the runway level and longitudinal position, a synthetic reference glidepath was computed and used as the basis for the MFD control laws for nonprecision approach.

Collins designed and analyzed these control laws, and installed them in the DC-10 simulation computer at Long Beach. They were tested, along with the precision-approach MFD, in phase 4, Task 2, piloted flight simulation tests in windshear conducted by the AWLS team at Douglas in December 1978-January 1979. These tests are described in a separate Task 2 report.[8] The results were excellent, both in terms of absolute performance and in terms of performance improvement over the conventional DC-10 approach-and-landing flight director system.

The final subtask was to adapt the MFD algorithms to a government test aircraft. The FAA Grumman Gulfstream I was selected. The MFD steering and thrust commands were redesigned for the aerodynamic characteristics of the Gulfstream I, analyzed and tested with a computer model, and installed in the airplane's flight director. Flight tests will be conducted by the FAA.

Much of the work was done in coordination with the flight simulation windshear exercises conducted by the other members of the AWLS team (SRI and Bunker Ramo Corporation) under Task 2 at Douglas and NASA Ames Research Center. Collins engineers supported these exercises on site, checked out the simulation of the control laws, and monitored the operation of the algorithms in test. Collins also participated in the presentations and demonstrations that were held for the aviation community after the simulator tests.

B. Organization of Report

The work under Task 5 was documented in a long series of interim technical reports by Collins. This final report collects the major points of these interim reports. Section II describes the review of background studies of inertial augmentation for approach and landing systems. The development and comparison of the inertially augmented autoland control laws for the CV-880 airplane are discussed in Section III. Flight director control laws, both steering and thrust management, for the DC-10 are described in Section IV; this includes the systems for both precision and nonprecision approaches. Section V contains a discussion of the B-727 simulation model developed by Boeing and the Collins modified flight director algorithms for the B-727. Implementation of the modified flight director in the Grumman Gulfstream I test airplane is the subject of Section VI. The last section, VII, gives general conclusions drawn from all the work on Task 5 and related efforts. Appendices contain technical details of certain computer models.

II BACKGROUND REVIEW*

T. J. Schuldt

Previous work on inertially augmented approach couplers has been directed primarily toward the use of inertial platform data to improve the performance of approach couplers on noisy ILS beams. Various evaluation criteria have been used to show improved tracking performance and reduced control activity in the presence of noisy ILS signals when inertial platform data are used. Improved ILS tracking in the presence of random gusts and windshears has also resulted from the tighter control and the use of signals which are not sensitive to windshear. Although autothrottles have been used or assumed in some of the previous work, there has been little emphasis on the autothrottle control laws and little effort to optimize them for atmospheric disturbances.

The following sections review the limitations of "conventional" control laws and the ways by which acceleration and velocity information can improve performance. Previous efforts related to the current tasks are summarized.

A. Conventional vs Inertially Augmented Approach and Landing Control Laws

Previous reports[5-7] provide background discussions on approach and landing control laws and the sensor inputs from which they are derived. Pitch and roll axes are treated separately.

1. Roll Axis

A typical conventional bank command generated by an approach mode control law is the sum of localizer deviation, integrated localizer deviation and a damping, or rate, term as shown in Figure 1a. Development work has been directed toward achieving a more nearly ideal damping term and toward improving the direct localizer path by using complementary-filter or other estimator techniques as shown in Figure 1b.

---

*This section is excerpted from T. J. Schuldt, "Inertially Augmented Approach Couplers--A Review of Previous Work," report by Collins Radio Group, Rockwell International, Cedar Rapids, Iowa (March 17, 1976).

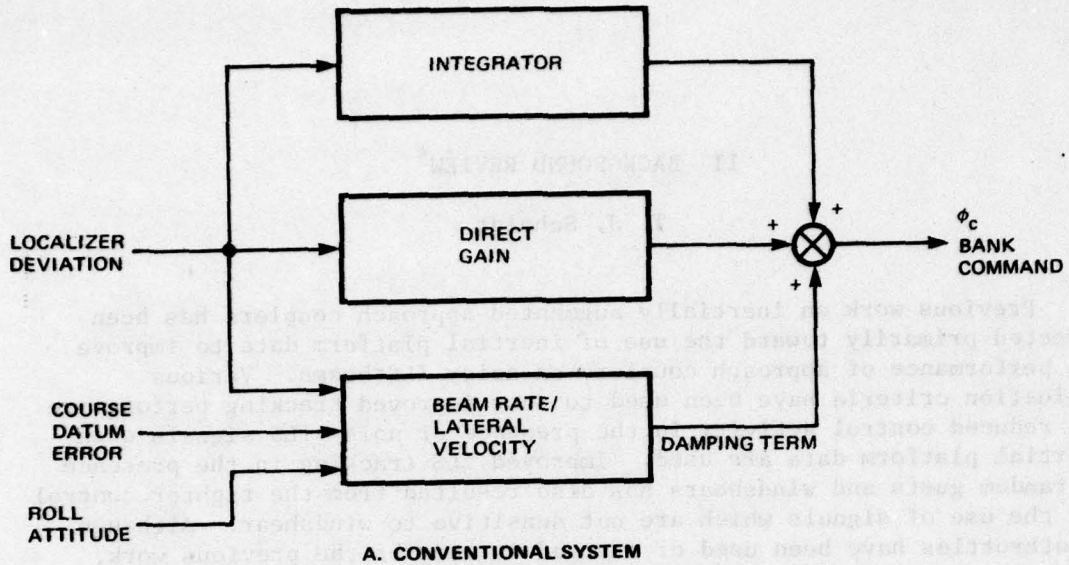

A. CONVENTIONAL SYSTEM

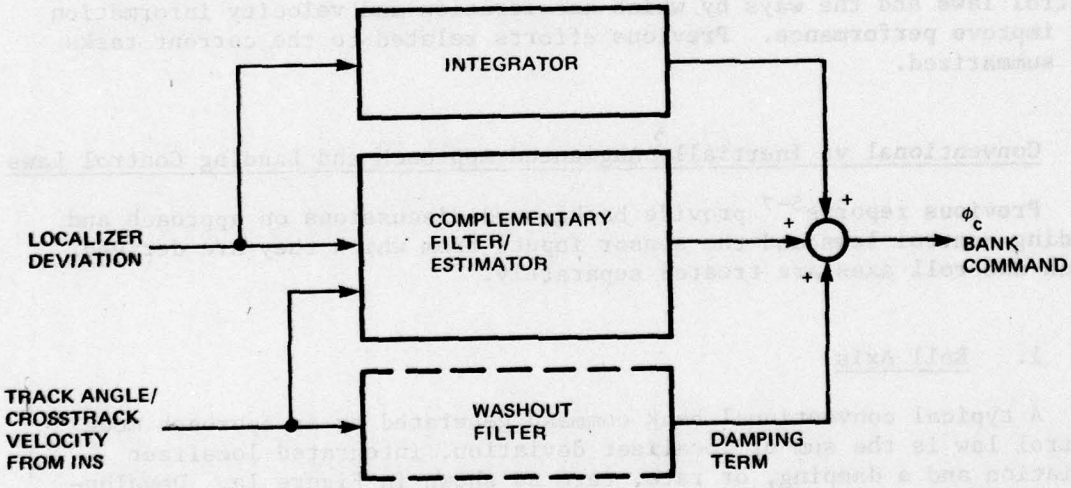

B. AUGMENTED SYSTEM

FIGURE 1 SIMPLIFIED BANK COMMANDS

Path Damping--Estimating Lateral Velocity. Various sensors and transfer functions have been used in conventional systems to estimate or approximate lateral velocity, which provides the path damping term in the bank command. Derived beam rate, lagged roll, and course datum error have been used to estimate lateral velocity.

Derived beam rate ideally would be sufficient for path damping, but noise on the localizer signal is amplified by the beam rate deriver. To achieve acceptable system activity and localizer dispersion, the time constant of the rate deriver must be increased and the derived rate gain decreased significantly from the values required for adequate damping.

Lagged roll is an approximation to lateral velocity. When sideforces are ignored (i.e., if a coordinated turn is assumed), a heading change is equal to the integral of roll attitude. (A heading change is equivalent to a lateral velocity change.) Another approximation, as the term "lagged roll" implies, is that roll attitude is processed through a lowpass (lag) filter, rather than through a pure integrator because of system offsets.

Course datum error represents lateral velocity if there is no sideslip. However, since sideslip is not completely eliminated during maneuvers, the gain of the course datum error must be less than ideally desired to avoid reduced stability at the Dutch roll frequency. A further restriction on the use of course datum error is its sensitivity to cross-wind conditions. A washout filter will remove the steady-state course datum error, which corresponds to a constant cross wind, but in the presence of a cross-windshear the course datum error term causes offset localizer tracking.

In many systems, a combination of beam rate, lagged roll and course datum error have been used to provide path damping. In more recent systems the course datum term has been eliminated because of its cross-windshear sensitivity. In at least one autoland system, roll attitude has been combined with a lateral accelerometer (body-mounted) output to remove some of the restrictions on the use of lagged roll.

Significant improvements in localizer tracking have been achieved by using INS track angle or crosstrack velocity from the INS as an alternate signal to replace the conventional damping terms. It does not have the dynamic approximation errors of the conventional terms (assuming negligible sample data effects), and it is limited only by INS drift and the use of a washout filter to remove low frequency errors. Since track angle is a more nearly ideal representation of lateral velocity, the damping gain can be increased to provide improved stability and tracking performance.

Complementation of Localizer Deviation. Another means for reducing control activity and improving tracking performance is to replace the direct localizer deviation contribution to the bank command with an

inertially smoothed localizer deviation signal, which is the output of a complementary filter as shown in Figure 1b. The complementary filter removes the higher frequencies of the localizer signal and replaces them with short-term position information derived from INS track angle (or crosstrack velocity). By this technique the localizer signal is smoothed, and the complementary use of short-term position information derived from velocity data replaces the dynamic portion of the localizer signal, which is removed by the filter.

An important consideration in the use of complementary filters is the initialization of the filter at the beginning of the approach. Since the filter time constant is on the order of 20 s, an improper initial condition, when the localizer track computations are engaged, can cause unacceptable offsets. Proper initialization or synchronization must be accounted for in the design of the complementary filter.

More complex means for estimating lateral position involve combining ILS and inertial information. One method is to minimize the integral square of the difference between inertially computed displacement and ILS-sensed displacement. The second is to use the Kalman filtering technique to minimize the sum of the mean-square differences between the estimated and actual values of several variables based on inertial and ILS information. Kalman filter techniques require the use of digital computations.

The use of INS data improves localizer tracking by smoothing the localizer signal and providing improved path damping. Both improvements allow channel gains to be increased with resultant increases in system bandwidth; they also reduce control activity and improve path tracking in the presence of a noisy localizer signal, gusts, and windshear.

2. Longitudinal Axis Control Laws

Previous work in the area of longitudinal axis performance improvements has been directed in a manner similar to roll axis improvements. The glideslope error signal has been smoothed by complementary filter techniques. Pitch attitude damping has been replaced by vertical acceleration damping and by increased dependence on altitude rate. In addition, the previous work includes the replacement of normal accelerometer and barometric altitude rate data by INS data. Figure 2a shows a simplified control law, which includes pitch damping. Figure 2b illustrates the use of vertical acceleration damping.

Longitudinal Path Damping. The use of vertical acceleration to replace pitch attitude for inner loop damping and stability improves glideslope tracking in vertical gust conditions. The use of pitch attitude can cause commands which oppose the tendency of an inherently stable airplane to trim and can accentuate the effect of a gust in

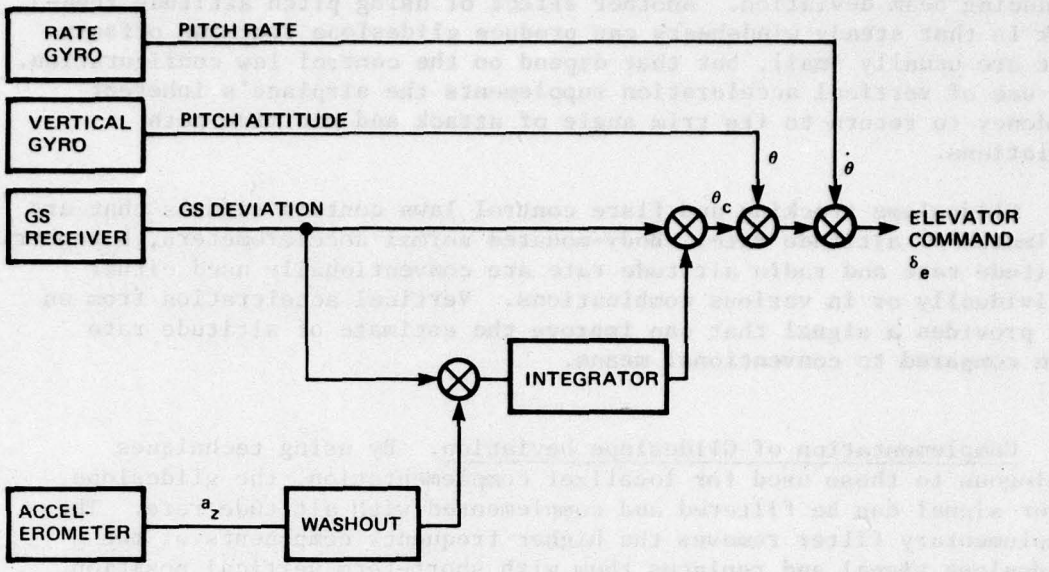

A. PITCH ATTITUDE

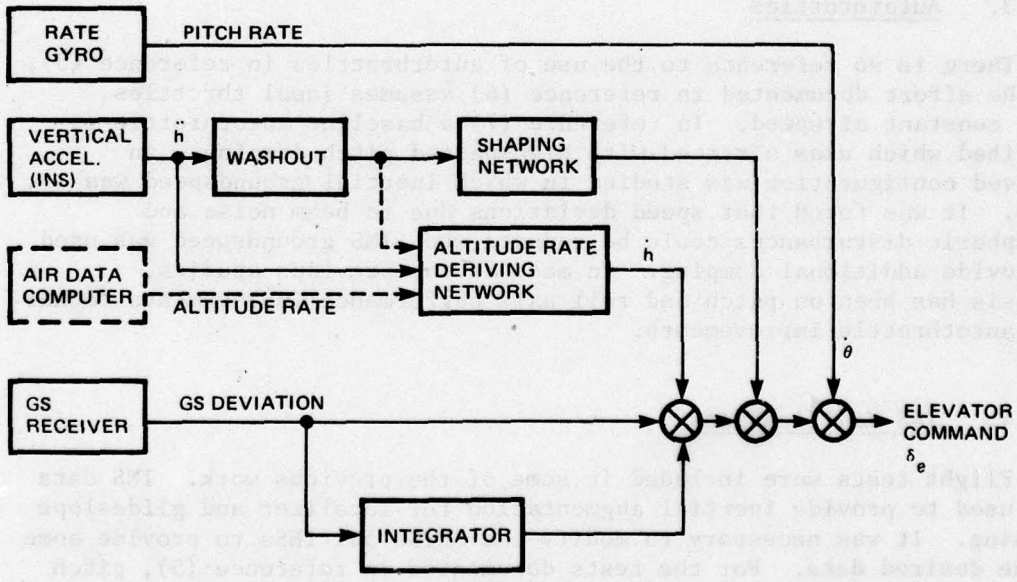

B. VERTICAL ACCELERATION

FIGURE 2 DAMPING METHODS

producing beam deviation. Another effect of using pitch attitude feedback is that steady windshears can produce glideslope tracking offsets that are usually small, but that depend on the control law configuration. The use of vertical acceleration supplements the airplane's inherent tendency to return to its trim angle of attack and minimize path deviations.

Glideslope tracking and flare control laws contain signals that are estimates of altitude rate. Body-mounted normal accelerometers, barometric altitude rate and radio altitude rate are conventionally used either individually or in various combinations. Vertical acceleration from an INS provides a signal that can improve the estimate of altitude rate when compared to conventional means.

Complementation of Glideslope Deviation. By using techniques analogous to those used for localizer complementation, the glideslope error signal can be filtered and complemented with altitude rate. The complementary filter removes the higher frequency components of the glideslope signal and replaces them with short-term vertical position information derived from altitude rate. The complementary use of altitude rate allows smoothing of the glideslope signal without introducing unacceptable system lags.

3. Autothrottles

There is no reference to the use of autothrottles in reference (5), and the effort documented in reference (6) assumes ideal throttles, i.e., constant airspeed. In reference (7) a baseline autothrottle is described which uses airspeed with high-passed pitch damping. An improved configuration was studied in which inertial groundspeed was added. It was found that speed deviations due to beam noise and atmospheric disturbances could be reduced when INS groundspeed was used to provide additional damping. In most of the previous studies, emphasis has been on pitch and roll axis performance improvements rather than autothrottle improvements.

4. INS Modifications

Flight tests were included in some of the previous work. INS data were used to provide inertial augmentation for localizer and glideslope tracking. It was necessary to modify the ARINC 561 INSs to provide some of the desired data. For the tests documented in reference (5), pitch and roll attitude and vertical acceleration analog outputs were available and used unmodified. Groundspeed and track angle were used in digital format. Software changes were made to increase the data rate of the track angle output from once every 600 ms to once every 200 ms. An operational consideration is that the magnetic runway heading reference had to be corrected with local magnetic variation before combining it with track angle to obtain track angle error.

For the flight tests described in reference (7), software changes were also required for the INS. Some changes in computation rates were required, and software changes to allow entry of the glideslope angle and true runway heading via the control display unit were made. Since the experimental autopilot hardware used analog computations, software changes were made to replace some of the existing analog outputs with outputs required for the inertial augmentation tests, e.g., crosstrack velocity.

B. Inertially Augmented Automatic Landing System: Autopilot Performance With Imperfect ILS Beams[1]

The Boeing work documented in reference (1) compared the performance capabilities of three sets of pitch and roll axis autoland control laws for a commercial jet transport in the presence of ILS beam anomalies. The control laws had varying degrees of dependence on INS inputs. The three sets of control laws were:

- Conventional control laws with no INS inputs
- Control laws which use INS information for path damping
- Control laws which use INS inputs for both path damping and inertial smoothing of the ILS beam inputs.

Specific objectives of this program were to:

- Identify the advantages of inertial smoothing
- Define the limitations of inertial smoothing
- Determine criteria which will permit exploitation of the advantages of inertially smoothed systems.

The system A control laws were the conventional control, used as a baseline. The roll axis used a combination of beam rate, heading and roll attitude inputs for path damping. The pitch control law generated a pitch command which was summed with pitch attitude and pitch rate to generate an elevator command. Both localizer and glideslope deviation were gain-programmed with radio altitude. The system B control laws used inertial data for path damping. The roll axis control law used track angle from the INS to provide path damping instead of the conventional control law damping. The pitch axis control law had the pitch attitude deleted, an improved estimate of altitude rate derived from barometric altitude rate and vertical acceleration from the INS, and vertical acceleration through a shaping filter to replace pitch attitude. The system C control laws included the addition of localizer and glideslope smoothing to the inertial path damping of system B. Localizer deviation was filtered and complemented with INS track angle. Glideslope was filtered and complemented with an altitude rate error computed from INS groundspeed, glideslope angle and derived altitude rate.

One of the objectives was to determine performance criteria with which to compare the three sets of control laws. These performance criteria were designed to be compatible with the pilot's assessment of satisfactory performance. For the pitch and roll axes a "footprint" criterion and a "maneuver" criterion were defined, related to similar performance criteria in AC 20-57A and AC 120-39.[1,2]

The roll axis footprint criterion was a closed curve in the y-$\dot{y}$ plane, representing the satisfaction of four inequalities defined to restrict position, velocity and corrective maneuvers from 100 ft altitude to touchdown to routine, acceptable values:

$$J \geq |y|$$

$$-J \leq R\dot{y} + y - \frac{\dot{y}^2}{2A} \qquad \text{for } \dot{y} \leq 0 \text{ and } 0 \leq h \leq 100$$

$$J \geq R\dot{y} + y + \frac{\dot{y}^2}{2A} \qquad \text{for } \dot{y} \geq 0 \text{ and } 0 \leq h \leq 100$$

$$|\dot{y}| \leq (10 - R)A$$

where

J = threshold value (60 ft)

A = crosstrack acceleration criterion (1.125 ft/s^2)

R = pilot reaction time (1.0 s)

The roll axis maneuver criterion was based on pilot confidence and passenger comfort. It expressed all appropriate state variables in one inequality to represent the pilot's integrated assessment. The roll axis maneuver criterion was expressed by the inequality:

$$Y \geq |y + K_1 \Delta\psi_G + K_2 \phi|$$

where

Y = roll axis maneuver criterion threshold value

$Y = \frac{h - 100}{5.3} + 60$ ft for $h \geq 100$ ft

$Y = 60$ ft for $0 < h < 100$ ft

$$K_1 = 17 + \frac{h - 100}{65} \text{ ft/deg for } h \geq 100 \text{ ft}$$

$$K_1 = 17 \text{ ft/deg for } 0 < h < 100 \text{ ft}$$

$$K_2 = 5 \text{ ft/deg}$$

y = lateral displacement in ft

$\Delta\psi_G$ = ground heading error $\propto \dot{y}$

ϕ = roll attitude $\propto \ddot{y}$

The pitch axis footprint criterion was based on assumptions involving Boeing airplane characteristics and autoland performance. The footprint is an area in the $\Delta h - \Delta\dot{h}$ plane. It was assumed that each system evaluated included a flare control law whose performance met Category III dispersion requirements. Then maximum altitude and altitude rate deviations from the nominal (for altitudes between 50 and 100 ft) were determined which produced touchdowns at the extremes of the allowable touchdown zone. As a conservative measure, each of the extremes was translated 5% into its favorable region.

The pitch axis maneuver criterion was expressed by the inequality:

$$F(h) \geq |\Delta h + C_1 \Delta\dot{h} + C_2\dot{\theta}|$$

F(h) was estimated from the AC 20-57 tracking requirement:

$$F(h) = 0.089h \qquad \text{for } 180 \leq h \leq 700 \text{ ft}$$

$$= 16 \text{ ft} \qquad \text{for } h < 180 \text{ ft}$$

The values of C_1 and C_2 were determined by simulating a sinusoidal beam bend which caused system A to barely exceed the footprint criterion. It was assumed that the same bend should also produce marginal performance relative to the maneuver criterion. C_1 and C_2 were adjusted until the maneuver inequality was satisfied.

$$C_1 = 3.5$$

$$C_2 = -3.5$$

Both simulation runs and flight tests were performed, but only a brief review of flight test results is included in this summary. During test flights, beam disturbances were simulated; Figure 3 shows some examples.

Figure 4 shows footprints for the pitch control laws. Note the concentration of footprint trajectories near the origin for systems B and C when compared with system A. Further distinctions between systems B and C were masked by atmospheric upsets having greater effects than the simulated beam disturbance. Figure 5 shows roll axis footprint trajectories and shows clearly the relative performance improvements for systems B and C. Although the prime objective of this study involved demonstrating improved performance in the presence of ILS disturbances, improved performance in the presence of atmospheric disturbances was also demonstrated qualitatively by comparing system performance over a short period of time.

System C control laws were the most sensitive to INS errors because both path damping and complemented beam deviation are derived from INS outputs. The pitch axis was less sensitive than the roll axis and had no significant path offsets due to INS errors. The roll-axis errors were a bias and ramp error in track angle as well as signal format properties of granularity, data rate, and computation time delay. Track angle bias errors were cancelled by the path integrator after several minutes of localizer tracking. Ramp errors resulted from platform tilt and accelerometer biases.

A successful approach was defined by the footprint and maneuver criteria. By using a combination of flight test data, simulator runs with deterministic beam bends, and turbulence-induced dispersion data from other studies, estimates of the performance attainable on ILS beams of varying qualities were made. The system C control laws provided the most performance margin and were least affected by beam bends. System C, particularly the lateral axis, was judged as being capable of Category II performance on most Category I beams and Category IIIa performance on most category II localizers. Constraints to achieving improved performance were localizer misalignment and the permissible variation in glideslope beam center location with respect to the touchdown zone.

C. Application of Inertial Navigation and Modern Control Theory to the All-Weather Landing Problem[2]

The project reported in reference (2) was an analysis and simulation study which used both a simplified aircraft model and Boeing B-2707 phase IIC SST aerodynamic data. The study had a twofold emphasis:

- Implications of inertial navigation technology for all-weather landing
- Application of modern and classical control theory for effective use of inertial equipment.

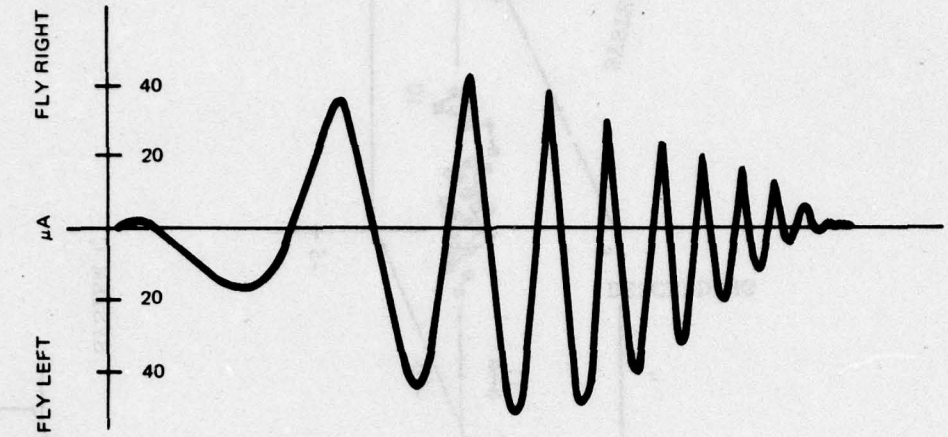

A. HIGH-ALTITUDE OVERFLIGHT

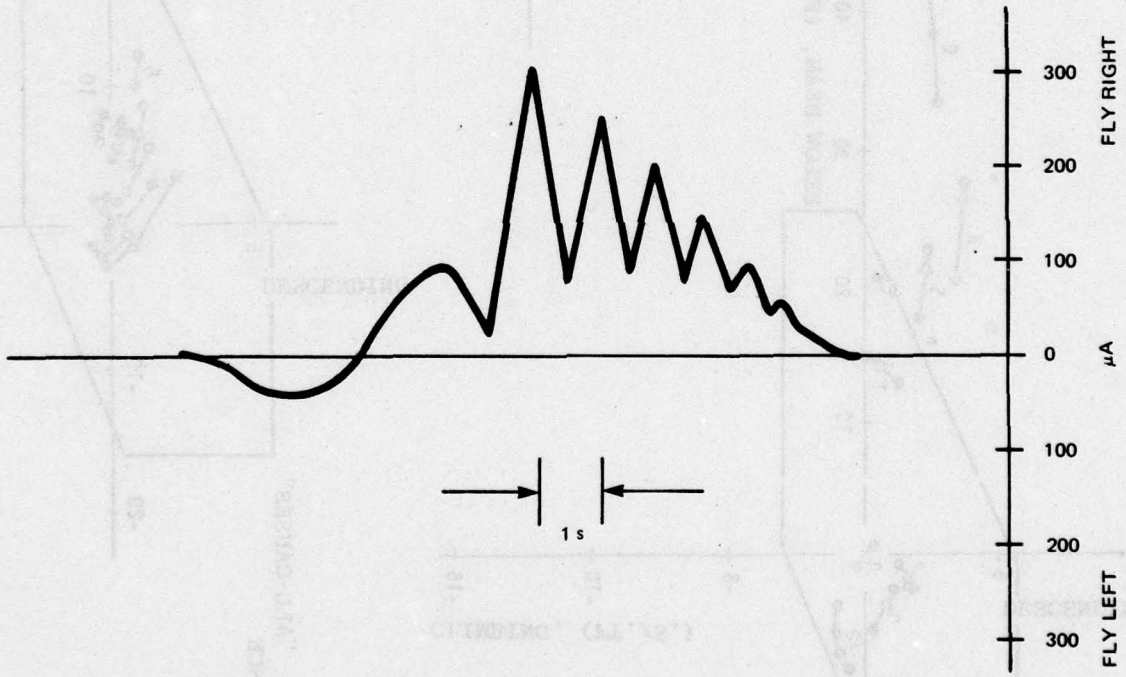

B. LOW-ALTITUDE OVERFLIGHT

FIGURE 3 SIMULATED LOCALIZER DISTURBANCES

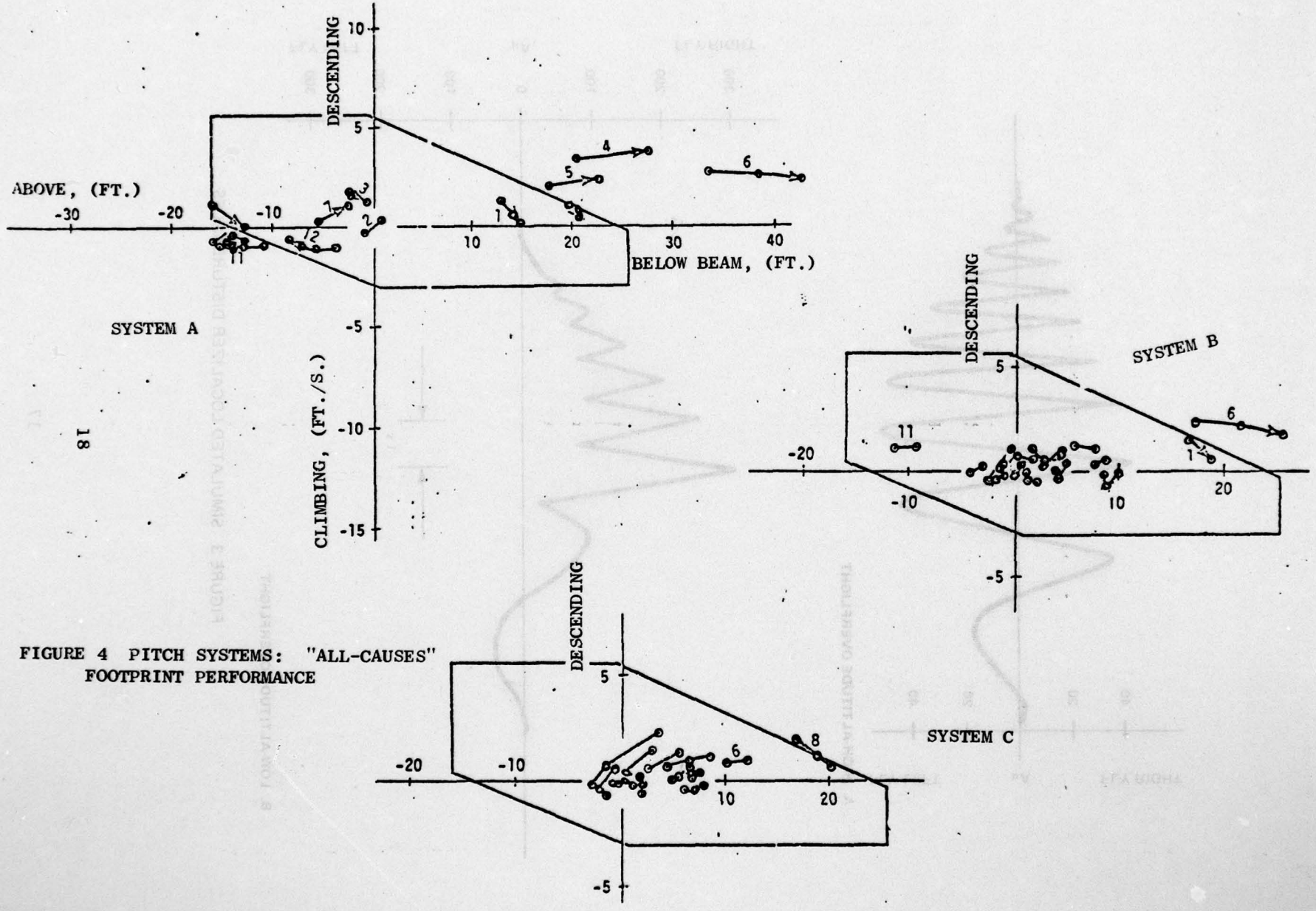

FIGURE 4 PITCH SYSTEMS: "ALL-CAUSES" FOOTPRINT PERFORMANCE

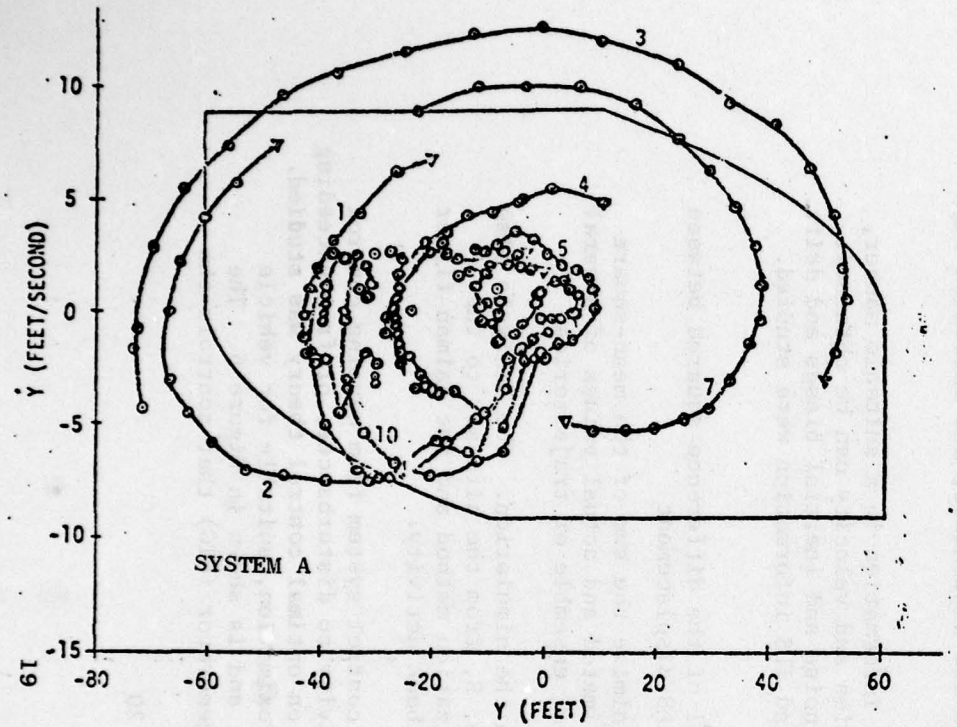

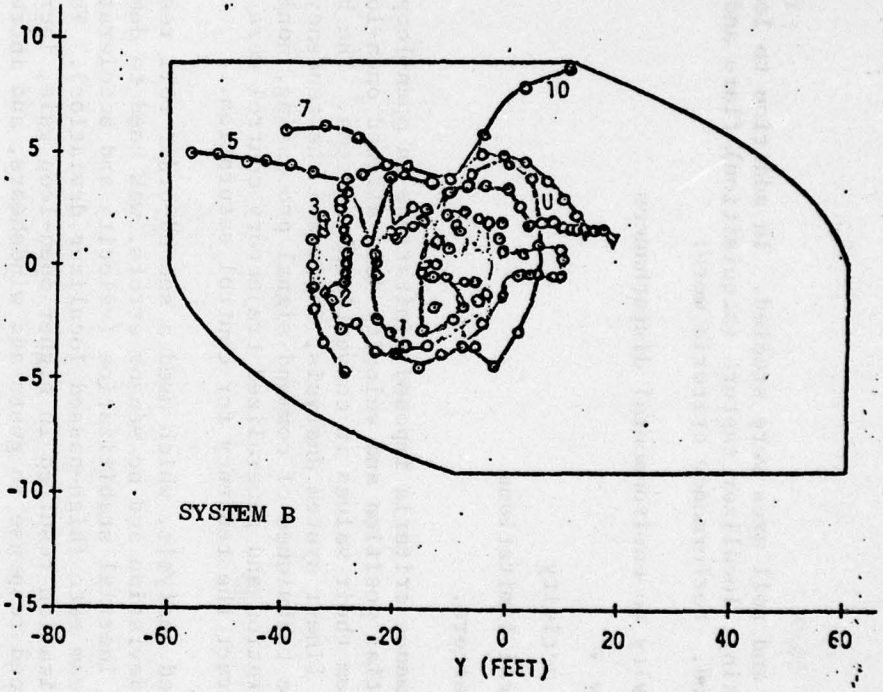

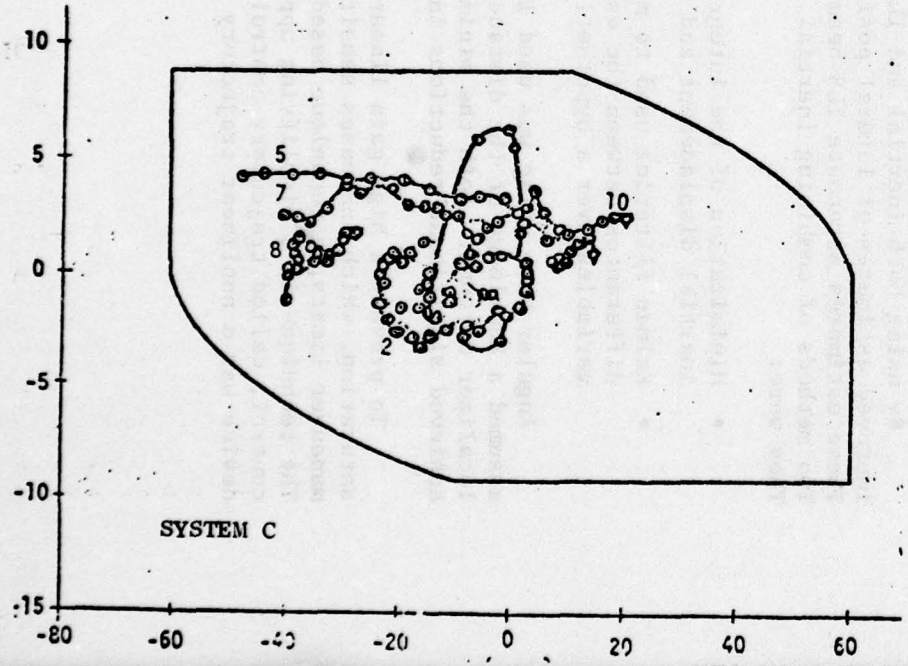

FIGURE 5
ROLL SYSTEMS: "ALL-CAUSES" FOOTPRINT PERFORMANCE

Both pitch and roll axes were studied. In addition to localizer and glideslope tracking, localizer capture (acquisition), flare and decrab were investigated. Performance criteria were:

- Sensitivity to environmental disturbances
- Accuracy
- Control activity
- Structural limitations
- Human factors.

The performance criteria imposed limitations on open-loop gain, but the use of inertial position and velocity data allowed open-loop gains to be increased from their values in conventional systems. The higher gains, based on linear system analysis, increased the tendency for control saturation. The techniques of command signal processing, nonlinear trajectory generation and generalized trajectory control were studied as means to counteract the tendency for control saturation.

A simplified analysis, which used a second-order roll response and assumed linear deviation and no sensor errors, was used to demonstrate the benefits of inertial stabilization (velocity and acceleration) compared with beam rate (high-passed localizer deviation). The use of inertial stabilization resulted in higher open-loop gain, increased bandwidth, reduced response to gusts and windshears, and increased beam noise sensitivity.

By using both inertial and ILS information in a suitable manner, improved estimates of lateral position and velocity can be obtained. These estimates attenuate ILS beam noise and inertial biases and drift. Two methods of combining inertial and ILS information were studied. They were:

- Minimization of the integral of the difference squared between inertial displacement and ILS displacement
- Kalman filtering used to minimize the sum of the mean-square differences between the estimated and actual values of several variables over a hypothetical ensemble of trajectories.

Angular beam noise was used in the simulation. The analysis also assumed a knowledge of the distance, R, from the aircraft to the localizer antenna. Both the minimization method and the Kalman filter achieved significant reductions in bank activity.

To prevent a high gain linear control system from causing control saturation, which increases sensitivity to disturbances, or from exceeding maneuver limits, a technique based on optimal control theory was studied. The technique is a simplifying approximation, suitable for vehicle control, called trajectory control, and is shown in Figure 6. The device was a nonlinear trajectory generator (NTG) that controls the

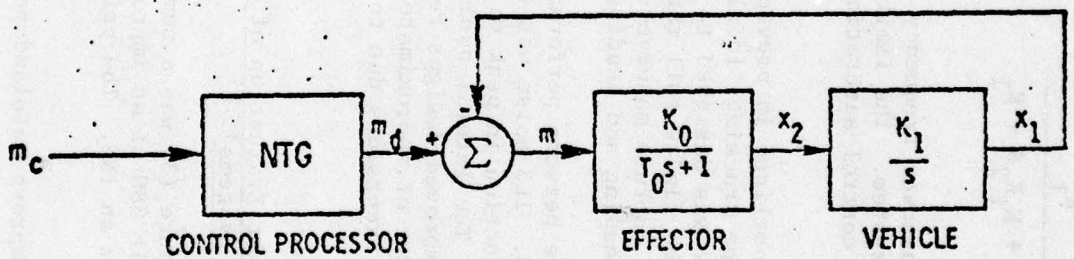

FIGURE 6. ILLUSTRATIVE MODEL OF A TRAJECTORY CONTROL STSTEM. THE VALUE OF x_1 SHOULD FOLLOW THE VALUE OF m_d CLOSELY.

bandwidth of the input and modifies the input by limiting the first and second derivatives. A linearized model of the NTG is a second-order filter whose transfer function is

$$\frac{md}{mc} = \frac{K_1}{S^2 + K_1K_2S + K_1}$$

and whose bandwidth equals the crossover frequency of the open-loop transfer function of the control system. The limits were set at values less than those which would cause control saturation to allow control authority for disturbances.

The techniques and concepts outlined in previous paragraphs were applied to localizer and glideslope tracking, localizer capture, flare and decrab. The localizer capture was designed to be a fixed-bank-angle capture with allowance made for the finite roll rates desired at the initiation and termination of the capture manuevers. The decrab system used an NTG to control aircraft heading and heading rate.

Several comparisons were made between performance of the improved systems and a conventional system. ILS noise was the primary disturbance simulated. A factor of three reduction in peak roll angle while tracking localizer was achieved. The lateral position trajectory was also noticeably smoother. The improved designs reduced lateral velocity excursions due to gusts by a factor of approximately two. In the vertical axis, vertical velocity excursions due to vertical gusts were reduced by approximately 0.6.

D. Design, Development and Flight Evaluation of Inertially Augmented Automatic Landing Systems[3]

The work discussed in reference (3) was a combination of simulation and flight test in the FAA Convair 880 of an improved automatic landing system which used parameters from an INS. The primary objectives of this study were:

- Use INS information to improve autoland performance with minimum modification.
- Implement a system for flight evaluation.
- Flight test the system in a turbojet transport aircraft to confirm simulation predictions.

Two system designs emerged. One system, identified as "AUG," used inertial parameters with the assumption that errors accumulated during

a flight of several hours duration. The second system was labeled "I/AUG" and used inertial data with the assumption that the inertial data had been updated to keep errors small.

A simulation study was performed to compare the inertially augmented systems with the existing (or "normal") Lear-Siegler AWLS on the FAA CV 880. The study included both ILS beam and wind disturbances. The approach simulations were initiated at glideslope capture. It was the goal of the study to obtain a factor of two improvement in performance. The performance criteria were based on maintaining or improving system stability, beam tracking accuracy, windshear capability, and gust and turbulence sensitivity.

It was determined that the best uses of INS would be (1) to augment the ILS receiver outputs (glideslope and localizer deviations) and (2) to replace beam rate damping with INS velocity and acceleration. The I/AUG lateral system differed from the existing in the replacement of beam rate and lagged roll damping by crosstrack velocity, $\dot{y}$. In the I/AUG system the position gain was effectively increased by summing inertial position (y) with localizer deviation. This configuration worked well with no errors but was sensitive to INS position errors. No gain programming was used.

In the lateral AUG system the damping was the same as the I/AUG system but the suppression of beam noise was accomplished by a complementary filter which combined localizer deviation and inertial crosstrack velocity. The localizer gain was increased by a factor of four. The AUG system used crosstrack velocity and course angle error to generate the decrab command.

In the I/AUG longitudinal system a reference altitude Z_R was computed from inertial groundspeed and the glideslope angle. Vertical acceleration from the INS was integrated twice to obtain vertical rate and displacement. The vertical rate replaced a vertical rate signal obtained in the normal system by complementing barometric altitude rate with body-mounted normal acceleration. The direct glideslope gain was reduced by a factor of eight.

The longitudinal AUG system was similar to the I/AUG system except that the use of inertial vertical position data was replaced by a complementary filter which used inertial vertical rate to complement glideslope deviation.

This study is the only one of those summarized in this report which included autothrottle performance. The autothrottle was used to control airspeed, but the addition of inertial groundspeed as a damping term provided improved damping.

The AUG system was the more practical user of inertial data. The I/AUG system was sensitive to INS position drift error and required

knowledge of the glideslope angle. The performance improvements indicated by the results of this study were significant. When inertial information was used, wheel activity, aircraft motion and excursions from ideal localizer and glideslope beams were reduced by more than a factor of two. The lateral offset due to an 8-knots-per-100-ft windshear was reduced by a factor of three during an altitude change of 200 ft and a factor of 10 over 300 ft of altitude. Improved tracking accuracy (at the expense of wheel activity and angular rates) in the presence of gusts was also demonstrated.

A significant portion of the flight testing was used to identify and correct problem areas, many of which were related to the improper initialization of the inertial signals. Longitudinal axis performance was inconsistent during flight tests but appeared satisfactory near the end of the flight test period. The primarily lateral axis results were documented in the reference.

The result of this combined simulation/flight test effort were:

- The lateral performance improvements of the AUG system can be predicted by simulation and confirmed by flight test correlation
- Proper initialization of the inertial terms is essential
- Improved performance in the lateral axis is more pronounced than in the longitudinal axis.

E. General Results

Several other previous investigations were reviewed and reported. They ranged from theoretical studies to combined simulation/flight test efforts. In general, each of the previous efforts used a baseline or "conventional" system and an improved system which included inertial platform data and performance criteria, all of which differ from the other efforts. All of the previous work reviewed, however, showed that the systems using inertial platform data resulted in improved performance on noisy ILS beams when compared to their corresponding "conventional" systems by using the appropriate performance evaluation criteria. It has also been noted that systems which use inertial platform data provide improved responses to atmospheric disturbances.

Performance improvements have been achieved by:

- Replacing derived beam rate with acceleration and velocity information from the inertial platform
- Using inertial velocity information to complement glideslope and localizer deviation signals.

Schemes ranging from single-order lowpass filters to more complex estimation techniques have been tested or studied. In those instances where flight tests have been performed, the ARINC 561 inertial navigation systems have required modifications to provide some of the signals used in the improved control laws.

III AUGMENTATION OF THE CV-880 AUTOLAND SYSTEM*

F. B. Benson, L. V. Miller and R. J. Rudig

The goal of this subtask was to design and specify an accelerometer-complemented automatic flight control system for a transport aircraft that would have approach-and-landing performance comparable to a more expensive INS-based control system. The FAA Convair 880 test airplane was selected. The flight condition was chosen to correspond as closely as possible to anticipated test conditions:

- Gross weight = 155,000 lb
- Flaps at 50°, gear down

---

*This section is a compilation of excerpts from the following Collins documents prepared on AWLS Task 5:

Rudig, R. J., "Candidate Longitudinal Axis Control Laws for the Study of ILS and MLS Glideslope Beam Complementation," (2 December 1975).

Miller, L. V., "Candidate Lateral Axis Control Laws for the Study of ILS and MLS Localizer Beam Complementation," (4 December 1975).

Benson, F. B., "Evaluation Plan for Task 5 of DoT Contract FA75WA-3650," (8 December 1975).

Miller, L. V., "Analysis and Simulation of Aircraft, Roll Loop, and Yaw Damper to be Used for SRI Inertial Augmentation Study," (19 December 1975).

Rudig, R. J., "Analysis and Simulation of Longitudinal Aircraft, Pitch Loop, and Autothrottles to be Used for SRI Inertial Augmentation Study," (5 January 1976).

Miller, L. V., "Analysis and Simulation of Localizer Control Laws to Be Used for SRI Inertial Augmentation Study," (18 February 1976).

Rudig, R. J., "Analysis and Simulation of the Baseline Glideslope Control Laws for the SRI Inertial Augmentation Study," (25 March 1976).

Miller, L. V. and R. J. Rudig, "Report of Task 5, Phase I, AWLS-Inertial Augmentation," (10 August 1976).

- Approach speed = 265 ft/s
- Runway at sealevel

Longitudinal, or pitch, axis control was investigated, and, in a separate activity, lateral axis control laws were studied. Frequency responses were analyzed with the Collins CHAIN program on a Univac 1108 digital computer. Longitudinal system models were run at 1000 times real time on an EAI 680 analog computer simulation, with statistical data being gathered by a Pacer 100 digital computer. Similarly, lateral axis models were tested in separate simulations. The lateral and longitudinal axes were not coupled because of expense and because experience had shown that good results could be obtained treating the two axes separately.

The modes simulated for the longitudinal or pitch axis included glideslope capture and track, flare, and autothrottles. The autothrottles were adjusted to have a response time that did not react significantly to short-term longitudinal wind turbulence and that approximately simulated a slowly reacting manual operation. The autothrottles were adjusted such that an error in airspeed was reduced by a minimum of 90% in approximately 18 s. For the lateral axis, localizer capture and track, yaw damper, and a forward slip mode were set up for simulation and analysis. Forward slip was used to provide a maneuver comparable to that expected from a manual slip.

Captures of the ILS glideslope or localizer beams were provided to ensure a realistic treatment of initial conditions. In the complementation of the beam, initializing filters can be a very significant problem. Captures were included, therefore, to analyze initial condition problems and to synthesize solutions.

For both the longitudinal and the lateral axes, three typical systems using inertial data in different ways were specified and analyzed. The three were also compared to a conventional air transport system. Control laws involving accelerometer smoothing of beam data were compared with INS-data-smoothed laws to show equivalent performance. The accelerometer-smoothed laws were also compared with unsmoothed laws now in Category III certified service. The unsmoothed system also used accelerometer information, but primarily for rate damping rather than beam noise smoothing. All three systems studied were highly capable and demonstrated considerable improvement over a typical Category II autopilot conventional system.

The systems were evaluated through the capture, track, and landing phases of operation under a wide variety of environmental disturbances including beam noise, wind turbulence, and, of course, windshear. The wind profiles, turbulence models and ILS beam noise and beam disturbance models are given in Appendix A.

A. Longitudinal Axis and Autothrottle

The aircraft longitudinal linearized equations of motion for this flight condition are presented below:

- Test conditions
  - Altitude = 0 ft
  - V_{true} = 265 ft/s
  - Weight = 155,000 lb
  - Gears = down
  - Flaps = 50°
- Linear equations of motion

$$-\dot{\upsilon} - 0.03815\upsilon + 0.3297\alpha - 0.562\theta + 0.206\delta_{throt} = 0 \quad (1)$$

$$-\dot{\alpha} - 0.053\upsilon - 0.624\alpha + 0.969\dot{\theta} - 0.02817\delta_{stab} - 0.0027\delta_{throt} - 0.00704\delta_{te} = 0 \quad (2)$$

$$-\ddot{\theta} - 0.181\dot{\alpha} - 0.455\alpha - 0.48\dot{\theta} - 0.74\delta_{stab} + 0.07\delta_{throt} - 0.184\delta_{te} = 0 \quad (3)$$

$$\ddot{\delta}_e + 11.5\dot{\delta}_e + 189\delta_e = -165\delta_{te} - \dot{\theta} - 24.2\alpha \quad (4)$$

$$\delta_{te} = \delta_e - \delta_{tec} \quad (5)$$

Of particular interest are the elevator equations. The CV-880 control surfaces are aerodynamically actuated through control surface tabs. Equations (4) and (5) represent this activation. Several things are noteworthy:

- The elevator tab actuation contains a mechanical feedback from elevator deflection, reducing the tab deflection as the elevator deflects.
- Elevator deflection is affected by pitch rate and angle-of-attack as well as elevator tab deflection. These terms model the effect of aerodynamic forces upon the surfaces.

The time response of the CV-880, open loop, in this approach-and-landing condition displayed a poorly damped 48-s phugoid mode.

The CV-880 autothrottles provided for its digital autopilot are based on an airspeed error signal with pitch and longitudinal acceleration for damping. Shown in Figure 7 is a simplified version of the autothrottle simulated for this study. A comparison of the corresponding

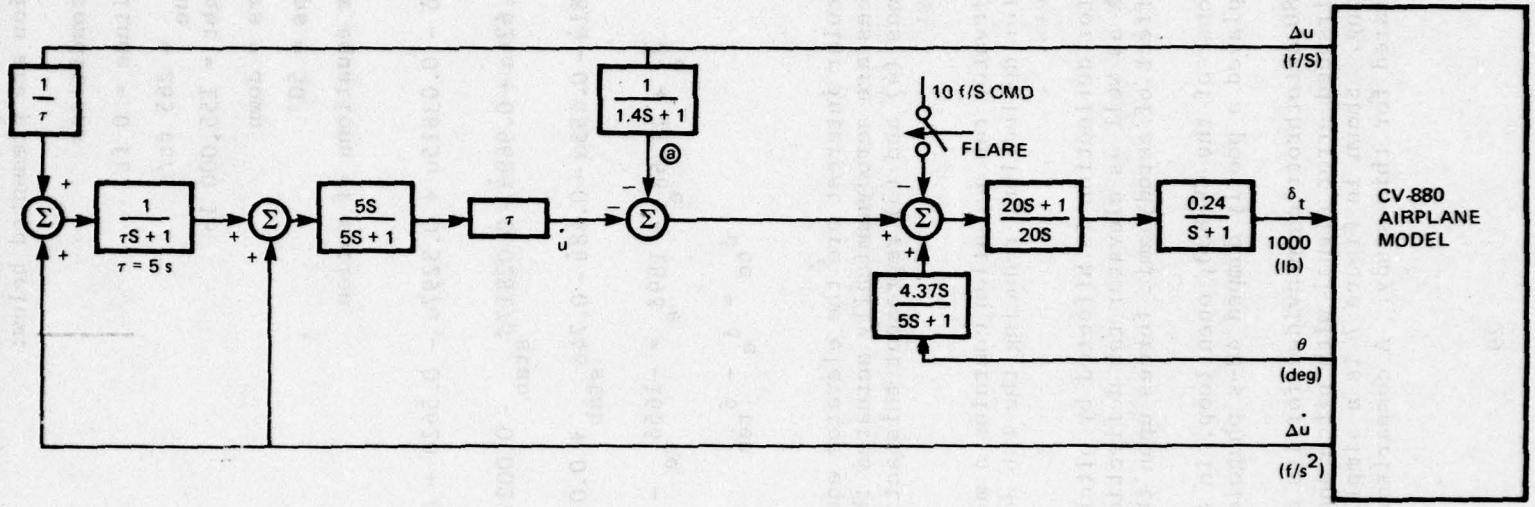

FIGURE 7 SIMPLIFIED AUTOTHROTTLE MODEL

responses of a model of the complete system and of the simplified version showed no significant differences. Frequency analysis of the simulated system showed stability margins satisfactory for a well-damped response and bandwidth satisfactory for an airspeed system.

The pitch loop accepts the autopilot pitch commands and moves the airplane elevators. Figure 8 shows the simplified model of this system used for this study; it is identical to the actual system except for some high bandpass filtering. With this loop and the autothrottles engaged, the phugoid mode was definitely suppressed. The conventional autopilot (A/P) put in its pitch command to this loop and the switch was down. The three systems for comparison put in a pitch rate command so the switch was up.

Figure 9 is a block diagram of the conventional system control law. From glideslope capture until 50 ft (radio altitude), glideslope deviation is controlled to zero. Below 50 ft, the flare programmer reconfigures the computation to command a -2 ft/s descent rate, at touchdown, in a smooth and transientless fashion. Prior to capture, the synchronizer cancels any command from the radio path. During the capture maneuver, the synchronizer smoothly fades in the radio path. Path damping is provided with vertical acceleration, derived vertical rate, and washed

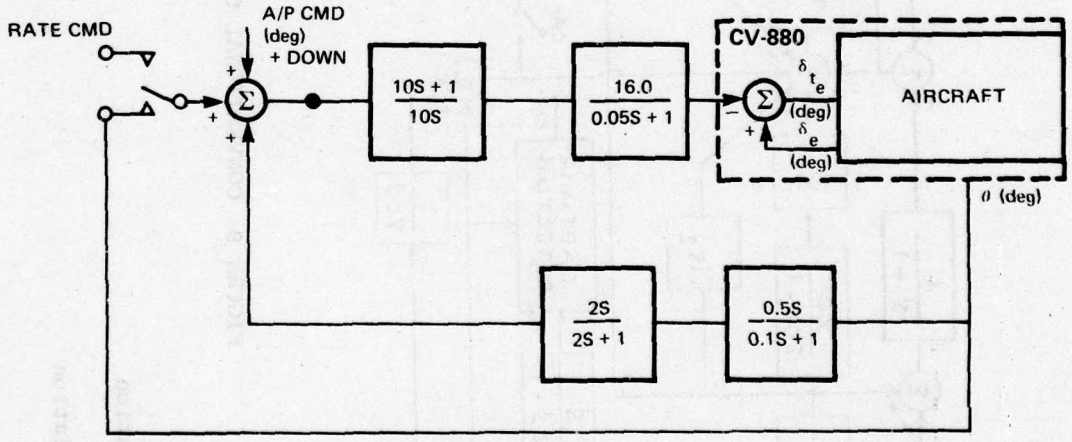

FIGURE 8 SIMPLIFIED CV-880 PITCH LOOP

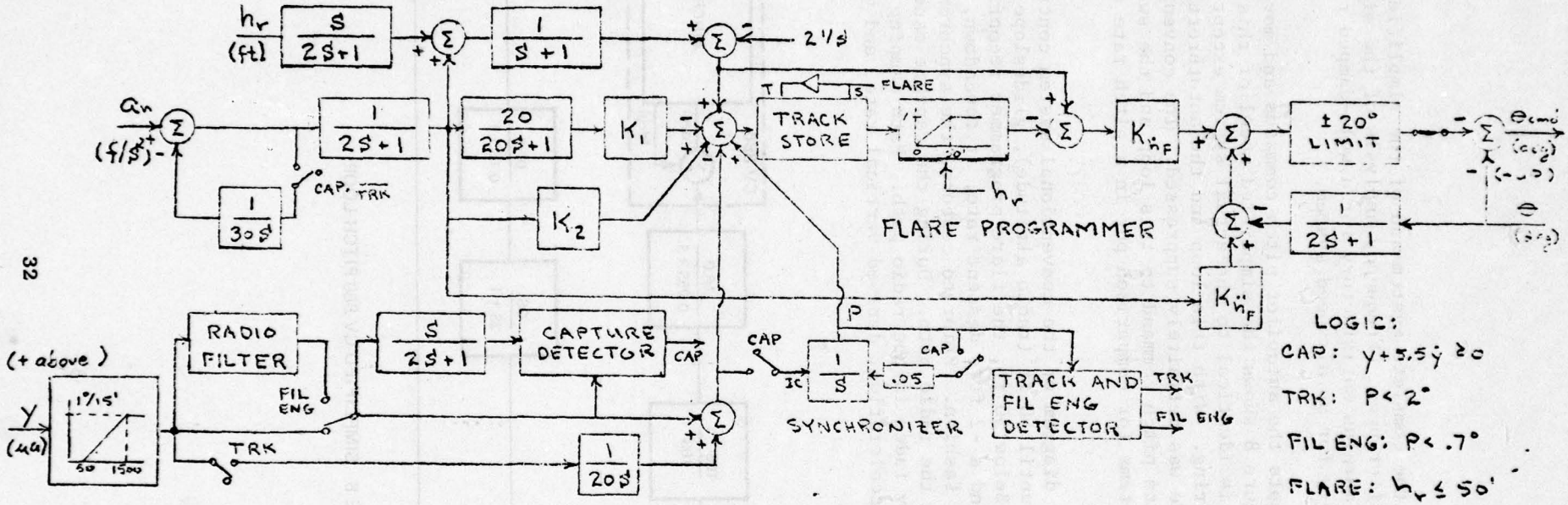

FIGURE 9 CONVENTIONAL CV880 CONTROL LAW

h_r = radio altitude

a_n = normal acceleration

y = glideslope deviation

θ = pitch angle

out pitch. A 2-s noise filter is placed on the normal accelerometer output to reduce steering needle and column activity. Since the summation of vertical rate and acceleration is proportional to pitch, in the short term, the lag introduced by the noise filter is offset with washed out pitch. The accelerometer data are washed out to remove biases and low-frequency errors. The washout is disengaged during capture to avoid a false charge on its output due to the capture maneuver. Beam standoffs are removed by the integrator in the radio path. To avoid charging the integrator to undesirable levels, it is not engaged until the capture maneuver is completed. The radio gain programmer is adjusted to give 1° of command per 15 ft of deviation (at the rate command output) below 1500 ft. The pitch limiter will command an absolute limit of 20° of pitch attitude.

Four conditions are detected and used to reconfigure the control law: capture, track, filter engage, and flare. Assuming the aircraft is on a course which will intercept the glideslope beam from below, the summation of radio deviation and deviation rate will become positive prior to the point of interception. The capture maneuver is initiated prior to interception and the trip point will be a function of closure rate. The synchronizer output decays to zero after glideslope capture. The time constant is greater than the beam closure rate, and the bias will therefore cause the airplane to pitch over prior to intersecting the glideslope.

The magnitude of synchronizer output is monitored to specify the track and filter engage conditions. The synchronizer output level is essentially a timer for the capture maneuver. The track condition engages the forward path integrator and reengages the accelerometer washout. A lower synchronizer output level specifies the filter engage condition. The final condition, flare, is set true when radio altitude is less than or equal to 50 ft. All of the logic levels above are latched when the appropriate conditions are met so that ambiguous situations are not encountered due to variations in input data.

Three different candidate autoland systems were implemented to study the performance capabilities of inertial complementation algorithms and inertially referenced data sources. Inertial platform data were employed in one system, while less expensive body-mounted accelerometers were employed in the others. Two of the systems included an inertial beam augmentation scheme to demonstrate the benefits this technique offers for reducing the effects of radio noise and beam anomalies. The salient features of the three systems were as follows:

- Platform System
  - Inertial platform data
  - Inertially referenced path damping
  - Inertially complemented radio filtering

- Accelerometer System
  - Conventional sensor data (body-mounted accelerometers)
  - Inertially referenced path damping
  - Pitch-complemented path damping filter
  - Inertially complemented radio filtering
- Unaugmented System (certified Category III system)
  - Conventional sensor data (body-mounted accelerometers)
  - Inertially referenced path damping
  - Pitch-complemented path damping filter

The platform and accelerometer systems provide a performance comparison between an inertial-platform-based system and a conventionally sensored system. The unaugmented and accelerometer systems provide a basis of comparison for the benefits of the radio complementation filter. Figure 10 is a functional diagram of the three different systems.

1. Unaugmented System

In Figure 10, the unaugmented system is engaged with switches S5, S6, and S7 in the A position. Prior to glideslope capture, the synchronizer cancels any command from the radio path. At glideslope capture, the synchronizer smoothly fades in commands from the radio path. The capture point is determined from a combination of radio deviation and deviation rate. The capture maneuver will therefore begin at a distance from the intercept point, which is a function of beam closure rate. This adaptive behavior allows a smooth capture to be performed under a wide range of atmospheric conditions. The synchronizer output decays to zero after glideslope capture. The decay rate is selected such that the aircraft will pitch down prior to intersecting the glideslope.

The path integrator (UA1) is not engaged until 8 s have elapsed following capture. At that time, switch S3 is thrown to the A position. The accelerometer washout circuit (UA11) is also bypassed during the capture maneuver. Both of those circuits would accumulate a false charge if engaged during acquisition. The accelerometer output is high-passed to remove long-term accelerometer errors. Similarly, the vertical rate deriver does not operate on long-term information and will therefore produce a displacement rate relative to the glideslope beam.

The control law remains in the tracking configuration to an altitude of 50 ft. During this period, vertical rate and acceleration are obtained from the accelerometer input and are the primary path damping and gust alleviation feedback signals. The acceleration signal has considerable high frequency content due to wind gusts perturbing the aircraft and is therefore filtered to avoid excessive control activity. The pitch complementation filter is added for short-period damping and stability.

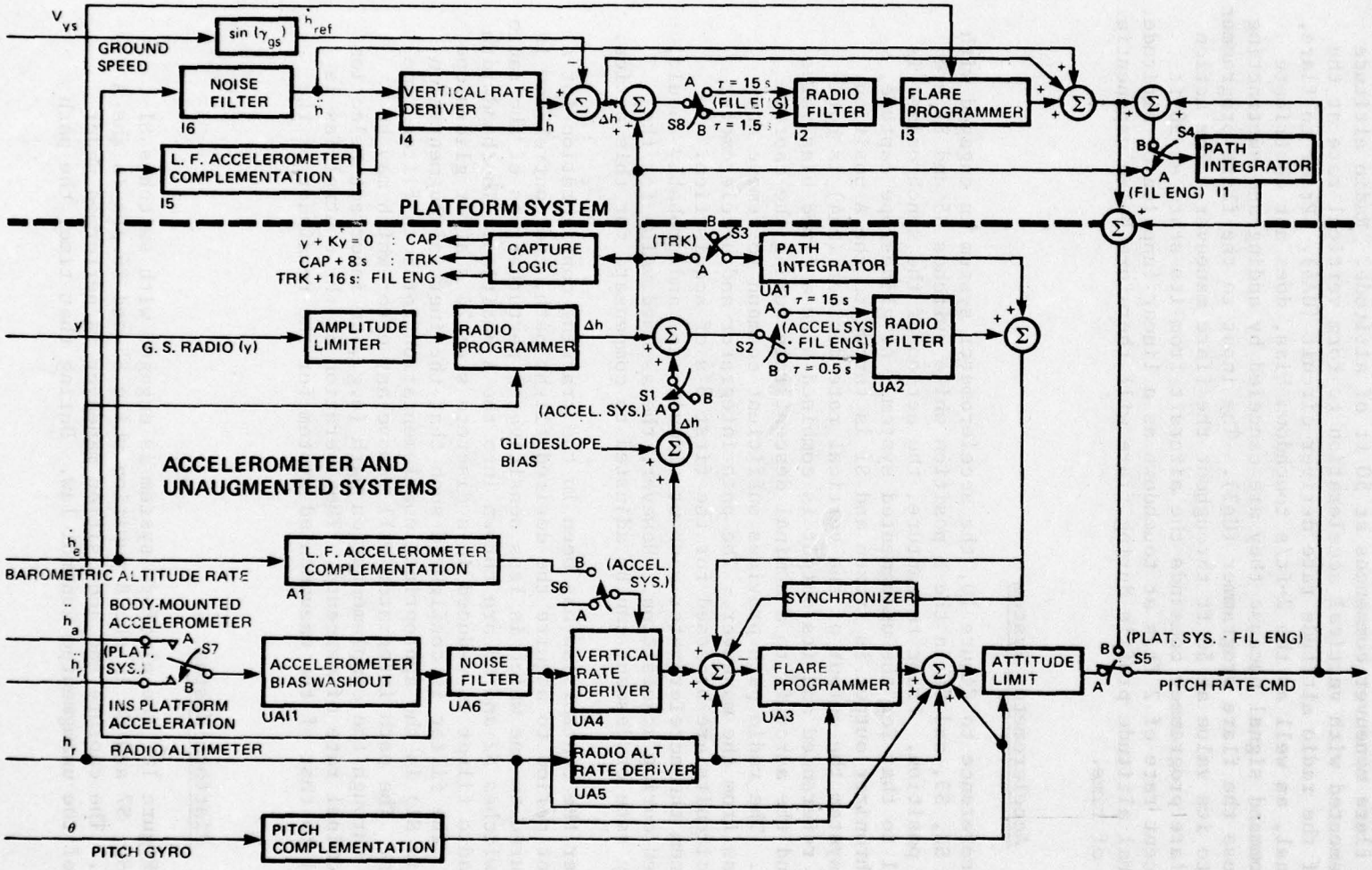

FIGURE 10 GLIDESLOPE CONTROL LAWS, FUNCTIONAL DIAGRAM

The flare maneuver commences at 50 ft of altitude. Radio altitude is complemented with vertical acceleration to form vertical rate at the output of the radio altitude rate deriver circuit (UA5). Prior to flare, that signal, as well as the 2-ft/s touchdown bias, does not contribute to the command signal because they are canceled by adding and subtracting them across the flare programmer (UA3). The input to the flare programmer is held to its value at 50 ft throughout the flare maneuver. The action of the flare programmer commands the aircraft from its state at 50 ft to a descent rate of 2 ft/s at touchdown as a linear function of altitude. The nominal altitude profile during flare will therefore be an exponential function of time.

2. Accelerometer System

In reference to Figure 10, the accelerometer system is engaged with switches S2, S3, and S6 in the B position while switches S5 and S7 are in the A position. Prior to capture, the action of the synchronizer is identical to that for the unaugmented system. At glideslope capture, the synchronizer output is frozen and S1 is thrown to the A position. In this system the output of the vertical rate deriver (UA4) is horizontally referenced and its output is combined with a fixed bias value to command the aircraft to a nominal descent rate during the capture maneuver. The radio path provides sufficient command to remove any abruptness from the maneuver. The path integrator and accelerometer washout circuits are bypassed for the first 8 s of acquisition. In this system the accelerometer washout circuit can, and probably should, be engaged during acquisition. However, the assumed value for the reference rate of descent can be adjusted to compensate for this action.

After the control law has been in the tracking configuration for a sufficient period to acquire the desired flight path, the control law is reconfigured to one which is less sensitive to perturbations of the radio beam. Switches S2 and S3 are thrown into the A position. The bandwidth of the radio filter is reduced in a discrete step 24 s after glideslope capture. The filter is configured such that the inertial augmentation input (via S1) is the appropriate complementation for both filter time constants. The path integrator will remove any error which may be injected through the complementation path (e.g., an incorrect selection of the nominal rate of descent). The operation of the control law is identical to that of the unaugmented system for the remainder of the landing.

3. Platform System

In Figure 10, the platform system is engaged with switches S1 through S4, S7 and S8 in the B position while S5 and S6 are in the A position. The capture and acquisition maneuver is performed under control of the unaugmented control law. During that time, the path

integrator (I1) time constant is set to an extremely fast value. This allows it to be used to equalize the command signals on both arms of switch S5. Control is transferred to the platform system 24 s after glideslope capture by switching S5 to the B position and S4 to the A position. At the same time, the radio filter (I2) is transferred to the low bandwidth position (S8-A) and the forward integrator time constant is reduced to its normal value. A smoother transition than in the case of the accelerometer system is attained as a result of using the path integrator as a synchronizer. Biasing errors, which at some point must be removed by the path integrator, will have been removed while the integrator was operating as a synchronizer.

The major differences in the platform and accelerometer systems during glideslope tracking were the use of inertial platform data (acceleration and groundspeed) and the absence of pitch complementation. The bandwidth of the accelerometer noise filter must be considerably wider than that in the other systems in order to maintain adequate stability margins. Groundspeed was employed to establish the nominal rate of descent in contrast to the fixed bias of the accelerometer system. This modification would be of greater benefit if the estimate of the reference vertical rate were used as a control parameter prior to switching the radio filter time constant.

As in the other systems, flare commences at 50 ft of altitude. The input to the flare programmer (I3) is not latched to its value at 50 ft; however, the programmer gain is linearly reduced to a near zero value at touchdown. As a consequence, the programmer operates in a similar manner to that of the accelerometer and uncomplemented systems (UA3). More significantly, the aircraft is commanded to a zero rate of descent at touchdown causing it to have a tendency to float along the runway if the radio filter path does not provide sufficient command to force a touchdown.

4. Performance

Each system was subjected to the four FAA-supplied windshears shown in Appendix A. These included logarithmic (neutral boundary layer), nighttime stable boundary layer, frontal, and thunderstorm cold air outflow shear profiles. All three candidate systems were capable of maintaining good glideslope tracking after acquisition and the aircraft state at 500 ft is well controlled. The accelerometer and unaugmented systems completed the autoland without difficulty. The touchdown was extended only 300 ft past the nominal as a result of the shear, well within accepted dispersion limits. The platform system also appeared to have good control of the flare maneuver. There was comparable performance for the three candidate systems in the presence of the nighttime boundary-layer shear and the frontal windshear. All three exhibited adequate tracking throughout the landing.

The most challenging wind profile was the thunderstorm. In it, the conventional control law was not capable of maintaining control of the aircraft. Less than one mile from the runway threshold a peak descent rate of 43 ft/s was observed. The system was not able to regain control and the aircraft contacted the ground 1/2 mile in front of the runway threshold at a descent rate of 21 ft/s. Peak deviations off the glidepath of 60 ft at 1.1 nmi and 55 ft at 2.4 nmi were also observed. In contrast, maximum deviations of 10, 30, and 20 ft were observed for the platform, accelerometer, and unaugmented systems. Descent rate was held below 15 ft/s and path deviation was within 10 ft of the glideslope beam at flare altitude. Acceptable landings were completed by all three of these systems.

Vertical gusts were simulated with 0.113-second-correlated white noise having a 3σ value of 4.5 knots. Figure 11 shows typical time traces of the conventional and the three candidate systems. They demonstrate the superior gust alleviation qualities of systems using inertial sensors, either body-mounted or platform, over a conventional control. Much improved control of vertical rate was obtained through the use of inertial sensors. Improved performance in vertical turbulence was achieved by implementing the pitch-complemented filter in the acceleration channel. The accelerometer and unaugmented systems show a reduction in elevator activity of nearly 2 to 1 over the platform system. The vertical rate traces show a corresponding reduction in excursions.

Longitudinal gusts were simulated with 2.26-second-correlated white noise having a 3σ value of 14.5 ft/s. The accelerometer and unaugmented systems were found to have significantly reduced elevator activity as a result of the pitch complementation. Longitudinal turbulence has the greatest impact upon the motion of the aircraft along the glidepath and improved throttle control was clearly indicated. The platform and accelerometer systems exhibited marginal glideslope tracking performance and further refinement of the radio augmentation filter was therefore indicated for both of these systems. The inertially referenced systems were shown to be a vast improvement over the conventional pitch control in turbulence. Comparable performance for the accelerometer and inertial platform-based systems also established the body-mounted accelerometer as a viable inertial sensor.

A noise model of 4-second-correlated 15 μA (3σ) white noise was employed to compare system performance in the presence of beam noise. The unaugmented system exhibited tighter tracking performance at the expense of considerably increased pitch activity on the 300 to 50 ft altitude interval (3σ). Figure 12 is a plot of the 3σ values for pitch at discrete altitudes, illustrating increased control activity for the unaugmented system. The accelerometer and platform systems had significantly reduced elevator activity as a result of the radio augmentation filter. Peak-to-peak elevator dispersions are reduced nearly 5 to 1 over the unaugmented system, while the data indicated comparable tracking performance by all three systems above 300 ft. The data indicated the unaugmented system has superior capabilities below 300 ft in the presence of beam noise.

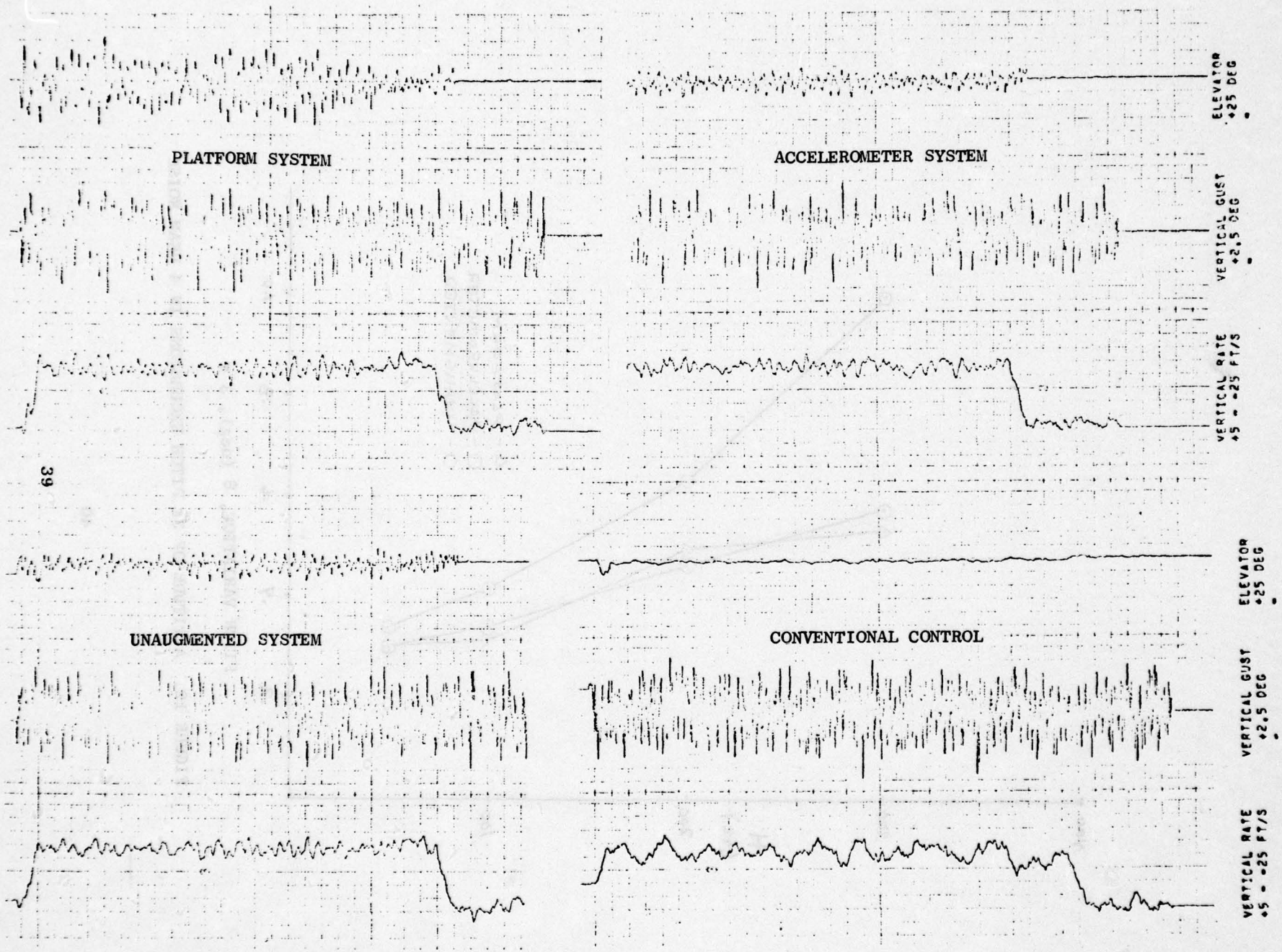

FIGURE 11. COMPARISON OF SYSTEMS WITH VERTICAL GUSTS

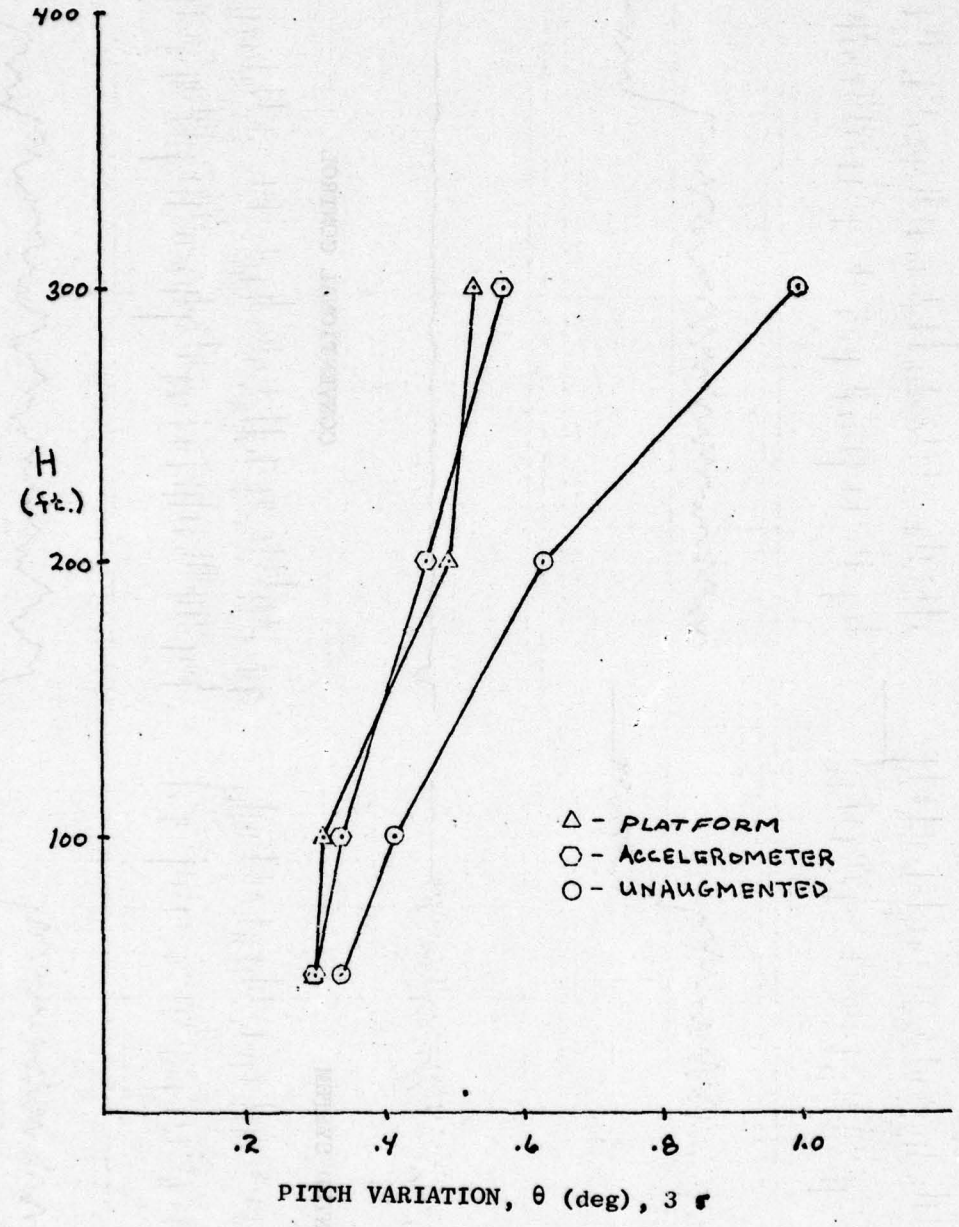

FIGURE 12. ALTITUDE OF 3σ PITCH EXCURSIONS IN 4 BEAM NOISE

Two types of beam anomalies were simulated in this study. A reasonable representation of what is commonly referred to as a bend in the glideslope beam was simulated with 10-second-correlated white noise of 30 μA (3σ) intensity. To simulate system response to phenomena such as beam outages and flyovers, a saturation of the radio input for a varying duration (1-8 s) was applied to each system at an altitude of 200 ft.

All candidate systems were found to have comparable tracking capabilities in the presence of the 10-second-correlated beam noise. The unaugmented system had slightly superior tracking qualities (and correspondingly greater pitch activity) below 300 ft. Elevator activity was greatly reduced by the beam augmentation filters employed in the accelerometer and platform systems. A suppression of the high-frequency content in pitch activity was also evident in those systems. Comparison of the glidepath dispersion for 4- and 10-second-correlated beam noise also indicated the augmented systems were much less sensitive to both the amplitude and frequency content of beam noise.

Figure 13 illustrates system performance in the presence of beam outages of varying durations. The radio augmentation filters in both the platform and accelerometer systems provided substantial improvement in performance over the unaugmented system. Peak-to-peak variations in pitch attitude of 7 to 9° were measured for the unaugmented system. The accelerometer and platform systems exhibited less than 6° of pitch variation which is within 1° of the normal variation caused by the flare manuever. Maximum perturbations off the flight patch, established prior to the outage, ranged from 11 to 60 ft for the unaugmented system and 6 to 28 ft for the platform and accelerometer systems. Peak-to-peak variations in g forces of 0.27 to 0.65 g for the unaugmented system, and 0.13 to 0.18 for the accelerometer and platform systems were measured.

Assuming the runway threshold is roughly 1100 ft from the glideslope antenna, the unaugmented system did not reach the runway for outages exceeding 4 s in duration. Descent rates greater than 5 ft/s and positive accelerations above 0.25 g at touchdown, indicating hazardous impact levels, were experienced for outages exceeding 5 s. The accelerometer and platform systems were capable of successful landings in all cases.

The accelerometer and platform systems exhibited comparable performance in the presence of beam noise and hardovers. Both systems had significantly reduced control activity in beam noise and were far less sensitive to beam outages when compared to the unaugmented system.

Statistical distributions of various flight parameters were collected with the systems subjected to wind gusts and beam noise in conjunction with the logarithmic shear. Results from the three candidate systems are summarized in Table 1; the performance of the conventional control was not comparable.

In Table 1 the statistical data indicates acceptable performance in the presence of the logarithmic shear. Examination of the airspeed

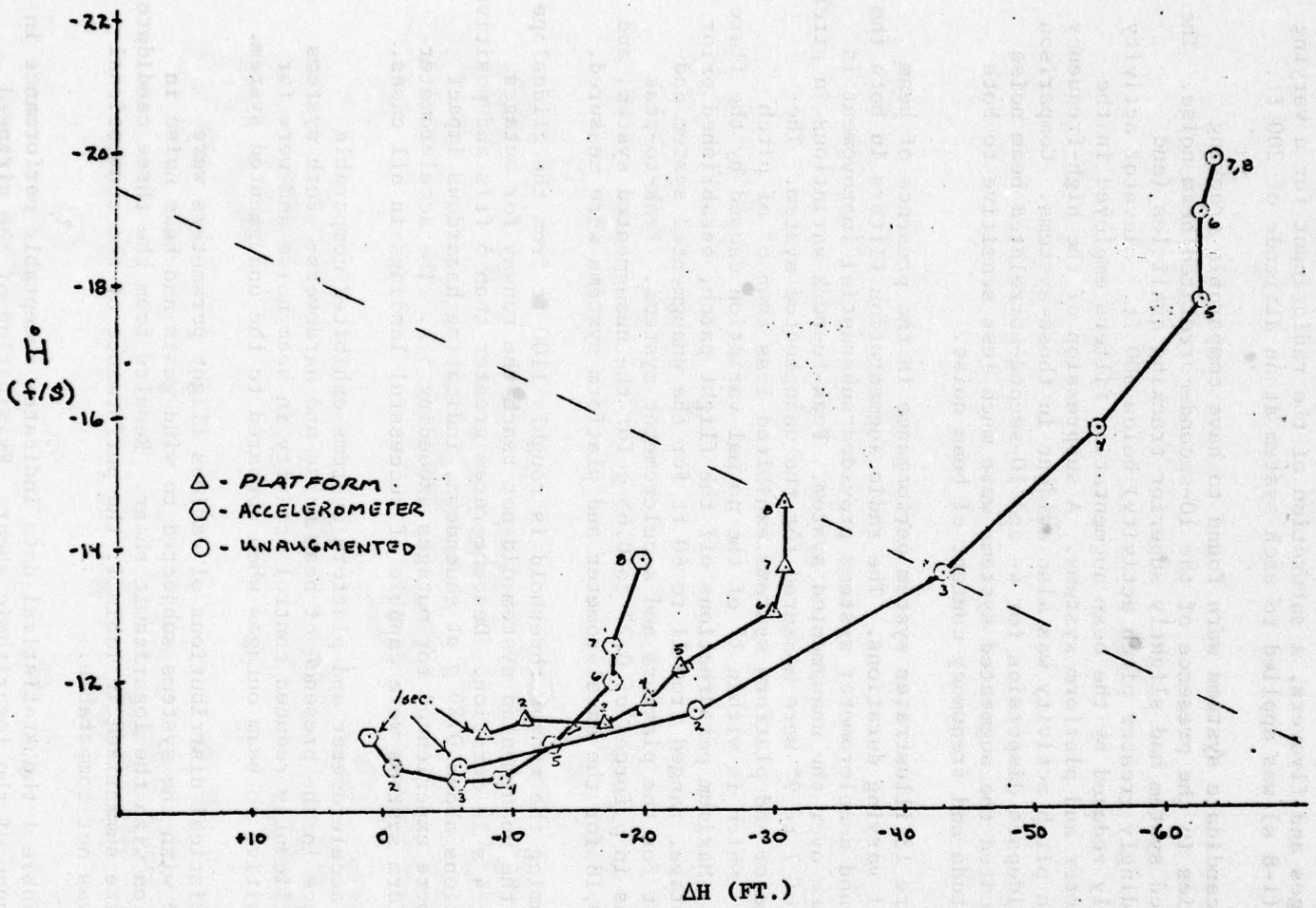

FIGURE 13. BEAM OUTAGE DATA: VERTICAL RATE VS PATH DEVIATION AT 50FT

Table 1

LONGITUDINAL STATISTICAL DATA

Parameter	Alt (ft)	System	DISTURBANCE													
			Longitudinal Gusts		Longitudinal Gusts + shear		Vertical Gusts		Vertical Gusts + shear		Longitudinal + Vertical Gusts		Beam Noise (4 sec)		Beam Noise (10 sec)	
			3σ	m	3σ	m	3σ	m	3σ	m	3σ	m	3σ	m	3σ	m
Distance, ft	0	UNAUG	700	610	920	700	460	635	690	860	633	625	395	640	480	640
		ACCEL	860	610	1140	720	500	600	690	775	760	525	485	595	595	560
		PLTFM[a]	760	700	4370	3590	1116	550	3280	3000	836	590	580	380	510	365
Airspeed, f/s	0	UNAUG	17	255	25.8	253	1.9	254	5.9	250	14.5	256	---	---	---	---
		ACCEL	17	255	24.5	253	1.9	254	5.9	250	15.7	255	---	---	---	---
		PLTFM[a]	20.7	255	25.5	255	2.6	255	2.6	251	18.4	255	---	---	---	---
Descent rate, f/s	0	UNAUG	3.0	2.5	3.2	2.4	2.6	2.5	2.7	2.2	3.7	2.7	.51	2.5	.55	2.5
		ACCEL	3.0	2.5	3.2	2.4	2.6	2.4	2.6	2.2	3.8	2.7	.48	2.5	.48	2.5
		PLTFM	4.85	2.3	3.5	2.1	4.3	2.1	4.6	1.7	6.7	2.1	3.9	2.8	4.8	3.0
Pitch, deg	0	UNAUG	1.43	2.36	1.83	2.5	1.03	2.38	1.3	2.48	1.52	2.6	.5	2.35	.32	2.36
		ACCEL	1.47	2.36	1.85	2.53	1.05	2.38	1.2	2.53	1.58	2.6	.47	2.37	.31	2.38
		PLTFM	1.83	2.36	1.9	2.43	1.55	2.33	1.6	2.4	2.85	2.35	.533	2.37	.75	2.33
Deviation, ft	50	UNAUG	9.3	3.2	10.	2.4	4.2	5.2	3.8	1.5	10.7	3.5	5.6	2.7	11	3.0
		ACCEL	15.2	-3.2	15.3	-5.4	9.1	-2.2	9.9	-5.1	18.	-.2	10.	-5.	13.5	-3.5
		PLTFM	15.6	1.6	13.1	-.1	10.7	1.8	10.4	-1.2	17.	5.6	10.2	-1.	15	1.5
Descent rate, f/s	50	UNAUG	3.3	11.7	3.8	9.3	2.2	11.6	2.3	9.	4.3	11.9	1.3	11.7	2.1	11.7
		ACCEL	3.7	11.9	3.8	9.1	2.3	11.8	2.3	8.9	4.5	11.9	1.1	11.8	1.9	11.7
		PLTFM	3.3	11.8	3.0	9.1	2.5	11.7	2.7	9	4.1	11.9	.9	11.7	1.4	11.7
Deviation, ft	100	UNAUG	8.6	3.2	10.	2.3	4.3	3.8	4.3	2.	11.1	3.7	6.8	2.3	13.5	2.5
		ACCEL	14.6	-2.8	15.8	-4.6	8.6	-2.5	8.5	-4.8	17.4	-.7	10.2	-5.	15.8	-3.8
		PLTFM	14.5	1.5	13.7	.2	10.8	1.6	9.7	-1.1	17.4	5.	10.2	-2.	16.5	1.5
Deviation, ft	300	UNAUG	8.5	2.6	10.6	2.2	4.5	3.5	3.8	1.8	10.4	3.2	13.2	1.3	26.1	1.9
		ACCEL	15.	-4.	15.5	-4.1	9.9	-3.5	9.5	-4.4	17.9	-2.4	14.2	-7.8	26.2	2.5
		PLTFM	14.7	.3	13.	.7	11.5	.2	11.2	-.6	17.4	5.2	14.4	-4.7	26.4	-5.5
Airspeed, f/s	50-300	UNAUG	8	11.3	9	6	.27	.19	.57	-3.2	10.5	11.8	---	---	---	---
		ACCEL	8	11.3	9	6	.27	.19	.57	-3.2	10.5	11.8	---	---	---	---
$P(U - U_o) > X$		PLTFM	8	11.3	9	6	.3	21	.57	-3.2	10.5	11.8	---	---	---	---
Pitch[2], deg	50-300	UNAUG	.975	1.05	.975	.675	.5	.67	.45	.39	1.1	1.25	.45	.51	.525	.625
		ACCEL	.975	1.05	.975	.675	.525	.64	.45	.4	1.1	1.25	.275	.35	.525	.45
$P(\theta - \theta_o) > X$		PLTFM	.975	1.28	.9	.875	.725	1.37	.59	.9	1.0	1.675	.25	.32	.75	.38

[a] Minimum Dispersion

[b] Nominal Value of 2.5° and 1.5° (shear) has been subtracted

Shear = logarithmic wind profile

m = mean

traces indicated an increase in the last stage of the flare. This reaction to the airspeed loss in the shear caused lift to be increased and the aircraft had a lower rate of descent than normal. The length of time spent close to the ground is therefore increased and the touchdown parameters were more sensitive to turbulence than in the no-shear case. For most parameters, only small (less than 10%) increases in dispersions were experienced. In longitudinal turbulence, the 3σ values of distance, airspeed, and pitch attitude at touchdown increased 50% for the accelerometer and unaugmented systems as a result of the shear. In the presence of vertical gusts, touchdown dispersion increased 40 and 50% for the accelerometer and unaugmented systems, respectively, while pitch attitude dispersions increased 14 and 26%. Dispersion data along the glidepath did not appear to be greatly effected by the shear for any of the systems. However, augmentation of the radio with either body-mounted accelerometer on inertial platform data apparently yielded a less perturbable inertial path. The accelerometer system was least effected and all dispersion values remained within 10% of their values in a normal environment. The use of groundspeed for dynamical computation of the nominal rate of descent may account for the slightly improved performance. The unaugmented system exhibited a tendency to have increased dispersions when subjected to the shear at touchdown and along the glidepath.

In general the unaugmented system (Table 1) showed better glidepath tracking and smaller touchdown dispersions. These indicated a need for an improved flare law and more careful initialization of the filters in the inertially augmented controls. Overall, and particularly in comparison with the conventional control, significant performance improvements in turbulence and windshear were demonstrated through the addition of inertially referenced sensors. In addition, these sensors allowed control law configurations which were less susceptible to the quality of the radio beam. The performance capabilities of a conventionally sensored (body-mounted accelerometers) system were comparable to those of a system equipped with an INS platform. Consequently, the improvements in performance can be attained in an economically attractive manner.

B. Lateral Axis Control

The model for CV-880 lateral motion in the selected approach-and-landing flight condition is shown below:

- Test conditions
  - Altitude = 0 ft
  - V_{true} = 265 ft/s
  - Weight = 155K lb
  - Gear = down
  - Flaps 50°

- Linear motion equations, lateral axis

$$\ddot{\phi} + 1.109\dot{\phi} + 3.054\beta + 0.1275\ddot{\psi} - 0.8086\dot{\psi} = -0.4192\delta_a + 0.2989\delta_r + 1.012\delta_{sp} - 0.0614\delta_{t_a} \quad (6)$$

$$\dot{\beta} + 0.1330\beta - 0.1215\phi + 0.9887\dot{\psi} = 0.02863\delta_r - 0.01022\delta_{sp} + 0.0059\delta_{t_r} \quad (7)$$

$$\ddot{\psi} + 0.2347\dot{\psi} + 0.04675\ddot{\phi} + 0.08115\dot{\phi} - 0.6943\beta = 0.08837\delta_a - 0.4594\delta_r + 0.1224\delta_{sp} - 0.087\delta_{t_r} \quad (8)$$

$$\ddot{\delta}_a + 8.534\dot{\delta}_a + 212.3\delta_a + 6.575\dot{\phi} + 4.897\beta = -87.09\delta_{t_{a_c}} \quad (9)$$

$$\ddot{\delta}_r + 23.53\dot{\delta}_r + 124.8\delta_r - 42.79\beta + 1.0\ddot{\psi} + 7.659\dot{\psi} = -148\delta_{t_r} \quad (10)$$

$$\dot{\delta}_{sp} + 10\delta_{sp} = 2.72\delta_{t_a} \quad (11)$$

$$\delta_{t_r} - \delta_r = \delta_{t_{r_c}} \quad (12)$$

Of particular interest are the aileron and rudder equations. The CV-880 control surfaces are aerodynamically actuated through control surface tabs. Equations (9), (10), (11), and (12) represent this activation. Several things are noteworthy:

- The spoilers are geared to the aileron tab actuation.
- The rudder tab actuation contains a mechanical feedback from rudder deflection, reducing the tab deflection as the rudder deflects.
- Aileron deflection is affected by roll and sideslip, as well as aileron tab deflection. Rudder deflection is affected by sideslip and yaw rate as well as rudder tab deflection. These terms model the effect of aerodynamic forces upon the surfaces.

The time response of the CV-880 displayed, in particular, a 0.171-Hz (1.07 rad/s) Dutch roll mode.

The yaw damper suppresses the Dutch roll mode without affecting the heading control performance of the aircraft. To accomplish this, a bandpass feedback was provided in the region of 1 rad/s. The yaw damper provided a sufficient loop gain, therefore, in the frequency range of the Dutch roll mode to damp it. Figure 14 presents the block diagram of the yaw damper. The 0.2-s lowpass provided rejection of the noise well above the Dutch roll frequencies. The 4-s washout attenuated the low-frequency feedback, allowing heading control of the aircraft. The 0.006-s filter was added to further reject high frequency noise. The 20-rad/s servo model was representative of the servo used on the CV-880.

The roll loop is also shown in Figure 14. The frequency response with the roll loop broken at the servo and with the yaw damper coupled to the aircraft exhibited very good stability margins. The bandwidth (approximately the crossover frequency) was known from past experience to be adequate to support outer loop autoland control laws.

Figure 15 shows a block diagram of the localizer capture control law used in this study. The path damping was provided by mixing high-passed direct radio (radio rate) with partially washed-out course datum. This mix was less susceptible to crosswind standoff than the more common configuration that uses only course datum with a slow high-pass filter. A "pretrack" mode was provided after the initial phase of capture during which the remaining course datum was washed out with the addition of a 30-s washout. This completely eliminated beam offsets due to crosswinds. The gain programmer was used to maintain the radio loop gain to effect more optimum captures.

The capture law was utilized to provide a smooth transition from the original intercept heading onto the localizer centerline. To effect this transition, the aircraft must be in a linear region of the localizer beam, and the capture law must be commanding a roll away from the beam when the capture laws are engaged. The capture logic designed to assure these initial conditions was adaptive in that any factor which caused a difference in beam rate, such as aircraft speed or course cut, caused a proportional change in capture trip point. The pretrack phase, which washed out the remainder of course datum, was initiated when capture roll command was less than $|3.5|$ degrees. After pretrack, 45 s was allowed for the capture laws to stabilize the aircraft on the beam before the track law was engaged.

As was done with the longitudinal controls, three different candidate localizer-track control systems, each representing an advance over conventional control, were simulated and tested. The three candidates compared were:

- Unaugmented system (certified Category III)
- Inertial platform system, based on a full INS
- Accelerometer system, using body-mounted sensors

The conventional control was not included in this lateral study.

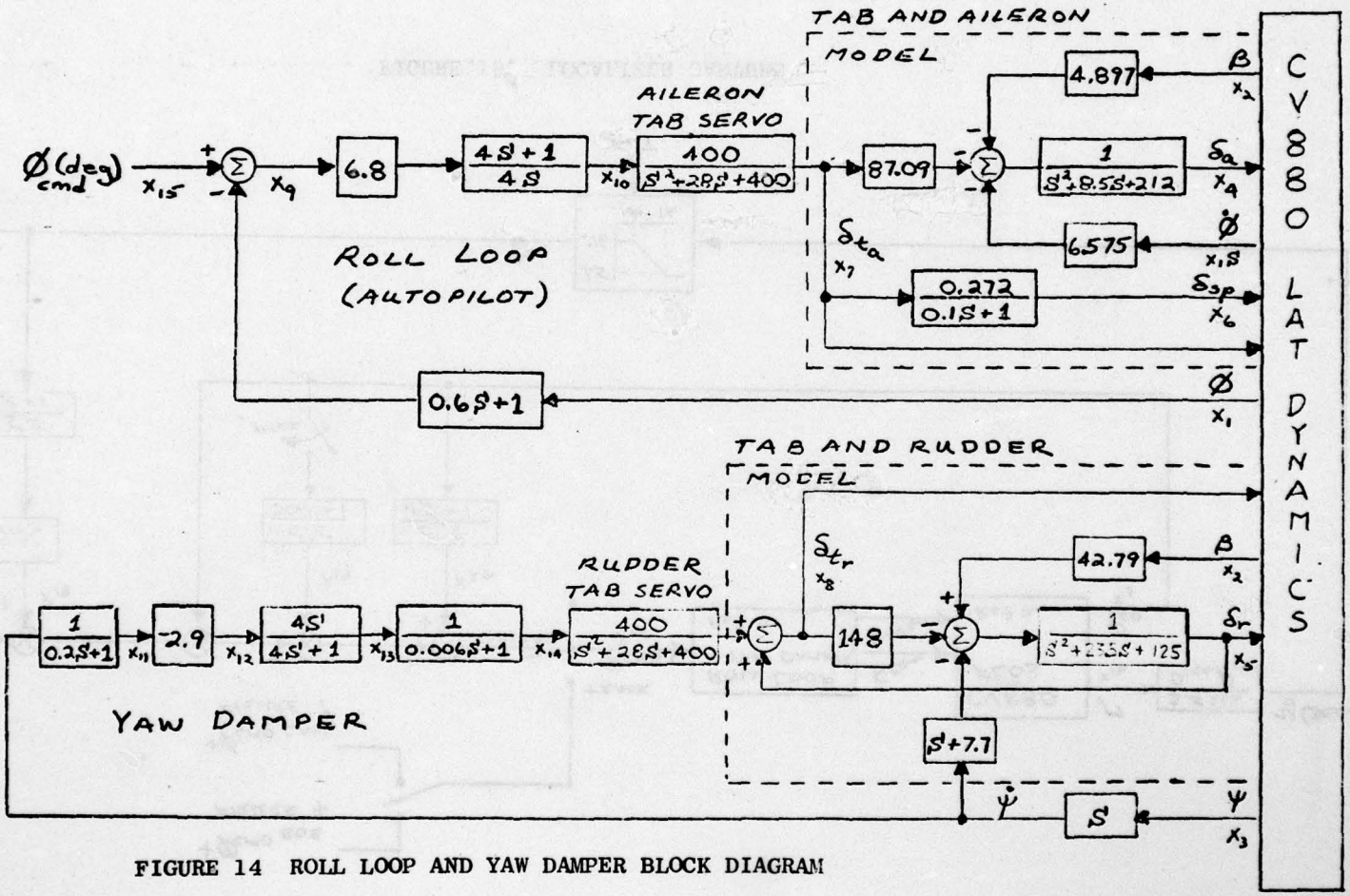

FIGURE 14 ROLL LOOP AND YAW DAMPER BLOCK DIAGRAM

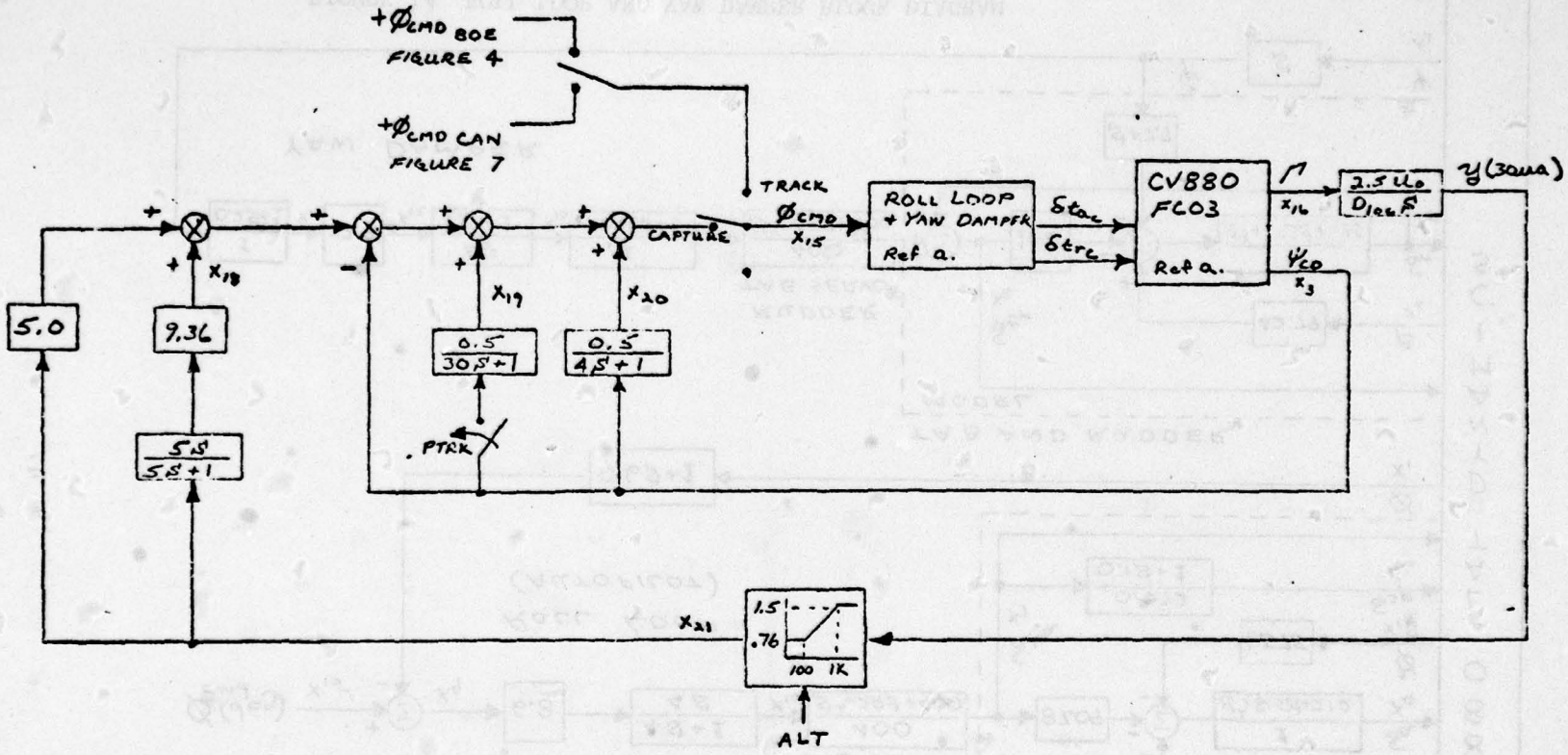

FIGURE 15. LOCALIZER CARTURE

1. Unaugmented Localizer System

Figure 16 presents the block diagram of the unaugmented comparison system. A 1-s filter was included on the localizer ahead of the gain programmer. The position feed was direct and contained no smoothing. A 30-s path integrator was provided to reduce localizer standoff due to roll mistrim. The rate damping term was derived from a 20-s single-order complementation of localizer deviation and lateral acceleration. The basic "weathercocking" effect of the airplane, the absence of heading in the track algorithm, and the relatively high rate gain allowed by using a rate estimator provided good windshear response. The use of a complementary filter on radio rate provided smooth rate information in the presence of beam noise; however, the unsmoothed position (localizer deviation) term allowed considerable control activity. A wind alleviation feed was included, which used accelerometer information to fight wind gusts and roll mistrim.

2. Inertial Platform System

Figure 17 presents the platform system. This system used a 20-s filter on localizer deviation complemented with track angle error from an inertial platform to estimate position. Track angle error was proportional to crosstrack rate and was also used for damping in this law. The system included a path integrator to cancel localizer standoff and synchronize control modes. Programming on localizer deviation included normal gain reduction proportional to reducing altitude.

Since track-angle-error is a flight path variable and not a direct heading term, and since the position and rate gains are high, the windshear fighting capability of this system should be equivalent to or better than that of the unaugmented system. The 20-s complementary filter on localizer suppressed most of the control activity produced by beam noise. This allowed the forward gain to be set relatively high.

3. Accelerometer System

Figure 18 is the block diagram of the accelerometer-augmented localizer track law. This system used a second-order filter complemented with lateral acceleration from a body-mounted accelerometer to estimate position. The complementary filter also contained an estimate of lateral rate, which was used for path damping. A wind alleviation circuit was included using lateral acceleration to help combat wind gusts. This signal also contained roll information, which was used during forward slip or thrust misalignment. Again, the absence of any heading terms in this law indicated the system should track well in windshear. The high position gain which was necessary to assure good localizer track in windshear necessitated heavy localizer filtering. This increase in filtering resulted in higher gains on accelerometer information and an increase in standoff due to accelerometer bias. An integration of the

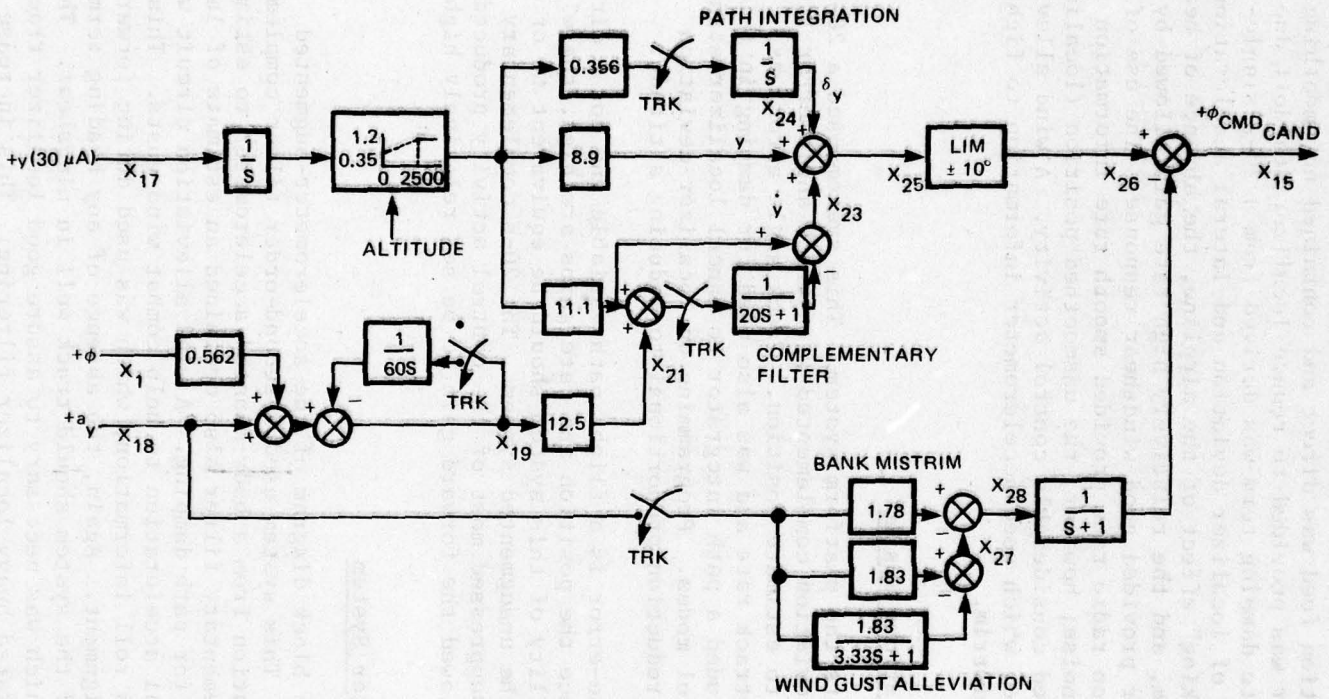

FIGURE 16 UNAUGMENTED SYSTEM LOCALIZER TRACK LAW

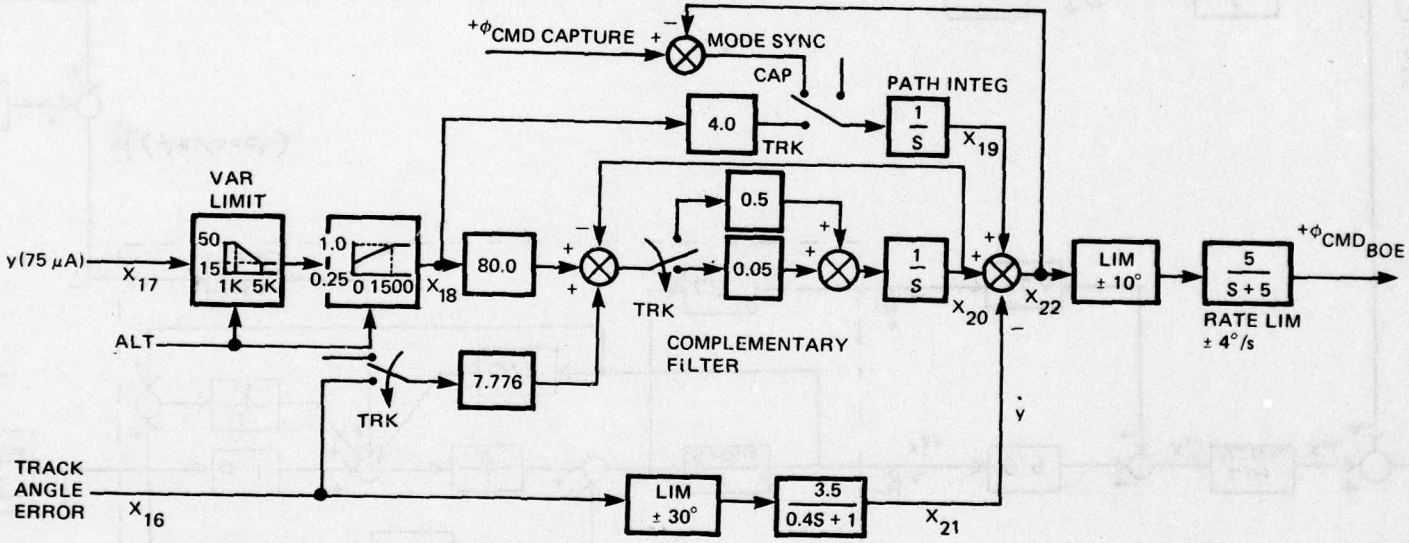

FIGURE 17 PLATFORM SYSTEM LOCALIZER TRACK LAW

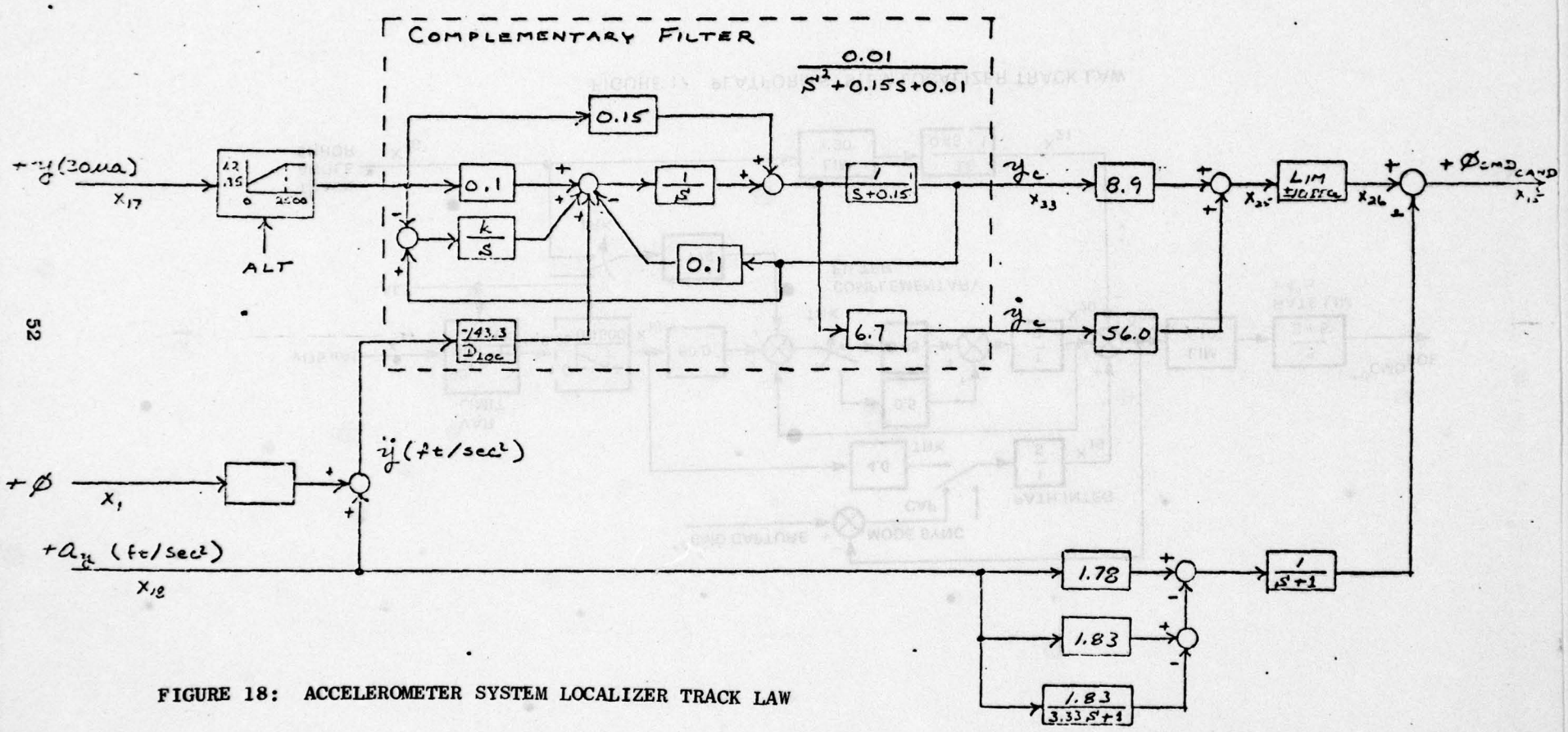

FIGURE 18: ACCELEROMETER SYSTEM LOCALIZER TRACK LAW

difference between localizer deviation and complemented position was used to decrease this standoff. However, this integration was destabilizing and it was desirable to keep the gain on this term low. The optimum design, then, was a compromise between desired beam filtering and accelerometer-bias-produced localizer standoff.

4. Performance

All approaches were run with initial intercept of 25° at a distance 10 nmi from localizer antenna. It was assumed the aircraft was tracking a 2.5° glideslope and no flare was simulated.

All the systems studies exhibited good immunity to lateral windshear. The most difficult profile, shear 2 (nighttime stable boundary layer), contained a large initial crosswind and a maximum shear rate of 17 knots/100 ft. Both the platform and accelerometer system flew this shear profile well. An aircraft center of gravity offset was caused by location of the localizer antenna on the vertical stabilizer. The distance from the aircraft center of gravity to the antenna was 68 ft. A crab angle of 11° should then produce an offset of 13 ft. As the crosswind decreased in shear, the aircraft should "weathercock" around the center of gravity. This moved the tail and localizer antenna off the center line, producing a localizer deviation. The platform and accelerometer systems responded to this deviation to bring it back to zero. Maximum localizer deviation for the platform system was approximately 3.0 μA and for the accelerometer system was 2.0 μA.

On shear 4 (thunderstorm cold-air outflow - Eastern 66/JFK) the magnitudes and shear rates specified for crosswind are very small (maximum 4.5° beta and 2.8 knots per 100 ft) and the aircraft response was negligible.

The resolution of shear 3 (frontal - Iberian 993/Logan) into the crosstrack direction resulted in a maximum shear rate of 12.8 knots per 100 ft. The maximum localizer deviations for the platform and accelerometer system were in the range of 2 to 3 μA.

Shear 1 (logarithmic profile) is comparatively stable down to an altitude of approximately 100 ft. Below this altitude, the shear rate increases drastically. We found no significant displacement of the aircraft center of gravity during the short period of severe shearing. Again, localizer deviation was a result of the aircraft weathercocking around its center of gravity.

Wind turbulence may cause major excursions in roll and heading. This effect was modelled by impressing on the sideslip angle of the CV-880 a 2.26-second-correlated random function of 2.1° (3σ) amplitude. The results indicated that the platform and accelerometer systems had comparable roll and heading response under this gust disturbance. Very small deviation in localizer deviation and linear position was noted.

The occurrence of turbulence is often accompanied by windshears. The response of the control systems under the combined disturbance of wind turbulence and the logarithmic profile windshear could loosely be compared to the sum of the wind turbulence alone and shear 1.

A more precise measure of the effect of gusts could be obtained by investigating the statistical dispersion of specific parameters of the systems under random turbulence. Table 2 presents the statistics for roll attitude at touchdown under the combined wind disturbances. It is extremely important that the probability of roll attitudes over 6° be very small due to the engine location on the CV-880 and the danger of scraping the outboard nacelles. We see that the 3σ magnitude of roll attitude for both the platform and accelerometer systems was 2.3°. The unaugmented system exhibited slightly less roll (3σ = 2.1°) but this was at the expense of considerably more lateral deviation. The 3σ magnitude of lateral deviation was 12.4 ft for the unaugmented system compared to 6.5 ft for the platform system and 4.9 ft for the accelerometer system. It is interesting to note the mean value of lateral deviation in these systems. The platform and accelerometer systems produced a mean lateral deviation of approximately 14 ft. This corresponded to the center of gravity offset due to crosswind crab. The unaugmented system was crossing through centerline on a small oscillation and exhibited a smaller deviation.

The accelerometer system would appear to perform adequately in wind gust and windshear; however, we need assurance that it will not respond unsafely in other disturbances. One of the limiting factors has been the response of a system to localizer noise. Since the desire is to fly AP/FD to altitudes less than 100 ft on Category I and II beams, we needed to prove that the maximum allowable beam bends for these facility categories did not cause unsafe excursions of the critical performance parameters. For worst-case Category II, the disturbance was a 15 μA (3σ) magnitude localizer noise with a 4-second-correlation time constant. As expected, the roll activity of the accelerometer system was less than that of the unaugmented system. From the statistical data obtained by inserting this same disturbance, we see the 3σ magnitudes of roll attitude at touchdown to be 1.5° for the platform system, 1.9° for the accelerometer system, and 2.9° for the unaugmented system. On localizer deviation, the three control laws provided equivalent performance. Lateral deviation at touchdown is a key parameter for noise response evaluation. Again the three systems seemed comparable in performance. Table 2 shows the platform system to have 3σ magnitude of 54 ft, the accelerometer system to have 63 ft, and the unaugmented system to have 61 ft.

If we extend our requirements to Category I beams, we will encounter beam disturbance of 30-μA (3σ) magnitude with a 10-s correlation time constant. At this disturbance level, the 3σ magnitude of lateral deviation was 175 ft for the unaugmented system, compared to approximately 120 ft for the platform and accelerometer systems. Roll dispersions also

Table 2

LATERAL STATISTICAL RESULTS

	Lateral Deviation (3σ)		Localizer Deviation (3σ)				Roll Attitude (3σ)	
	TD	50	TD	50	100	300	TD	50 ft
Localizer noise, 15 μA, 4 s								
Unaugmented	49 ft		26 μA				2.9°	3.1
Platform	43	46	22	23	22	21	1.5	1.6
Accelerometer	51	57	26	25	23	23	1.9	2.0
Localizer noise, 30 μA, 10 s								
Unaugmented	175 ft		78 μA				4.8°	
Platform	112	138	48	45	44	40	2.6	2.6
Accelerometer	125	144	54	48	47	49	3.6	3.4
Wind turbulence, 2.1° 2.26 s plus shear 1								
Unaugmented	12 ft		6.4 μA				2.1°	
Platform	6.5	6.6	4.2	3.6	3.0	2.0	2.3	2.4
Accelerometer	4.9	5.5	3.4	3.3	2.8	2.6	2.3	2.4

showed the effect of filtering the localizer signal. The unaugmented system had a 3σ roll amplitude of 4.8°, while the accelerometer system had 3.6° and the platform system had 2.6°.

Localizer hardover was simulated as a 300 μA, 6-s pulse on localizer deviation. For these runs, all rate limiters were removed and all systems were provided a 40-μA localizer deviation limit in the position feed. The unaugmented system responded to the hardover with an immediate roll limit command, producing high roll rates and causing an extreme flyoff rate. The return of localizer information produced another severe control command and a reverse roll. The servo command trace of the platform system showed no severe spiking, with a maximum excursion of 3°. The result was a considerably slower rollup and flyoff. The return of localizer produced a similarly slow roll response, allowing more flyoff to occur before the flight path could be corrected. The accelerometer system exhibited a filtered response to the hardover corners, but the combined effect of initial filtering and moderate response produced the best result. It would be necessary in a flightworthy system to provide more definitive protection against beam hardover, but the inherent immunity of the control systems to this type of disturbance was demonstrated.

The accelerometer system was shown to adequately control the aircraft in the presence of windshear and to operate in the presence of beam anomalies to allow the system to be flown below present minimum altitudes on beams of Category I levels. As presented, the system should not be considered flightworthy, but should provide a basic law around which a final product could be developed. More design effort would be needed in the areas of initialization, hardover protection, and unusual approach and attitude situations. The result of such an effort would be a flightworthy system of performance better than the present accelerometer system and equivalent to a platform-based system.

IV AUGMENTATION OF THE DC-10 FLIGHT CONTROL SYSTEM*

L. V. Miller, C. P. Shih, E. D. Skelley, D. A. Tiedeman

The CV-880 investigation showed that the inertial augmentation technique using body-mounted accelerometers held promise of improved performance. The next step was to study the application of the technique to other airplanes. The DC-10 model 10 had been selected for the piloted flight simulation tests in windshear being conducted under AWLS Task 2, and so Collins was tasked to design and analyze acceleration-augmented control algorithms for this aircraft. The flight condition was:

Gross weight = 350,000 lb

Flaps at 50°, gear down

Center of gravity at 20% of MAC

Approach speed = 142 knots (240 ft/s)

Runway at sea level, standard day

The approaches in the task 2 windshear simulation tests were being run with manual control supported by the flight director, simulating an ILS with 3° glideslope, so the Collins effort concentrated on the development of flight director control laws. In the process, however, both automatic and flight director control algorithms were designed and tested.

The first part of the study required that the phase 1 CV-880 autopilot algorithms be modified for flight director use. Once the algorithms were determined to provide good performance on the CV-880, the aircraft simulation was changed to a DC-10. An extensive set of simulator runs in both automatic and manual control modes showed that

---

*This section is a compilation of excerpts from the following Collins documents prepared on AWLS Task 5:

Miller, L. V. and Shih, C. P., "Final Report - Phase 2, GFC-41" (15 April 1977).

Skelley, E. D. and Shih, C. P., "Collins Development of an Integrated Fast/Slow Indicator and Modified Flight Director for Windshear, GFC-184" (26 January 1978).

Tiedeman, D. A., "Collins Development of a Modified Flight Director for Non-Precision Approaches, GFC-172" (31 January 1979).

the refined algorithms exhibited good stability and performance characteristics when used on the DC-10.

The primary technique for algorithm development was based on analysis using digitally generated time and frequency response data. Analog/hybrid computer simulation was used to demonstrate the performance, evaluate additional nonlinear characteristics, and present a more physical interpretation of the system performance. Use of digital analysis and analog simulation techniques was an iterative process. The gains and time constants of the algorithms were optimized to provide stiffness, bandwidth, and stability margins consistent with lateral and longitudinal track law performance requirements.

Linear, small-perturbation equations of a DC-10-10 aircraft were used, based on linearized aerodynamic data supplied by Douglas Aircraft Company. Pilot-in-the-loop simulations were performed using an air transport-type cab, which included a Collins 329B-9L Attitude Director Indicator with cross pointer commands. Vertical speed and barometric altitude were provided on peripheral instruments.

Runs were performed in both automatic and manual modes for each disturbance. Disturbances included four shear profiles, wind gusts, and glideslope radio noise (Appendix A). Runs were also performed with a combination of radio noise, gusts, and each of the four windshears.

Automatic pitch and roll inner loops were implemented to provide an objective basis for evaluation of the various systems and system modifications during the synthesis and analysis effort at Cedar Rapids. The automatic modes were also employed at Cedar Rapids to provide stripchart recordings with which to compare the verification runs at Long Beach for the checkout of the modified flight director and speed control system. Pilot models were not used extensively, but were employed to preclude any surprise results in the manual modes. Block diagrams of the longitudinal and lateral inner loops are presented in Figures 19 and 20, respectively.

A. Modified Flight Director (MFD)

1. Longitudinal Axis

The basic structure of the system chosen for control of the DC-10 in pitch corresponded to the "accelerometer system" of the CV-880 study. Neither glideslope capture nor flare were included, it being assumed that the simulated aircraft would start on glideslope in trim and that the pilot would flare to touchdown by visual reference.

Figure 21 shows a simplified block diagram of the glideslope track law that was developed. This law featured a complementary filter on glideslope deviation to increase beam filtering and an altitude rate inner loop to enhance windshear immunity.

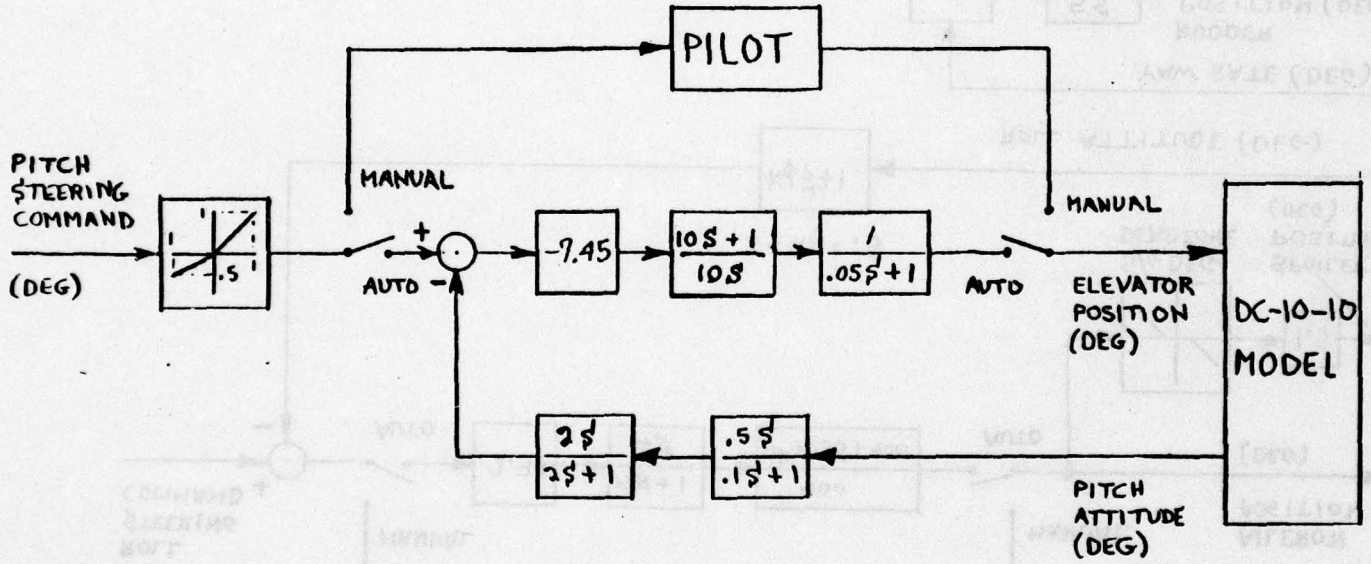

FIGURE 19 LONGITUDINAL INNER LOOP BLOCK DIAGRAM

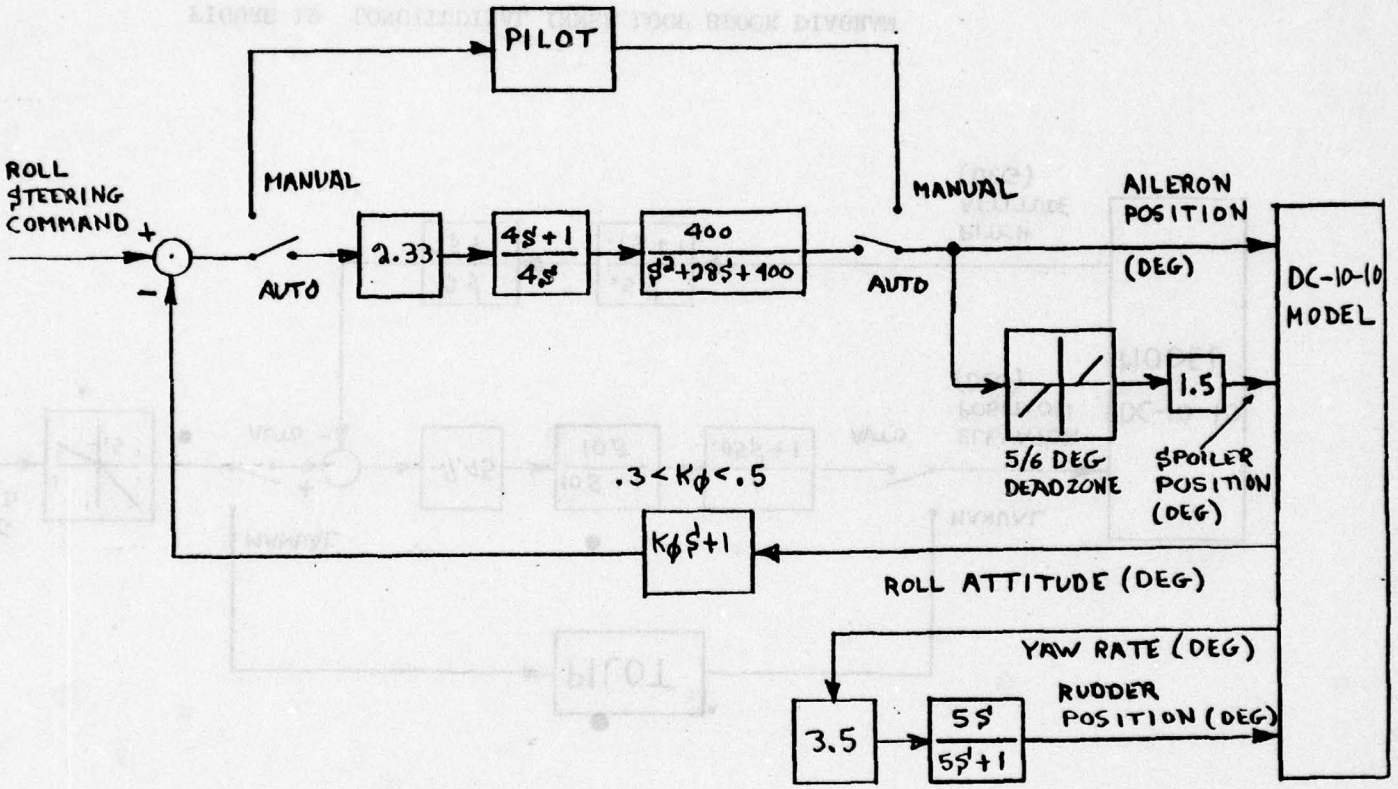

FIGURE 20 LATERAL INNER LOOP BLOCK DIAGRAM

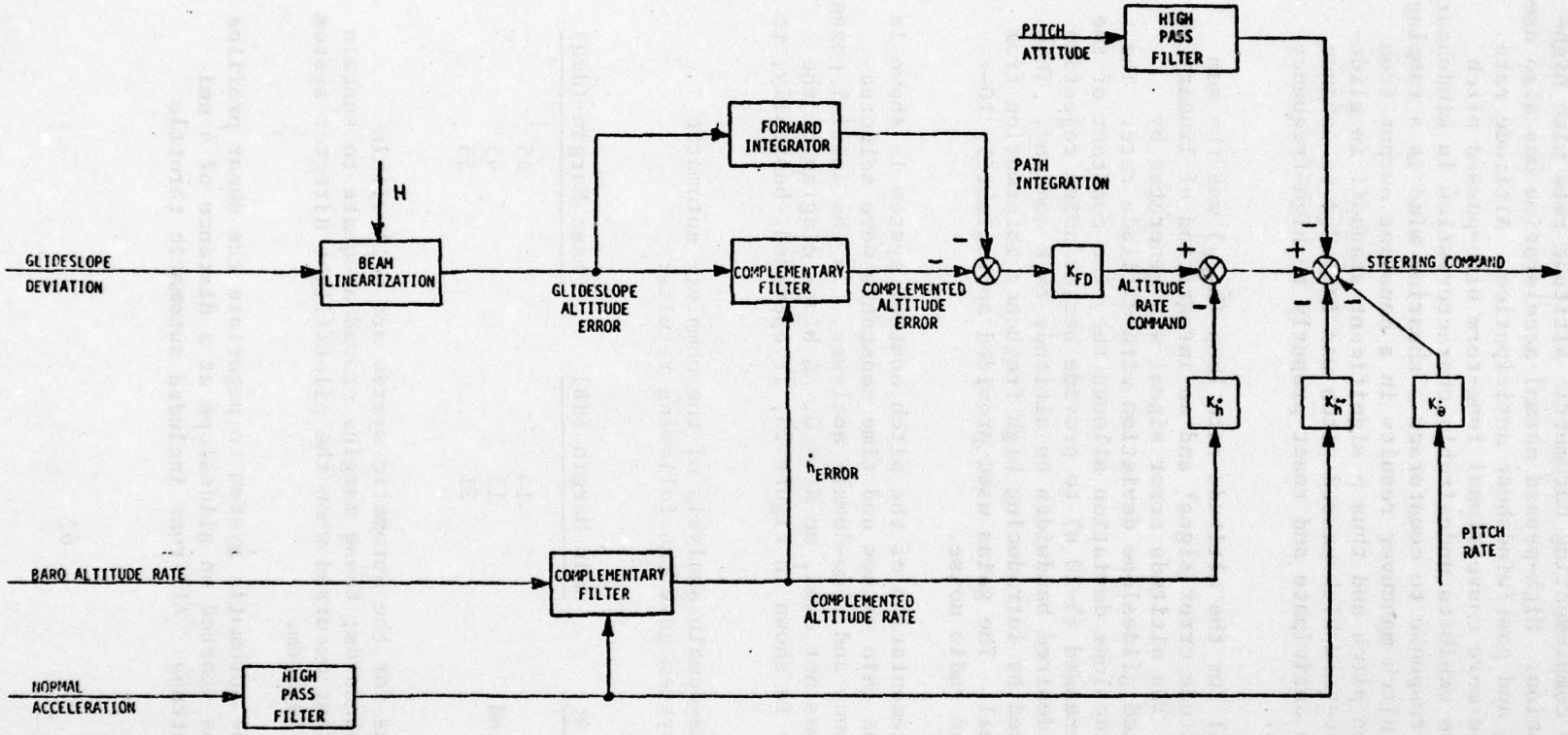

Figure 21 Simplified Longitudinal Control Law
For Modified Flight Director

The feedback signal for the altitude rate loop (complemented altitude rate) was generated by complementing barometric altitude rate with high-passed normal acceleration. High-passed normal acceleration was also used for inner loop damping and gust/windshear anticipation. Altitude rate was used instead of the more conventional long-term high-passed pitch because this pitch term exhibits undesirable characteristics in windshear. The required aircraft response to counteract a shearing wind is a ramping pitch attitude. This pitch maneuver results in a constant output from the high-pass filter on pitch and thus a significant standoff in glide-slope deviation. Short-term high-passed pitch was included to enhance the pilot's ability to anticipate and react properly to high-frequency pitch attitude changes.

The command signal for the altitude rate loop ($\dot{h}_{cmd}$) was the sum of a complemented altitude error signal and an integration of linearized glideslope deviation. The altitude error signal was generated by complementing linearized glideslope deviation with altitude rate. The complementation on glideslope deviation allowed the time constant of the noise filter to be increased (5-20 s) to provide better noise rejection while maintaining the desired bandwidth on altitude rate command. This bandwidth was maintained by introducing high frequency information from the altitude rate signal. The gains used provided approximately 10-s filtering on glideslope radio noise.

The detailed implementation of the pitch control system is shown in Figure 22. The various gain values and time constants were selected after extensive frequency and time-domain analyses. In the initial phase the pitch rate input was not used, so $K_{\dot{\theta}} = 0$. A block diagram of the simulated autothrottle is shown in Figure 23; it operated, basically, to null airspeed error.

Frequency and time-domain analysis of the complete automatic longitudinal control system gave the following results:

Control Loop Broken At:	Gain Margin (dB)	Phase Margin (deg)
Altitude error	14	45
Altitude rate command	15	45
Steering command	21	55

These stability margins for the automatic system are well within conventional design standards; these margins proved adequate to sustain the stability losses that occurred when the pilot/flight director system replaced the automatic system.

The ability of the automatic system to negotiate the shear profiles was tested. These runs started on glideslope at a distance of 4 nmi from the glideslope antenna. All runs included automatic throttle control.

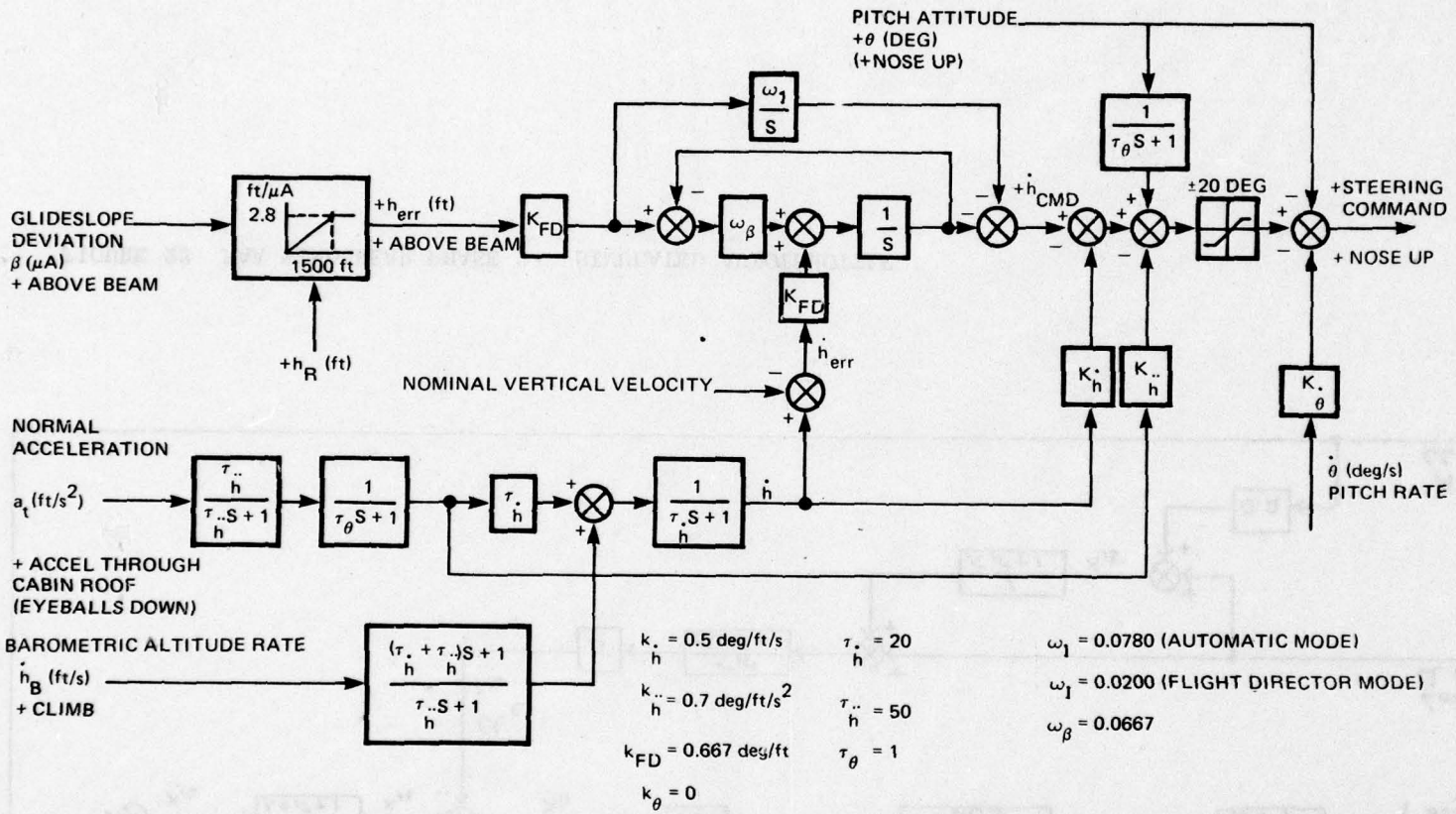

FIGURE 22 FAA WINDSHEAR PHASE 2: LONGITUDINAL CONTROL LAW

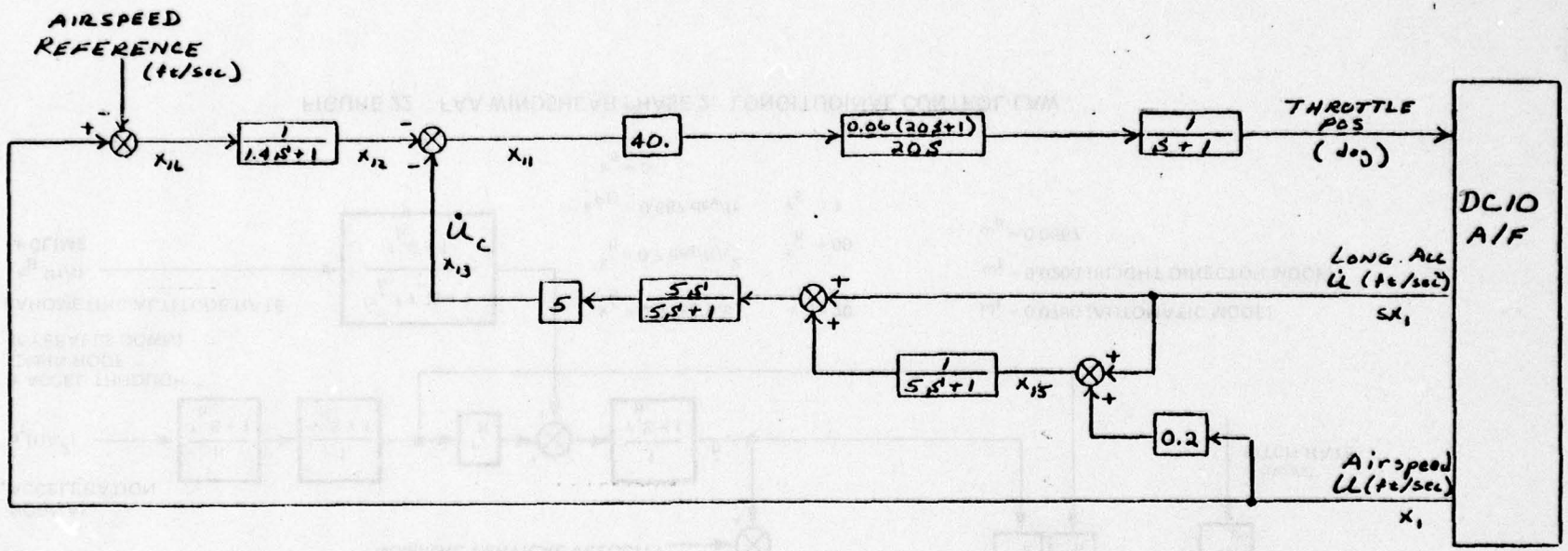

FIGURE 23 FAA WINDSHEAR PHASE 2: SIMULATED AUTOTHROTTLE

The logarithmic profile shear created no particular problem for this system. The maximum shear rate occurs over the last 100 ft and is equivalent to 6 knots/100 ft. The altitude error, except for initial trim upset, remained within a pen-width of zero.

The nighttime stable boundary layer shear profile represents a thermal inversion phenomenon. Maximum shear rate for this profile is 8.5 knots/100 ft. Maximum altitude error was 10 ft and occurred at the point where shear rate changed sign. Below 300 ft no deviations were recorded greater than 4 ft.

The frontal shear has a maximum shear rate of 21 knots/100 ft, occurring between 400 and 200 ft. The automatic system negotiated this portion of the shear adequately. Maximum altitude error of 25 ft occurred at 120 ft in a decreasing headwind shear of 6 knots/100 ft. At this altitude, the system was correcting for the undershoot and the aircraft situation at flare should be well within tolerances.

The thunderstorm cold air outflow shear profile presented the most complex and severe environment to the system. It has a horizontal component that varies from 50 ft/s headwind to 17 ft/s tailwind at touchdown. This profile includes a shear rate during one period of 20 knots/100 ft of decreasing headwind, which is 2-1/2 times the facility Category II certification limit. Correlated with this severe longitudinal shear is a rapidly varying vertical wind component. In portions of the two profiles, effects of the longitudinal and vertical components cause a multiplying effect on aircraft lift. Between 300 and 200 ft, the aircraft encounters the maximum decreasing headwind shear of 20 knots/100 ft and also encounters a downdraft that reaches 4 knots. The combined result is an extreme loss of lift. The Collins algorithms were successful in controlling altitude error in this area and allowed a maximum deviation from glideslope centerline over the entire approach of 20 ft. Glideslope deviation at the critical 100-ft altitude was 15 ft above centerline, and altitude rate indicated the aircraft would be in good position to perform a successful flare maneuver.

A pilot in the loop was simulated with a single pilot who was instructed to fly the command bars tightly. Autothrottle was used to control airspeed. The digital simulation with pilot models predicted good stability for the flight director system; conditions such as the thunderstorm shear showed this to be true. The request made of the pilot to fly the command bars tightly should have taxed the stability of the system, but these initial runs indicated very stable operation. In particular, small command bar and elevator activity and the smooth pitch attitude and altitude rate responses were noted.

For this control algorithm, response to gusts is a very good indication of system stability, and the traces of the runs indicated good stability and flyability. Comparatively minor activity in command bar and elevator was obtained for a relatively severe gust environment. With these small control activities, the autopilot and pilot were both able to maintain small errors on the glideslope.

One of the important improvements included in the modified control algorithms was a complementary filter on glideslope radio deviation. With this filter it was possible to put 10 s of filtering on radio deviation. The results of this filtering on system performance when subjected to Facility Category II level radio noise showed almost total absence of command bar activity, while the small altitude rate and altitude errors indicated that system stability had been maintained.

The combined effect of radio noise, gusts, and thunderstorm shear can be seen in Figure 24. These runs showed the same high stability and good performance seen in the single-disturbance runs. In the automatic mode approach, a maximum deviation of 30 ft was noted and the aircraft remained within 10 ft of nominal from 300 ft to run termination. Maximum pitch attitude deviation was 4.5°. The manual mode run exhibited the expected performance levels. Maximum altitude error was 40 ft; deviation at the critical 100-ft altitude was nearly zero. The long-term standoff of about 20 ft can be assumed to be caused by a mean radio noise value, as in previous traces. Pitch attitude remained less than 5° from trim.

2. Lateral Axis

The basic structure of the "accelerometer system" of the CV-880 study was again followed in developing the lateral control laws for the DC-10 modified flight director. The simulated aircraft was assumed to start on course and in trim, so ILS capture was not included. Also, it was assumed that the pilot would complete the landing by visual reference so no decrab or slip maneuver was provided.

Figure 25 is a block diagram of the accelerometer-augmented localizer track law for the DC-10 flight director system. The track law consisted of a second-order complementary filter utilizing radio altitude, gain programmed localizer deviation, and lateral acceleration from a body-mounted accelerometer to estimate linear beam deviation and rate. Also included was a bank mistrim and wind alleviation computation based on lateral acceleration. The complementary filter provided approximately 4-s filtering on localizer beam noise. This increased noise filtering allowed the forward loop gain (K_{FD}) to be increased for better performance in windshear. The bandwidth and damping ratio of the filter for the flight director were carefully selected to assure a fast response and well damped system. The beam rate signal was used for outer loop path damping. The roll feedback path closed the inner loop and roll rate feedback was included to assist the pilot in anticipating aircraft bank attitude changes. The bank mistrim and wind gust alleviation computations minimized localizer standoff due to bank mistrims and wind gusts. The gains and time constants of the system were optimized to provide stiffness, bandwidth, and stability margins consistent with track law performance requirements for a flight director system capable of handling the effects of severe windshears.

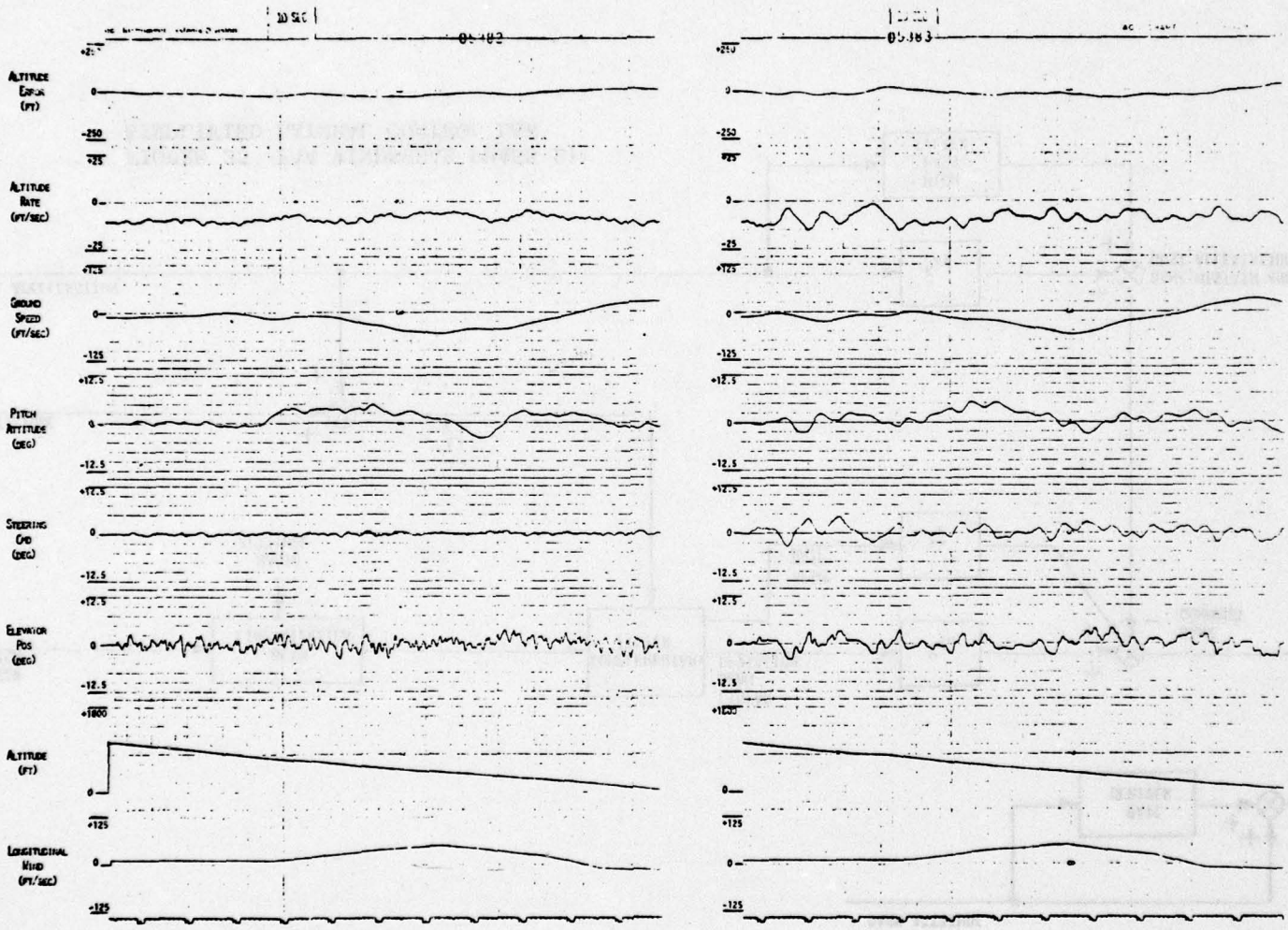

FIGURE 24. a AUTOMATIC MODE

FIGURE 24. b MANUAL MODE

FIGURE 24 GUSTS, RADIO NOISE, THUDERSTORM SHEAR

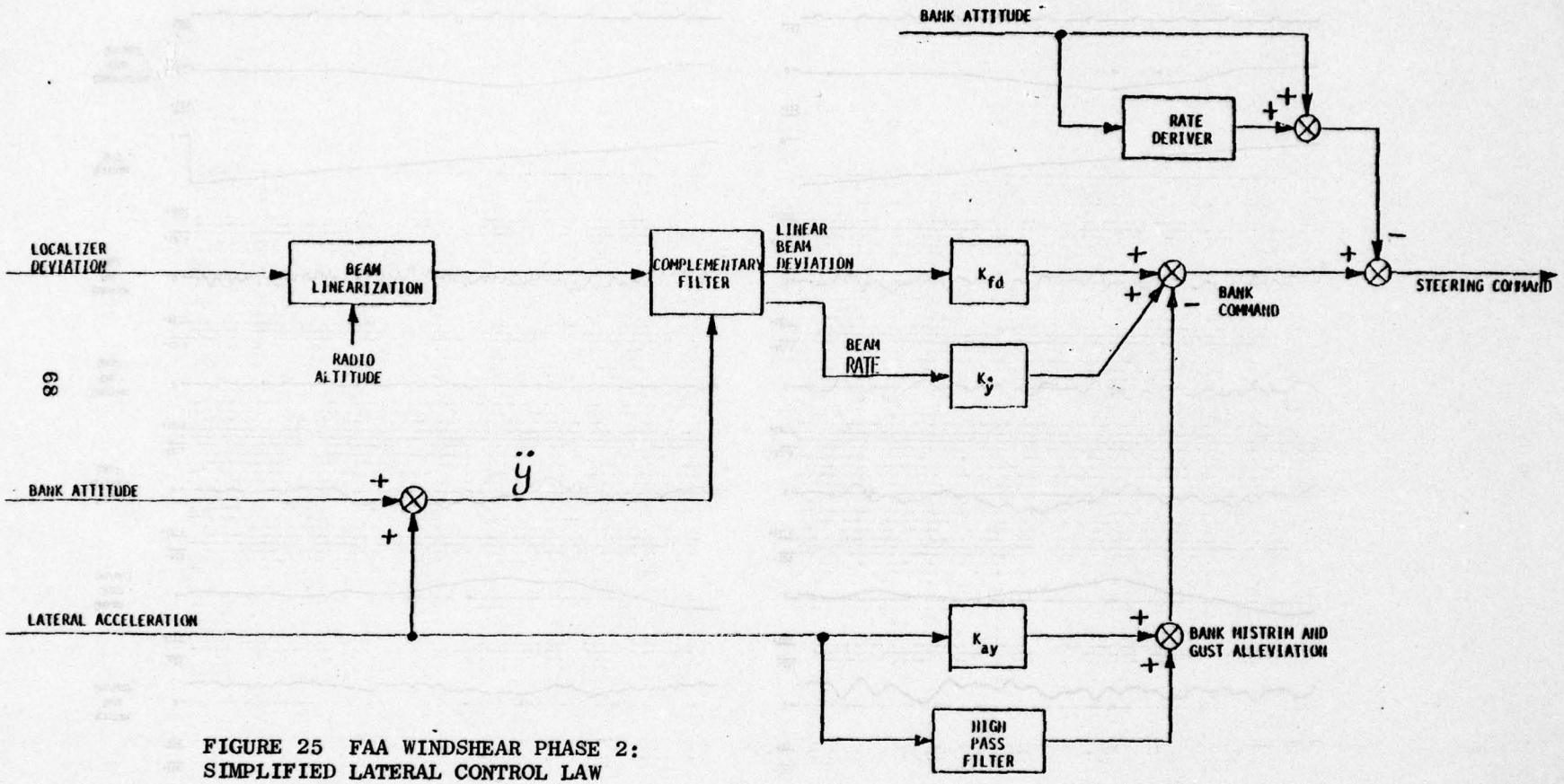

FIGURE 25 FAA WINDSHEAR PHASE 2:
SIMPLIFIED LATERAL CONTROL LAW

A detailed block diagram showing the implementation of the lateral-axis control is given in Figure 26. Frequency response analyses of the lateral system were run with two pilot models: a 0.1-s lag model $1/(0.1\,s + 1)$, and a 0.1- and 0.2-s lag model $1/[(0.1\,s + 1)(0.2\,s + 1)]$. The 0.1-s lag model was considered a better model for an average pilot. The results were:

Control Loop Broken At:	Gain Margin (dB)	Phase Margin (deg)
Steering command	22	70
Steering command error	17	45

The bandwidth and stability margins are consistent with the track law requirements of the flight director system.

The ability of the automatic system to negotiate the shear profiles used in this study was studied by runs that started on-localizer at a distance of 4 nmi from the glideslope antenna.

The logarithmic shear presented no problem for the Collins algorithm. Roll and aileron command activity were negligible and maximum localizer linear deviation was 13 ft. The system response to a nighttime stable shear was also small--maximum deviation from centerline being less than 13 ft. Roll command reached a maximum of 1°.

The frontal shear, which provided the most severe challenge to the lateral system, had a shear rate of 11.7 knots/100 ft at the critical lower altitudes. We noted increased aileron activity with a maximum of 2°. The resulting localizer linear deviation showed a maximum deviation from centerline of 18 ft.

The response of the automatic system to the thunderstorm shear was well controlled. Maximum lateral shear rate in the thunderstorm profile was 2.5 knots/100 ft. Roll and aileron command activity were negligible; maximum deviation from centerline was 12 ft.

In the same way, the corresponding flight director system (MFD) was tested with the analog computer and a test pilot operating the simulator controls. When encountering the logarithmic profile shear, the pilot-in-the-loop system exhibited good stability and performance. Maximum roll command was 2° and maximum deviation from centerline was 15 ft.

The system response to the nighttime stable shear showed adequate performance during the run except in a range from 300 to 100 ft. The roll command signal in this region was 5° with no equivalent increase in aileron command magnitude, indicating the pilot was distracted for that period and did not follow the commands given. It should be noted that the maximum deviation from centerline was still only 20 ft and the deviation reduced to 10 ft before altitude reached 50 ft.

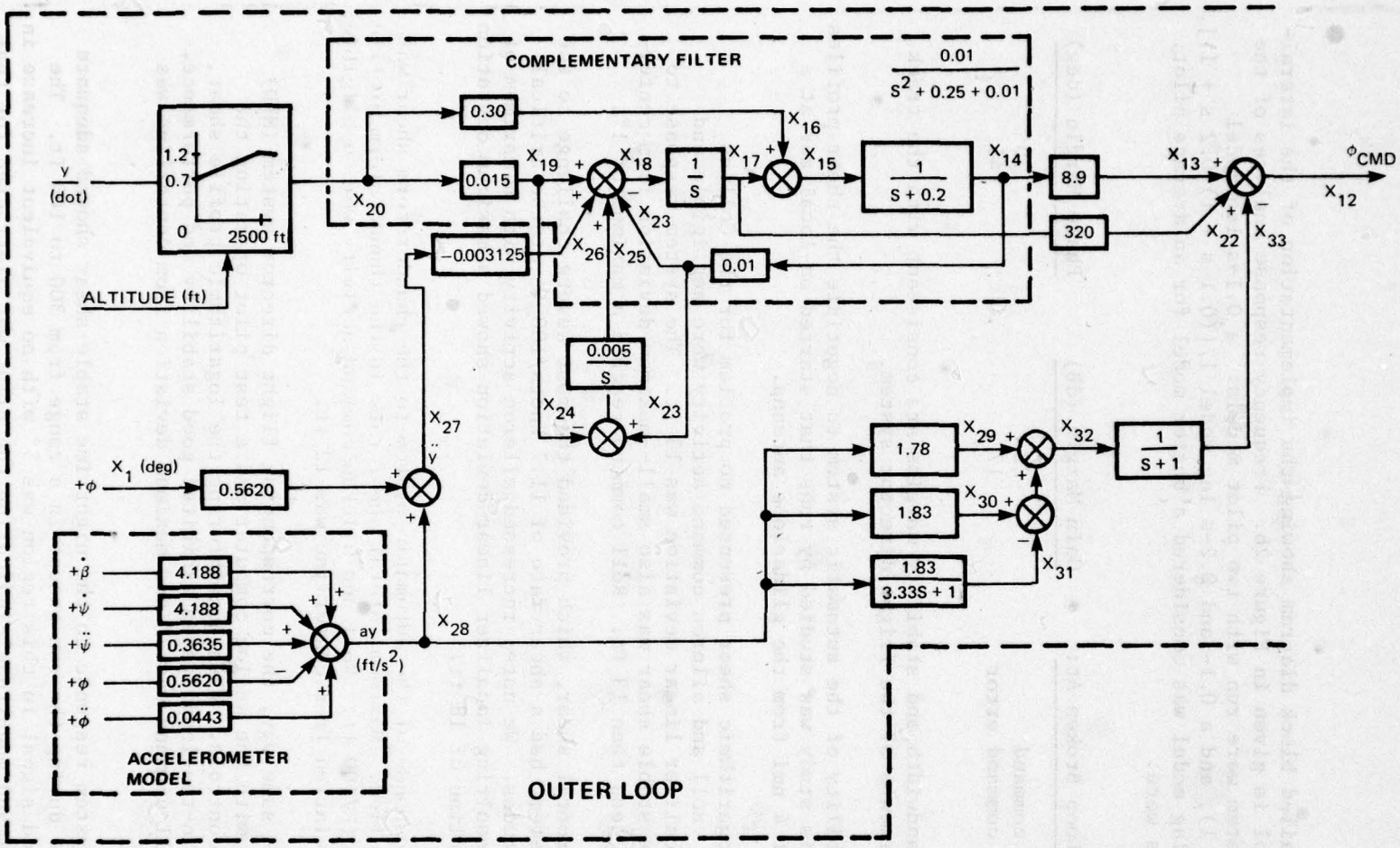

FIGURE 26 FAA WINDSHEAR PHASE 2: LATERAL CONTROL LAW

The response of the system to the frontal shear showed maximum roll of 3° and maximum localizer linear deviation of 30 ft.

The flight director system, when flown in the thunderstorm shear, showed a maximum roll command of 2° and maximum deviation from centerline of 23 ft. Below 200 ft, maximum deviation from centerline was 10 ft.

The response of a control system to gusts is a very good indicator of system stability. The gust model used is specified in Appendix A. The automatic system response showed good stability with maximum roll attitude of 1.5°, maximum roll command of 1.5°, and maximum lateral deviation from centerline of 15 ft. The flight director response exhibited acceptable increases in activity, with a maximum roll attitude of 2.5° and maximum roll command of 3°. Maximum deviation from centerline at altitudes below 300 ft was 20 ft.

The improved localizer noise filtering provided by the algorithm developed in this study was seen in runs showing the response of the system to Category II localizer noise of 3σ magnitude 7.5 μA. Description of the noise disturbance is found in Appendix A. The automatic system performance exhibited very low roll command activity with maximum value less than 1.5°. There was no high frequency activity on the command. The resulting lateral deviation from centerline was only 12 ft at 50 ft altitude and had a maximum of 25 ft overall. The flight director system performance showed equally good performance. Maximum roll command was 3° and the aileron command activity indicated the pilot did not have to track a noisy command bar. A relatively long-term lateral deviation of magnitude 30 ft was due to a nonzero mean value in localizer noise. The aircraft returned to centerline as altitude diminished, and was within 5 ft of centerline at 50 ft altitude.

Figure 27 shows the results of flying the automatic and flight director systems, respectively, through the combined disturbances of radio noise, gusts, and thunderstorm shear. The automatic system run shown in Figure 27a exhibited good performance in this combined disturbance. Maximum aileron command was less than 2.5°; maximum roll command was 1°. Localizer linear deviation at 50 ft altitude was 10 ft, while the maximum was 30 ft. The flight director system performance is shown in Figure 27b. Maximum roll command below 800 ft was 3°, and maximum aileron command was 5°. The localizer linear deviation indicated a standoff of 50 ft at 800 ft altitude, reducing slowly to 25 ft at 50 ft altitude.

3. Tests at Douglas Aircraft Company

The MFD algorithms thus defined were taken to Douglas for use on experiment 3, phase 2, of Task 2, accomplished at Long Beach, California during the period of January 17 through 27, 1977. The primary goal of

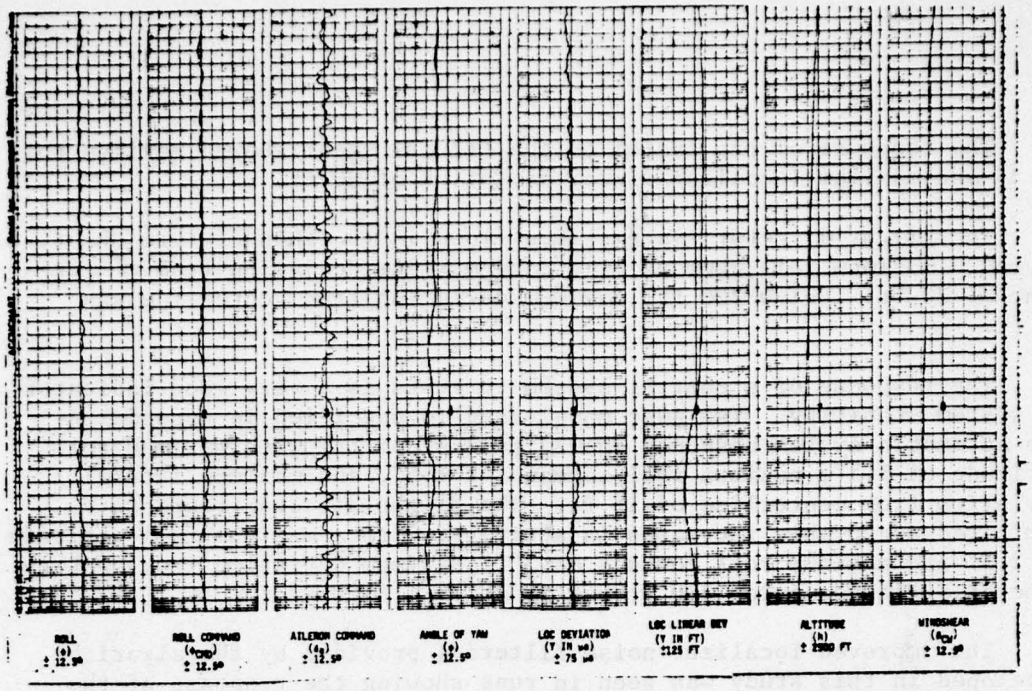

(a) LATERAL: AUTOPILOT SYSTEM

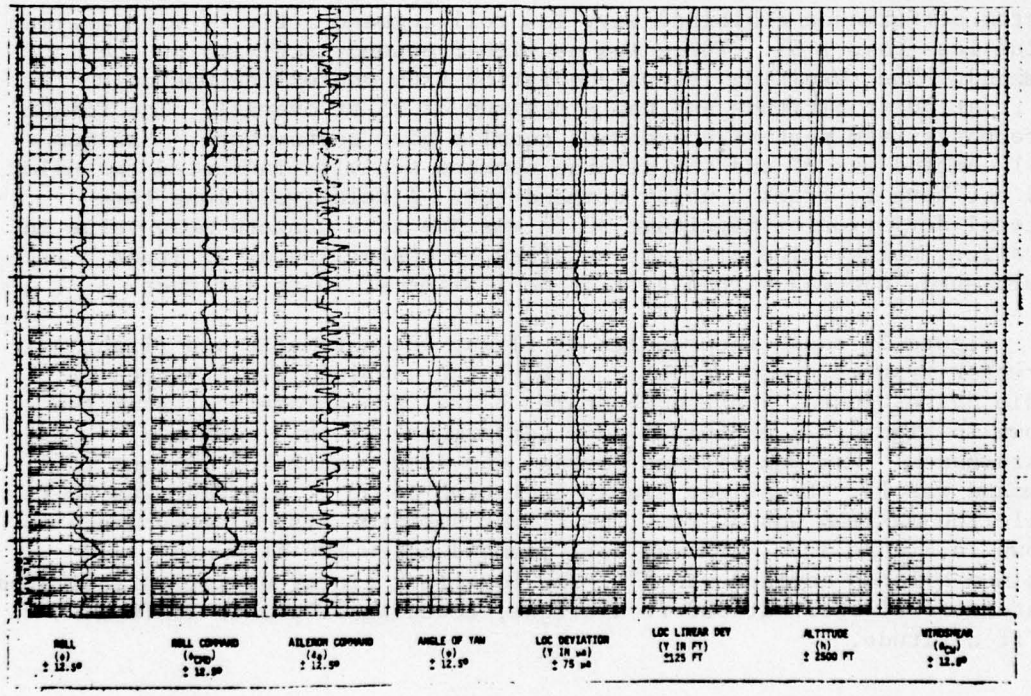

(b) LATERAL: FLIGHT DIRECTOR SYSTEM

FIGURE 27 GUST, LOCALIZER NOISE, THUNDERSTORM SHEAR

this experiment was to determine the effectiveness of the MFD concept relative to conventional approach management techniques in coping with low-level windshear.

The aircraft simulator used was the Douglas moving base research and development simulator. The cockpit simulation was basically a DC-10 with some modified equipment. The ADI used for this experiment was a Sperry Model 902. All controls were active, including rudder, flaps, and gear. Visual display was by way of a Douglas-designed asymmetric lens displaying a color TV visual of a Redifon terrain board produced at a scale of 750:1. The Douglas-designed motion base used two servo cylinders for each degree of motion to obtain the desired frequency and g capability. Commands to the cab and cockpit were linked from the main computer by a PDP11/40 digital system with digital-to-analog accessories. A Comcor CI 5000 analog computer was used for parts of the implementation. The aircraft motion and control algorithm simulation were implemented digitally in a Sigma 5, 32-bit computer using difference equations. All simulation programming was accomplished in Fortran.

The aircraft motion equations were six-degree-of-freedom, nonlinear, large disturbance equations of a DC10-10 at 350,000 lb gross weight. The approach simulated was an ILS with a 3° glideslope. The visual display simulated a 300-ft breakout with a 2400-ft RVR. The approach was initiated at 1500 ft on-glideslope, on-localizer. Windshears corresponded to those of Appendix A.

The MFD algorithms at Douglas for Phase 2 were the same as those tested at Collins (Figures 22 and 26) except that gain was increased slightly in the pitch control system; values were changed to $K_{FP} = 0.10°/ft$ and $\omega_\beta = 0.13$ rad/s (Figure 25).

The results of experiment 3 at Douglas have been reported in detail.[3] Briefly, the study concluded that the Collins-developed "modified flight director" algorithms, when compared with a "baseline flight directory system," significantly improved the pilot's chance of negotiating severe windshears. The report also concluded that further study, including speed control algorithm development, should produce a system able to negotiate severe windshear with an improved success rate.

B. Integration of Thrust Command in MFD

The next subtask in the Rockwell-Collins work on the DC-10 control algorithms was to design and test thrust (or speed) commands for display on the flight director Fast/Slow (F/S) indicator. The objective was to investigate the interaction between flight director steering and thrust commands in a windshear environment and to develop speed axis control strategies that would satisfactorily effect this interaction. A second objective was to refine further the flight director steering laws, particularly in concert with the thrust algorithms.

The pitch axis modified flight director algorithms implemented in the first DC-10 studies were employed as a starting point. Principal improvements on the pitch system were an increase in the bandwidth of the complementary filter and a compensatory increase in the $\dot{h}$ error gain for purposes of system damping. However, an increase in $\dot{h}$ error gain also required an increase in beam error gain to retain the symmetry of the filter. A power spectral density analysis (PSD) indicated that these gain increases would have to be limited since beam noise and vertical gust activity would be passed through the complementary filter in excessive amounts. A compromise was reached whereby some increases in the beam and $\dot{h}$ error gains were implemented as well as a pitch rate signal added to retain adequate system damping, yet restrict system activity due to noise and turbulence.

The lateral axis flight director algorithms remained essentially the same as those employed in the phase 2 study. A frequency domain analysis verified that adequate phase and gain margins existed while a PSD analysis demonstrated that the system noise characteristics were acceptable.

Prior to synthesizing a speed axis control system for windshear environments, an appraisal was performed of the effects due to reducing airspeeds in a landing configuration on the basic aircraft kinematics. Two aircraft having data readily available were examined: the C-5 (representing wide bodies) and the CV-880 (representing standard size vehicles). Aside from the obvious effects associated with a significant loss of airspeed, some stability derivatives varied by as much as 50% for a 20-knot loss in airspeed. These were the rolling moments due to aileron or rudder deflection, pitching moment due to angle-of-attack, and yawing moment due to roll rate. This adversely affects lateral handling qualities, the short period mode, and the directional divergence. Hence, it is necessary not only to maintain an adequate approach speed, but also to reduce airspeed transients to minimize the deleterious effects.

From the basic airframe equations, the aircraft's response to a throttle input had a time constant of between 6 and 8 s. The windshear profiles used for test had shear gradients as large as 44 knots/100 ft. Assuming a typical rate of descent of 12.5 ft/s, 44 knots could be lost in as little as 8 s in an extreme shear profile. Even in the majority of the profiles, shear gradients of 22 knots/100 ft are observed. Thus, to avoid stalling or even difficult handling of the aircraft, an immediate response to the shear should be initiated by the speed control system.

A pilot in the loop introduces considerable lag in the response to a windshear. This lag, combined with the shear gradient and response time of the airframe to a throttle input, can place the aircraft in jeopardy or even in an unrecoverable situation. Thus, some prognostication of an impending windshear situation must be employed whenever a human pilot is controlling the speed axis. Ten candidate speed control systems were proposed, encompassing airspeed error, angle-of-attack,

diminishing headwind shear, airspeed bias, ground speed error, and glidepath error. Some of these were rejected because of inadequate prognostication of the shear, others because of potential difficulty in their implementation. The airspeed error with diminishing headwind shear compensation was selected as providing performance (at least equivalent to any other method) with the greatest ease of implementation.

Figure 28 is a simplified block diagram of the speed axis control law. Longitudinal acceleration was complemented with airspeed to provide system damping. High-passed pitch was employed for anticipation, particularly in vertical shear situations. Airspeed and airspeed reference were differenced to form the basic airspeed error signal. Indicated airspeed and groundspeed (groundspeed corrected for altitude and temperature variations from a sea-level standard day condition) as well as headwind in the touchdown zone were combined, and filtered, then passed through a nonlinear network, which only had an output for a diminishing headwind shear condition. There was no command to retard the throttle(s) in an increasing headwind shear. The damping, high-passed pitch attitude, airspeed error, and diminishing headwind shear signals were summed and sent either to an autothrottle servo (perhaps with a lower gain to reduce throttle activity due to noise) or the flight director fast-slow needle. Whenever the flight director or manual mode was used, a high-passed throttle signal was employed. This had the overall effect of providing a pseudorate throttle command similar to a rate command autothrottle system. The results were smoother throttle activity by the pilot, particularly in turbulence.

A frequency domain analysis indicated that the speed control system had adequate gain and phase margins. PSD plots of the system's response to vertical and longitudinal gusts were obtained for each control path. These PSD plots indicated the sensitivity of each path to turbulence, where filtering would be required, and where gains could be increased to enhance performance.

The use of groundspeed in the diminishing headwind shear compensation raised the question of availability of this state, particularly if there were no inertial navigation system on the aircraft. In this study, this state was assumed to be available (from an INS, modified weather radar, or collocated DME) but the question of how much filtering could be tolerated still remained. Various groundspeed filters, ranging in value from 0 to 10 s, were evaluated in the simulation. With a 10-s filter, the rise time was 15% longer and the performance in a thunderstorm shear was "goosey." There was no noticeable effect for a 1-s filter and only a very slight effect for a 3-s filter. With a 5-s filter there was a noticeable effect; however, it could be tolerated. Based on this study, a 2.5-s filter on the groundspeed signal was selected for the speed control system.

Other filtering requirements of the system were established in a similar fashion. It was found that a 1-s lag on the indicated airspeed signal provided lower activity in turbulence without adversely affecting

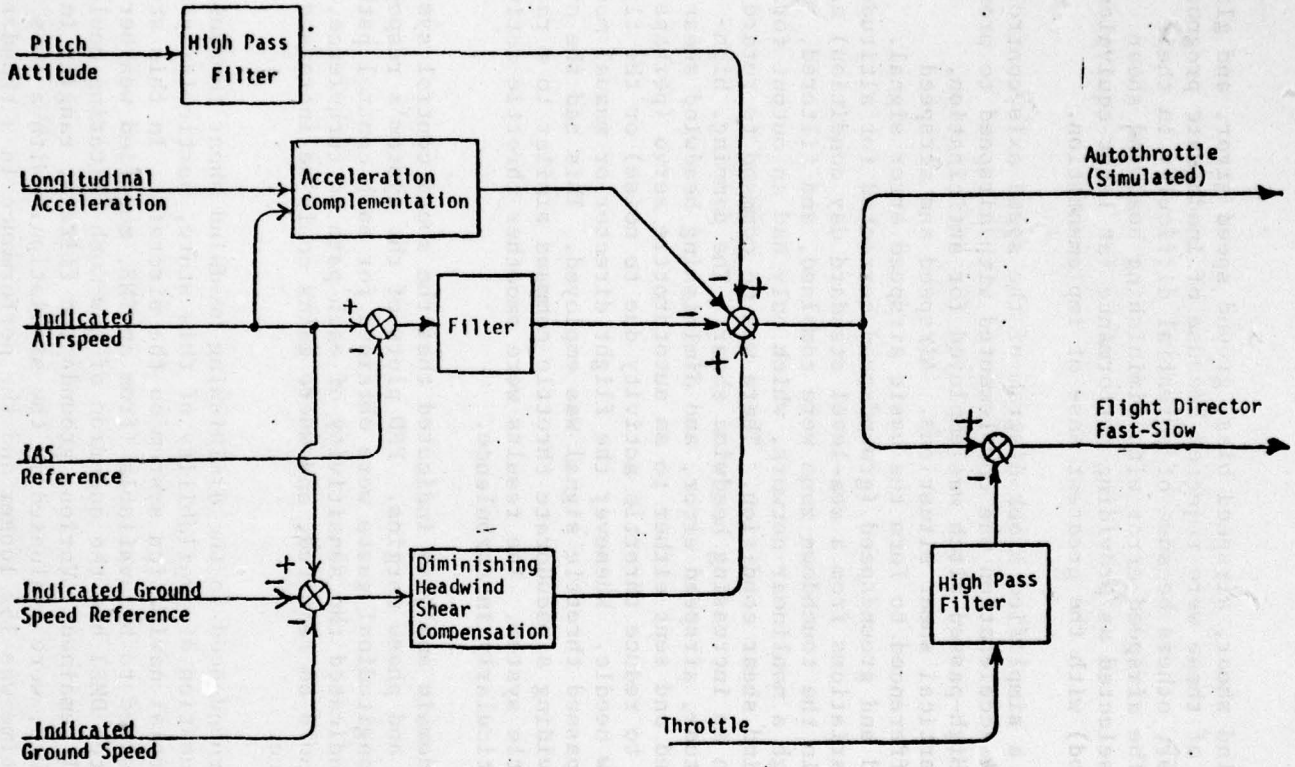

FIGURE 28 SIMPLIFIED SPEED AXIS CONTROL LAW (WITH GROUNDSPEED)

stability. Similarly, a 1.4-s filter on the airspeed error signal and a 1-s filter on the complemented acceleration signal were established.

The gain in the airspeed error path was set to twice the gain in the diminishing headwind path. In the B727 trials at NASA Ames Research Center in July 1977, the high airspeeds resulting from maintaining a minimum groundspeed at the "bug" setting caused unduly large pitch changes to occur, particularly in vertical shear. Thus, the augmented system was designed to weight more heavily the airspeed error (increase the bandwidth of this signal) and, incidentally, reduce the groundspeed pad, thereby reducing airspeed.

As in the first study, the DC-10-10 aircraft, inner loops, modified flight director laws, and speed axis control strategies were implemented on the Rockwell-Collins EAI-680 analog simulator. The runs with a human pilot employed a Rockwell-Collins 329B-9L flight director, with cross pointer commands, which was driven by signals from the EAI-680 computer for attitude and command information. The speed command was also computed in the control laws patched on the EAI-680 and drove the fast-slow needle on the flight director. Both the longitudinal system and the lateral system were flown in automatic and manual modes against each shear profile of Appendix A, with and without turbulence and radio noise.

The performance of the guidance and speed control systems in the logarithmic windshear profile showed deviations from the glideslope well within the limits specified at the inner marker (±28 ft altitude error, ±75 ft lateral error). Airspeed control was such that it never was below V approach.

A simulated encounter with a nighttime stable shear for the pitch axis again showed deviations from the glideslope well within the specified limits, while the airspeed never dropped below V approach.

The performance of the pitch axis modified flight director and speed laws in a simulated encounter with a frontal shear showed at the approach gate (inner marker) a deviation from the glideslope of less than 8 ft. The airspeed dropped below the reference, but by no more than 3 knots in the automatic mode and less than 3 knots in the manual mode.

The most severe challenge to the pitch guidance and speed axis control systems was presented by the thunderstorm profile. This was due to a sizeable shear gradient in the longitudinal axis, as well as significant vertical shears, both of which occurred close to the ground. Even though the aircraft deviated below the glideslope by 30 ft, this was outside the middle marker. Inside the middle marker and at the approach gate, vertical deviation below the glideslope was not more than 8 ft in either mode and the airspeed remained above V approach.

The behavior of the lateral axis was examined in a nighttime stable shear encounter. Although this was a relatively mild shear in the pitch axis, the lateral profile for this windshear was the most demanding of

THIS PAGE IS BEST QUALITY PRACTICABLE
FROM COPY FURNISHED TO DDC

those tested, exhibiting a maximum lateral shear gradient of nearly 15 knots/100 ft. However, there was no more than 20 ft of linear deviation from the localizer beam inside the middle marker.

The frontal shear also provided a severe challenge to the lateral guidance law because of the abrupt change of the shear gradient at low altitude. Deviation from the localizer in the automatic mode was no more than 18 ft. In the manual mode, the maximum deviation from centerline was 30 ft. Both deviations resided well within the specified limit of 75 ft at the inner marker.

Although the thunderstorm profile presented a severe challenge to the pitch axis, the lateral disturbances were relatively benign. Deviation from the centerline was less than 12 ft in the automatic mode and less than 23 ft in the manual mode, with better performance close in.

With the pitch axis control laws, the combination of beam radio noise, wind gusts or turbulence, and an encounter with a thunderstorm windshear profile showed that vertical deviation inside the middle marker never exceeded 20 ft and was less than 8 ft at the approach gate, even in this extreme situation. Airspeed, including gust peaks, was never more than 3 knots below V approach in the automatic mode and no more than 9 knots in the manual mode.

The lateral axis control was also tested with both automatic and the human pilots in the combined disturbances of radio noise, gusts, and thunderstorm shear profile. The automatic system exhibited good performance, with no more than 30 ft of linear deviation and no more than 20 ft inside the inner marker. With the manual mode, the maximum localizer deviation was 50 ft at 800 ft altitude and reduced slowly to 25 ft inside the inner marker.

Thus, the Rockwell-Collins modified flight director and speed axis control laws successfully negotiated all the shears in both the manual and automatic modes at Cedar Rapids.

Just prior to the September trials at Long Beach, SRI requested a second speed axis control system to test with the modified flight director. This second system was not to employ groundspeed. Several candidate systems were examined--the principal constraint being to develop and implement on the Douglas Long Beach simulation facility a system on such short notice. The candidates included a high bandwidth core airspeed error scheme, a glideslope offset system, an airspeed bias, and a combination of airspeed bias and glideslope offset. Figure 29 depicts the selected candidate, an airspeed bias scheme. This system provided better airspeed tracking and less sensitivity to noise and turbulence than the other candidates. This was especially true during the last 350 ft (altitude) of the approach where, of all the nongroundspeed candidates, it most closely duplicated the performance of the groundspeed system.

THIS PAGE IS BEST QUALITY PRACTICABLE
FROM COPY FURNISHED TO DDC

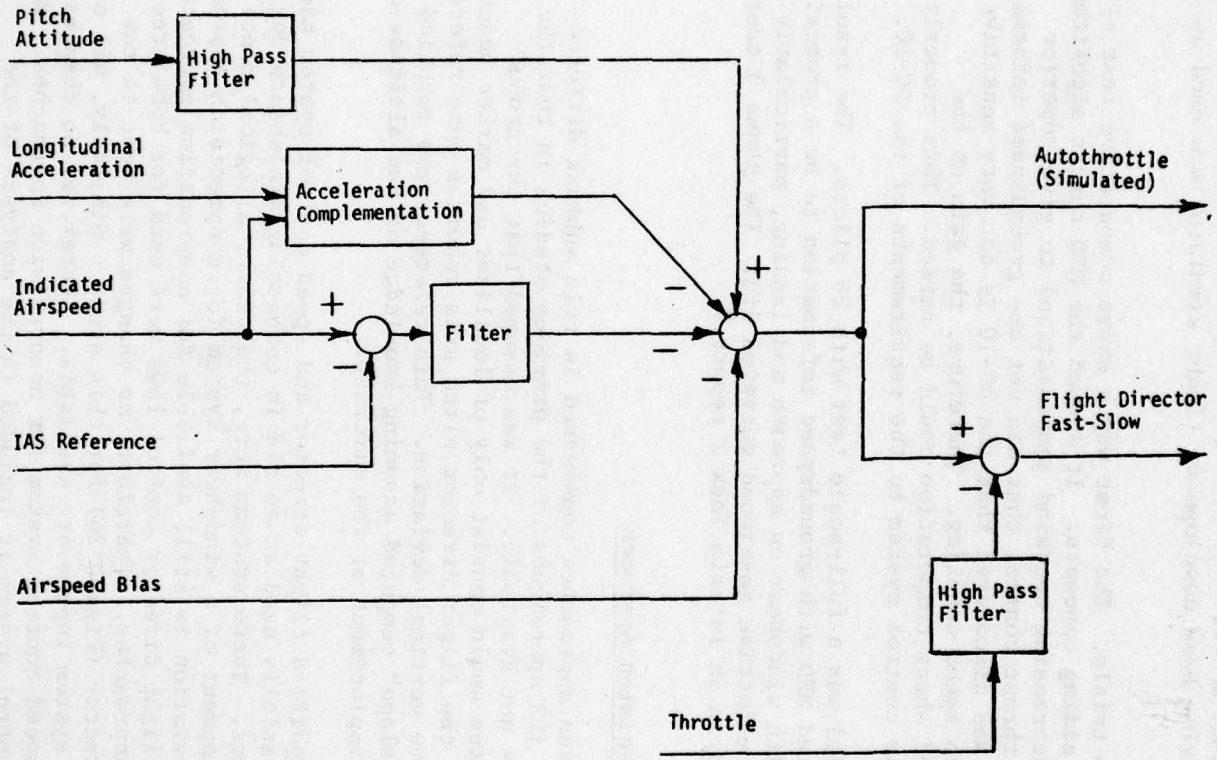

FIGURE 29 SIMPLIFIED SPEED AXIS CONTROL LAW (WITHOUT GROUNDSPEED INFORMATION)

These integrated MFD thrust and steering commands were implemented and further evaluated in the Task 2, phase 3, tests of DC-10 aids for coping with low-level windshear conducted by the AWLS team at Douglas Aircraft Company, Long Beach, California, in September and October 1977. The same Douglas moving base development flight simulator was used as in the phase 2 tests.

There were two trials. The first was a short comparative test of various individual aiding concepts. It showed the MFD thrust algorithm with groundspeed (decreasing headwind compensation) to give superior performance to the thrust control that did not use groundspeed information. However, it was discovered that the DC-10 is not very sensitive in the area of pitch speed coupling. Therefore, the gain on the diminishing headwind shear computation could be raised. This properly tuned the speed axis control system to the requirements of the DC-10.

The second trial was a full-scale test with 26 pilots. The results showed the integrated MFD with groundspeed information to be a promising method of coping with windshear on approach and landing, particularly if supplemented by an effective go-around decision aid. The phase 3 tests have been described in an interim Task 2 report.[4]

C. MFD for Nonprecision Approach

The nonprecision approaches considered in this subtask differed from the precision ILS approaches of the previous studies in that the glideslope beam was not available. It was assumed that the ground-based guidance system would consist only of localizer and marker beacons. In this condition, the flight director pitch axis requires some reference from which to derive vertical deviation. This reference was supplied by a "synthetic glideslope" computed assuming knowledge of the altitude and the longitudinal displacement of the aircraft.

The Collins-modified flight director and speed control system had already been successfully used as an aid in combatting windshears during precision approaches. These systems were, therefore, a logical place to start in the development of a windshear system for nonprecision approaches. Since localizer deviation is still available for nonprecision approaches, the same lateral flight director control laws were used for both precision and nonprecision approaches. Therefore, no changes were made to the lateral flight director (Figure 26) for this study. Similarly, all of the speed control system inputs are available. Therefore, no changes were made to the speed control system for nonprecision approaches. However, the speed control system is included in the analysis of the longitudinal flight director. The longitudinal flight director must be modified because glideslope deviation is no longer available for nonprecision approaches.

A block diagram of the Collins MFD (with groundspeed) speed control system is presented in Figure 30. The basic configuration of the MFD

THIS PAGE IS BEST QUALITY PRACTICABLE
FROM COPY FURNISHED TO DDC

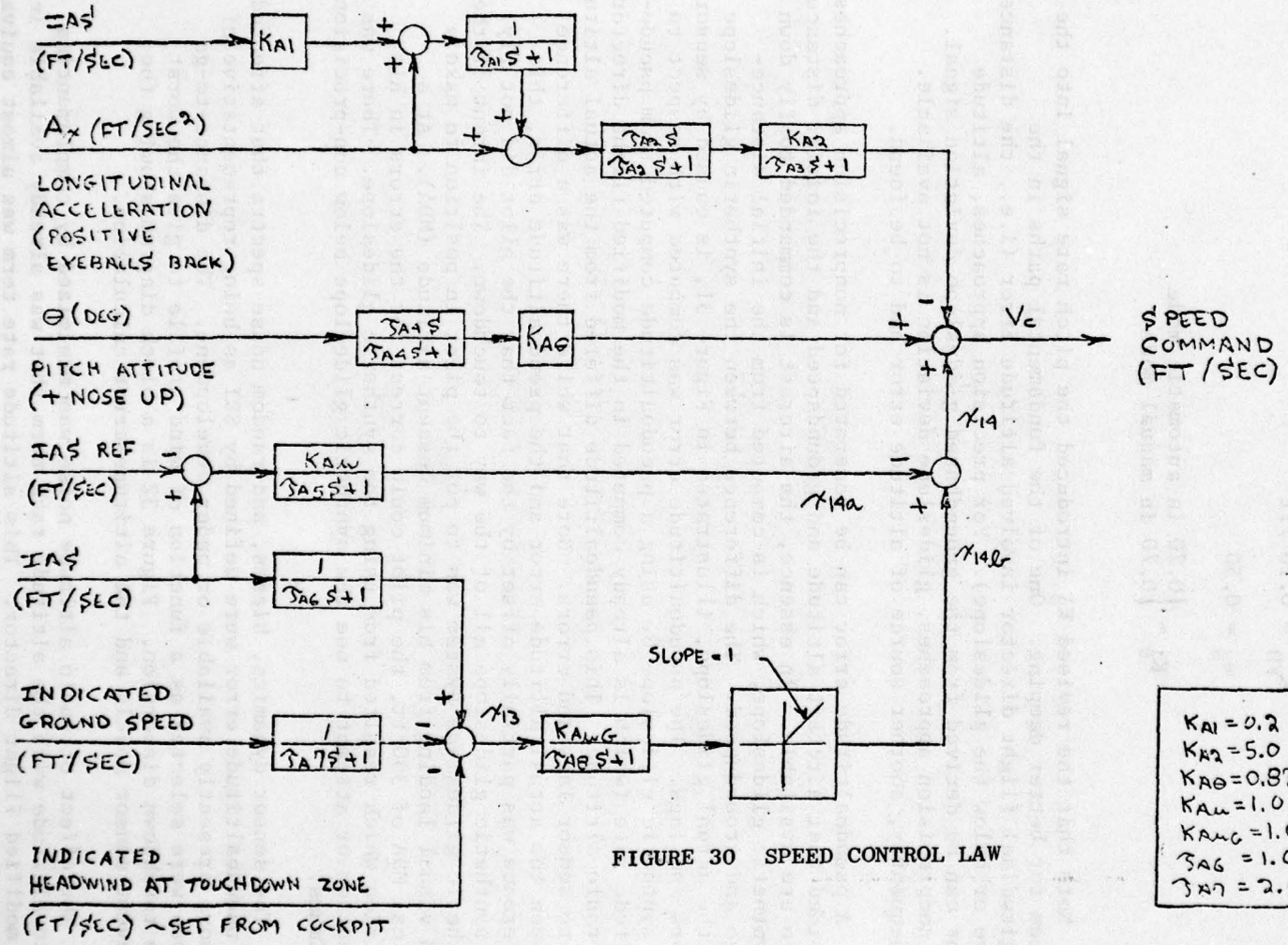

81

FIGURE 30 SPEED CONTROL LAW

$K_{A1} = 0.2$	$\tau_{A1} = 5.$
$K_{A2} = 5.0$	$\tau_{A2} = 5.$
$K_{A\theta} = 0.875$	$\tau_{A3} = 1.$
$K_{AW} = 1.0$	$\tau_{A4} = 5.$
$K_{AWG} = 1.0$	$\tau_{A5} = 1.4$
$\tau_{A6} = 1.0$	$\tau_{A8} = 1.4$
$\tau_{A7} = 2.0$	

THIS PAGE IS BEST QUALITY PRACTICABLE
FROM COPY FURNISHED TO DDC

pitch control system is shown in Figure 22. The only changes, which were dictated by experience with the DC-10 simulator at Douglas, were different values for three parameters:

$$K_{FD} = 0.10°/ft$$

$$\omega_{\beta} = 0.50$$

$$K_{\dot{\theta}} = \begin{cases} 0.20 \text{ in automatic mode} \\ 0.70 \text{ in manual mode} \end{cases}$$

Note that the revised $K_{\dot{\theta}}$ introduced the pitch rate signal into the system for better damping. One of the fundamental paths in the longitudinal flight director involved altitude error (i.e., the distance above or below the glideslope). For precision approaches, altitude error can be derived from the groundbased glideslope deviation signal. For nonprecision approaches, glideslope deviation is not available. Consequently, another source of altitude error had to be found.

A pseudoaltitude error can be generated for nonprecision approaches, provided that aircraft altitude and groundspeed and the initial distance-to-go are available. In essence, the aircraft is commanded to fly down a synthetic glideslope, which is computed from the initial distance-to-go and groundspeed. The difference between the synthetic glideslope and the actual glideslope, illustrated in Figure 31, is caused by sensor errors and lags. The pseudoaltitude error was computed with respect to the synthetic glideslope by using a pseudoaltitude computed from pseudo-altitude rate (which is already computed in the modified flight director) and radio altitude. This pseudoaltitude differed from the actual altitude due to sensor lags and errors. Note that while there was a difference between the actual altitude error and the pseudoaltitude error, this difference was partially offset by the fact that the pilot did not fly the synthetic glideslope all of the way to touchdown. The intent of the synthetic glideslope system was to put the pilot in position to make a good visual landing from his minimum descent altitude (MDA). At a typical MDA of 350 ft, the pilot could correct for the errors in his position which resulted from using the synthetic glideslope. There was no intention or attempt to use the synthetic glideslope below non-precision minimums.

The sensor dynamics, biases, and random noise spectra that affected the pseudoaltitude error were defined by SRI as being representative of sensors presently available or under development. The distance-to-go biases were selected as a function of wind profile to give the worst case touchdown dispersion. Figure 32 is a block diagram showing the relevent sensor models and the altitude-error calculation.

The effect of radio altitude noise was minimized by complementing radio altitude with the altitude rate term that was already available in the modified flight director. This altitude rate term was almost equivalent

FIGURE 31 PSEUDOALTITUDE ERROR COMPUTATIONS

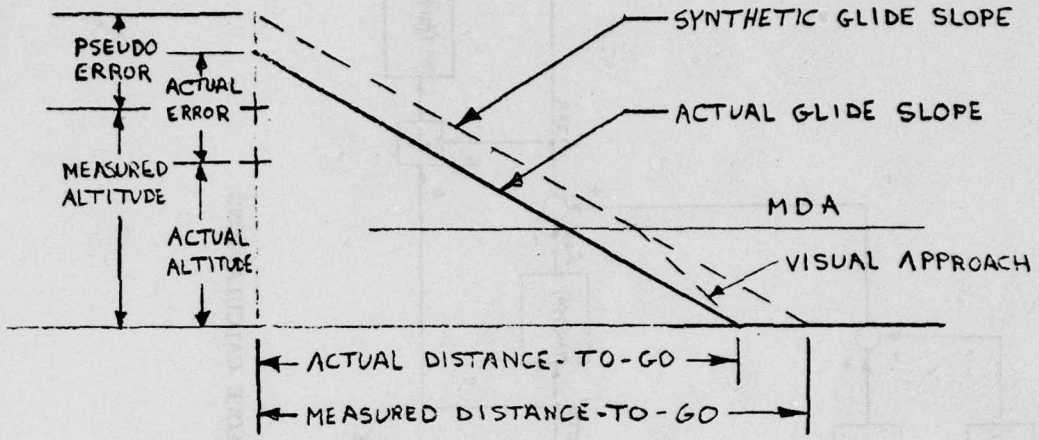

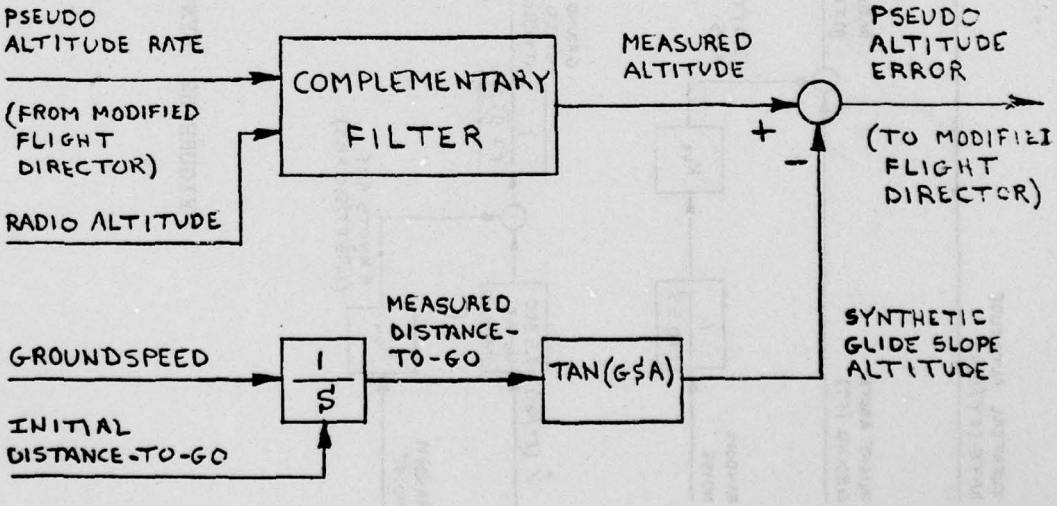

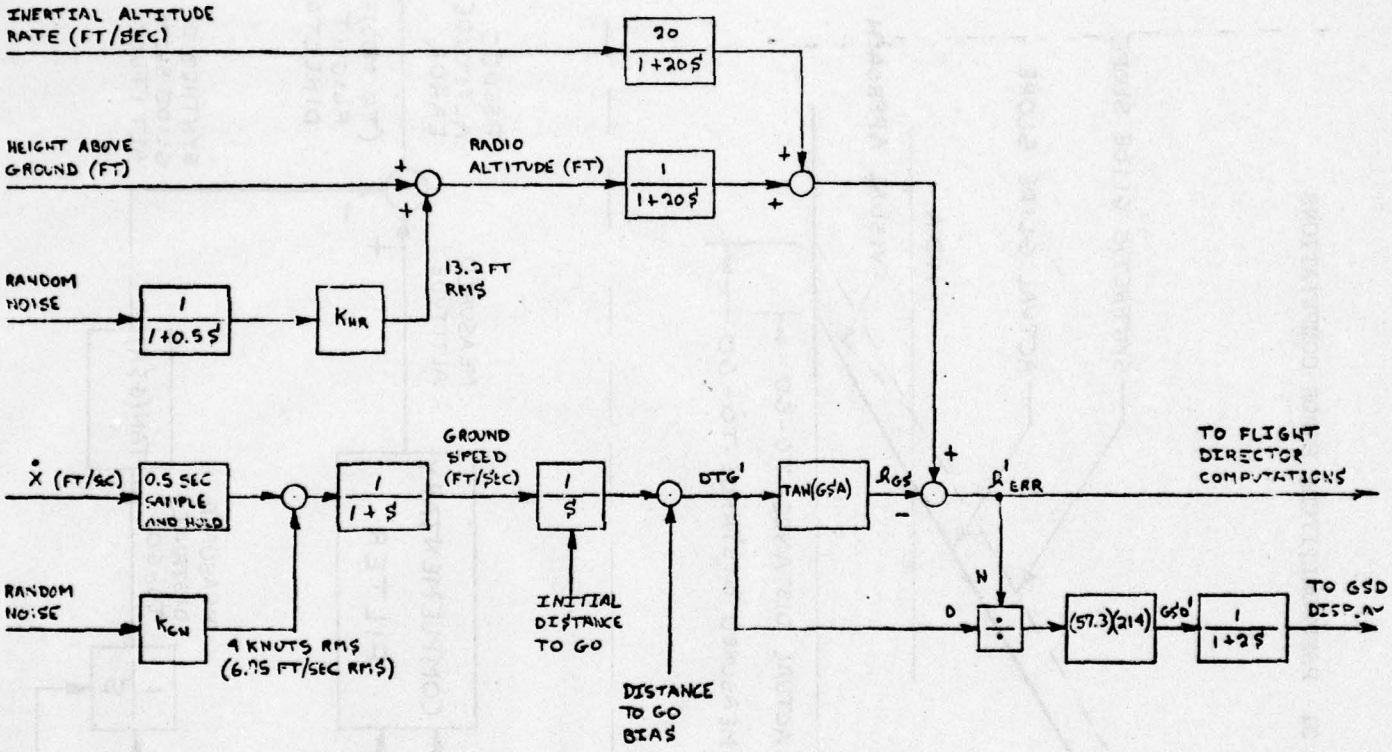

FIGURE 32 SYNTHETIC GLIDESLOPE CALCULATIONS

DAVE TIEDEMAN
23 JAN 79

to an inertial altitude rate. The groundspeed noise did not have a large impact on the flight director performance; consequently, no additional filtering was used for this signal. There was no way to compensate for the distance-to-go bias.

The DC-10-10 aircraft in the landing configuration was used for all of the nonprecision approach analysis and testing. The three-degree-of-freedom longitudinal equations of motion used were the same as for previous analysis work at Collins.

Preliminary analysis showed that, except for the pseudoaltitude error calculation, no change to the modified flight director and speed control systems were necessary to make them compatible with both precision and nonprecision approaches. This similarity meant that the modified flight director and speed control systems for nonprecision approach retained the adequate stability margins and noise suppression capability designed into the precision approach systems. The analysis task then was to determine what effect the sensor errors and biases had on the flight director performance during windshear and to adjust the flight director parameters to minimize that effect.

The analog computer simulation showed that no change to the basic modified flight director control laws was necessary to adapt them to the nonprecision approach problem. The 20-s complementary filter on the radio altitude signal in the synthesized beam calculations was found to be near-optimum for reducing radio altitude noise. Also, distance-to-go noise had much less of an impact on performance than did unfiltered radio altitude noise.

The performance of the modified flight director was examined by looking at the responses of the airplane to the headwind (μ_W) and downdraft (α_W) components of a windshear profile for several different conditions. An altitude error was observed, resulting from the lag on groundspeed, which acted like a distance-to-go bias. Except for this error, the response to the thunderstorm windshear was very similar to the precision approach response. Runs made with radio altitude noise, groundspeed noise, and the combination of both showed that the noise had little effect. With atmospheric turbulence, the effect could be seen on the pitch steering and speed command signals, but there was little change in the altitude error signal. For illustration, traces for a run on the thunderstorm wind profile with bias, noises, and turbulence are shown in Figure 33. The altitude error is with respect to the real glideslope, whereas the glideslope deviation is with respect to the synthesized glideslope. The altitude error shows the true performance of the system while the glideslope deviation shows the performance of the flight director (exclusive of the errors in computing altitude error).

Details of the modified flight director and speed control system for nonprecision approaches were transmitted to Douglas for use in the Task 2, phase 4, tests. Douglas programmed this information on their Sigma 5 computer and Collins checked their simulation. It was noted that the

FIGURE 33 NONPRECISION APPROACH RESPONSES

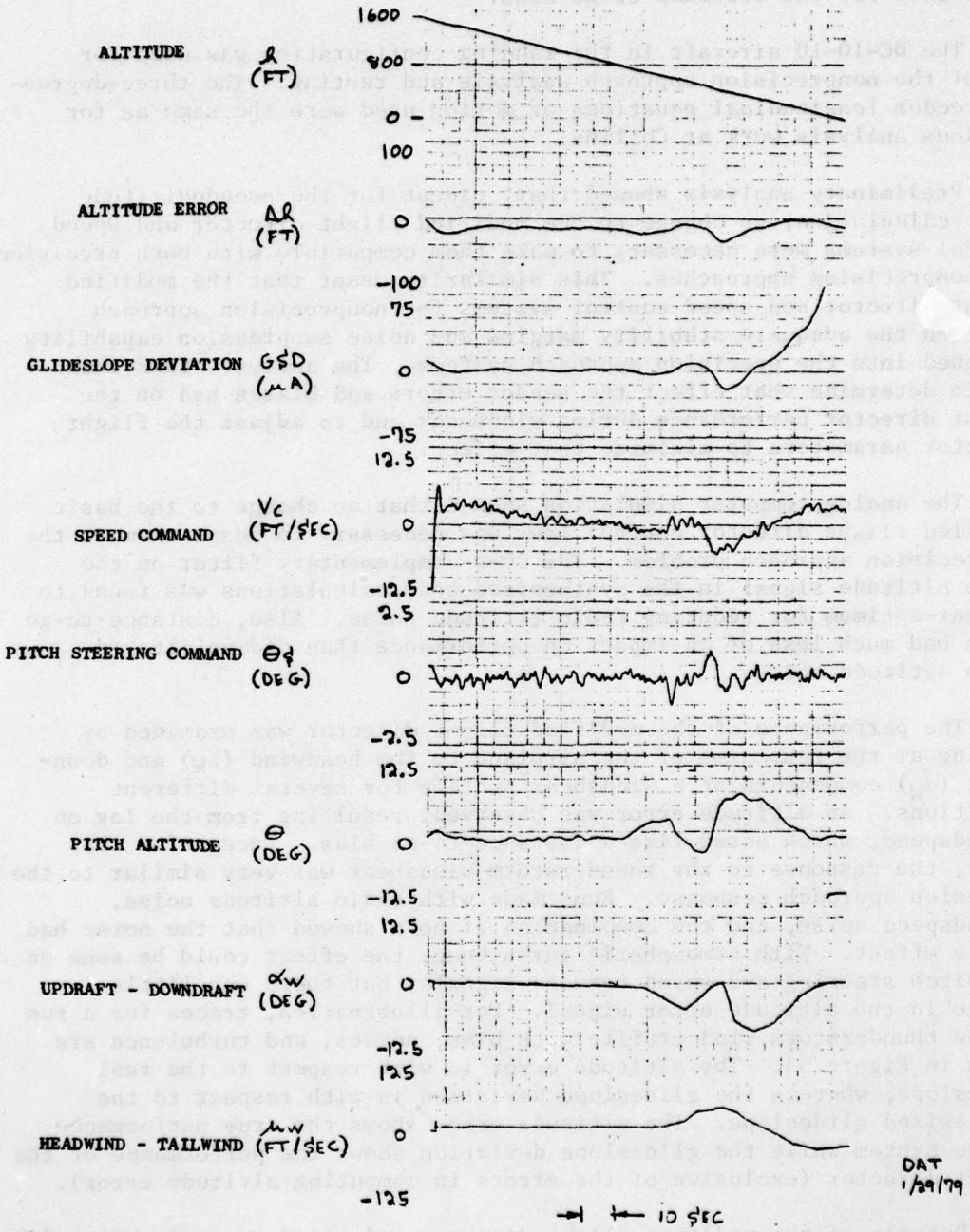

Douglas DC-10 engine model differed from that used at Collins; a block diagram of the Douglas model is shown in Figure 34.

The Collins synthetic glideslope, modified flight director, and fast/slow system were evaluated by airline and test pilots using the Douglas DC-10 moving base simulator during the period 8-12 January 1979. Pilot comments with respect to the Collins system were quite favorable. Details of these Task 2, phase 4, windshear tests are being presented in a report being prepared by SRI.[8] It was concluded that the nonprecision approach tests demonstrated that, by using a synthetic glideslope, the Collins modified flight director and speed control systems can be used to improve aircraft performance for nonprecision approaches in a windshear environment.

FIGURE 34 AUTOTHROTTLE AND ENGINE MODEL

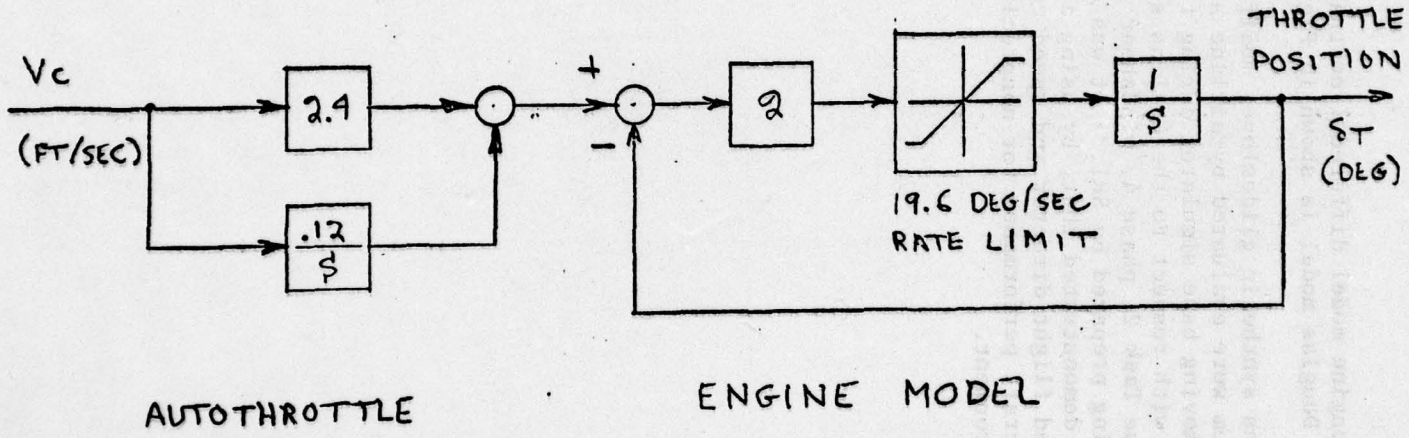

V AUGMENTATION OF THE B-727 FLIGHT DIRECTOR

L. V. Miller, D. J. Clymer

A. B-727 Simulation*

On 18 February 1977, SRI requested Boeing Commercial Airplane Company, Seattle, Washington, to submit a proposal to provide an approach-and-landing model of a B-727-200 airplane suitable for wind-shear simulations. Boeing's proposal B-9200-2-SRI-2 of 4 April was received and evaluated. A subcontract was negotiated and Boeing was authorized to start work on 14 April. Dave J. Clymer was the Boeing project leader.

Boeing's objectives were to provide SRI with a documented six-degree-of-freedom simulation model of the Boeing 727 airplane, and to confirm that the implementation of this model on the Flight Simulator for Advanced Aircraft (FSAA) at NASA Ames Research Center (ARC) accurately reflected the characteristics of the 727 airplane. The simulation was valid only in the approach, touchdown, and go-around modes of operation. Technical support was provided during the evaluation of the effects of atmospheric disturbances conducted by the AWLS team using this 727 simulation.

The simulation represented a typical production configuration of the 727-200 with JT8D-9/7 engines. Since this simulation was implemented on the FSAA installation, maximum use was made of an existing NASA library of simulation programs, including solution of the airplane equations of motion, kinetic equations, trim routines, FSAA motion and visual commands, atmospheric model, and landing gear model. The information provided by Boeing was limited to those modules required to define aerodynamic forces and moments, propulsion system, and flight control systems. Boeing provided the necessary coordination to ensure proper interfacing between the Boeing modules and the existing NASA programs. Boeing also provided the necessary aircraft geometric and mass properties.

The aerodynamic and system characteristics of the 727-200 were simulated for the following configurations and flight conditions:

---

*This section has been compiled from information in letters from Messrs. D. J. Clymer, J. W. Kerrigan, and Michael F. Hazen of Boeing to Dr. Wade Foy of SRI dated 3 May, 10 May, 31 May, and 15 June 1977.

THIS PAGE IS BEST QUALITY PRACTICABLE
FROM COPY FURNISHED TO DTIC

AD-A080 488 SRI INTERNATIONAL MENLO PARK CA F/G 1/2
INERTIALLY AUGMENTED APPROACH COUPLERS. (U)
JUN 79 D A TIEDEMAN, F B BENSON, L V MILLER DOT-FA75WA-3650
FAA-RD-79-118 NL

UNCLASSIFIED

2 OF 2
AD A080488

END
DATE FILMED
3 -80
DDC

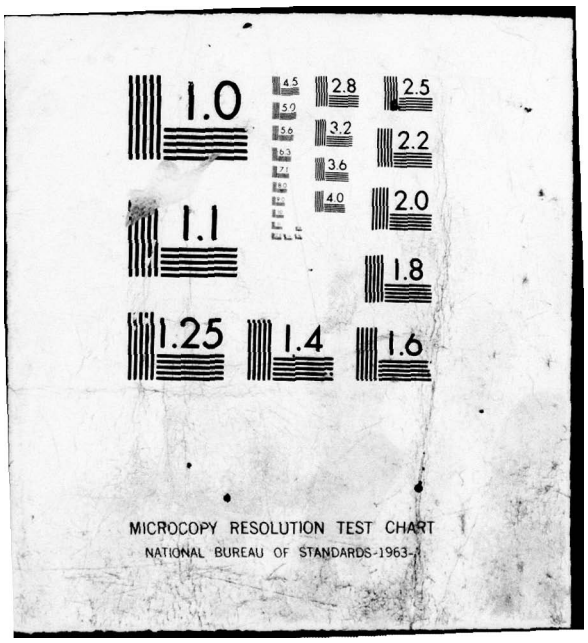
1.0
1.1
1.25
1.4
1.6
1.8
2.0
2.2
2.5
2.8
3.2
3.6
4.0
4.5
5.0
5.6
6.3
MICROCOPY RESOLUTION TEST CHART
NATIONAL BUREAU OF STANDARDS-1963-A

- Flap positions — 15°, 25°, 30°
- Gear — Up or down
- Thrust — Idle to maximum
- Weight — Landing, minimum to maximum
- Speed — 1 g stall speed to flap placard
- Altitude — Sea level to 20,000 ft
- Angle of attack — Not to exceed 25° in stall
- Cockpit — Standard 727 cab layout

All primary flight control systems were simulated in their normal "boost on" operational modes. Information was provided to simulate the following characteristics for the elevator, aileron, spoiler and rudder control systems:

- Control to surface gearing
- Surface rate limits
- Control and surface position limits (including blowdown)
- Pilot control forces
- Stick shaker for control column

Information was also provided to simulate the following secondary flight control systems characteristics:

- Stabilizer trim system rates and position limits
- Flap system rates and flap handle to surface gearing
- Yaw damper systems

Data for the following flight control systems were not provided:

- Speed brakes (spoilers will operate only for lateral control)
- Flight director
- Autopilot
- Autothrottle

Engine steady-state and transient response characteristics for a standard day were simulated for a typical JT8D-9 engine with optional limitations to provide JT8D-7 thrust levels as well. The flight simulation runs terminated upon touchdown, so thrust reversers, brakes, speedbrakes and nose wheel steering were not defined. Constants for the NASA gear model were provided to ensure that dynamics and static gear reactions at touchdown were representative of the 727 airplane. Ground effects were modeled for the longitudinal axis only.

Simulation modeling of ground-based navigational aids was not provided. Data for a linearized model of the 727-200 airplane were supplied to SRI and Collins. The following flight condition was selected:

- Weight = 133,000 lb
- Center of gravity = 25%
- Altitude = 500 ft
- Flaps = 30°, gear down
- Glideslope = 3°

Airspeed was V_{ref} for flaps 30 at 133,000 lb (125 kt) and V_{ref} + 20 kt (145 kt). Two sets of linearized equations were supplied. One set contained the aerodynamic derivatives excluding all thrust effects. The other set had thrust effects included in the speed and angle of attack derivatives.

The full six-degree-of-freedom nonlinear model had aerodynamic coefficient buildups presented in equation form with sketches of the typical magnitudes and variations in the data tables. Also included was a schematic showing the sign convention and an overall simulation block diagram to assist in integrating the aerocoefficient buildup with the existing NASA-FSAA simulation modules.

The control systems were presented in terms of required inputs and the resulting output parameters. Sketches of typical data magnitudes and variations were included. The yaw damper, stick shaker, and flap models were included in this section.

The engine model was presented in block diagram form with a list of parameter definitions. This format was deemed most straightforward owing to the complex empirical engine model gains required to simulate the engine dynamics accurately.

Data listings, data cards, and computer plots were prepared for all the control, aerodynamic, and engine functions. After NASA engineers had programmed the model in the FSAA computer, the model was checked. Boeing provided information to check out the following: static checkout, longitudinal trim, speed stability, wind-up turns, rate of climb, and level acceleration. In addition, output from a small disturbance computer program was included to provide typical values of phugoid, short period, and Dutch roll frequencies and damping.

Boeing engineering support was provided during checkout and validation of the simulation. A Boeing pilot conducted a qualitative evaluation of the FSAA flying qualities. Boeing personnel also monitored the B-727 windshear tests conducted by SRI and the rest of the AWLS team.

B. Modified Flight Director (MFD) for B-727*

The objective of this subtask of the Collins work was to implement both baseline and modified flight director laws and to evaluate their comparative performance in a windshear environment on a standard size airline aircraft, a B-727-200, on final approach.

A simulated pilot model, autothrottle, and yaw damper were employed to obtain objective analysis results and to provide a basis of verification for system checkout in the Ames FSAA. Human pilots were used to verify the flyability of the modified flight director system and to provide further comparison between the two systems. The baseline flight director system employed in the study was typical of those in service with the B-727 fleet. The modified flight director of the previous DC-10 study was used as a foundation for this development. Improvements on the design included an increase in the pitch complementary filter bandwidth, an increase in $\dot{h}$ error gain and additional pitch rate to retain adequate damping. This MFD design provided anticipatory signals in both the pitch and lateral axes to counter disturbances and reduce the tracking errors in shear conditions.

1. Pilot Models and Inner Loop Stabilization

Figure 35 is a block diagram of the pilot model used to close the pitch loop for system synthesis, analysis, and checkout. This model was chosen as representative of a human pilot's reaction to the ADI pitch command bar. Figure 36 depicts the autothrottle employed to control the speed axis during the synthesis, analysis, and checkout of the steering axes.

A first-order lag with a time constant of 0.1 s and a gain of 4.0° of wheel angle per degree of roll steering command were used to simulate a pilot's response to the roll command bar. The study employed a simplified yaw damper of the form:

$$\frac{\text{Rudder position (deg)}}{\text{Yaw rate (deg/s)}} = \frac{5\ s}{(0.8892\ s^2 + 3.162\ s + 1)}$$

---

*This section is a compilation of excerpts from the following Collins report:

Miller, L. V., "Collins Development of a Modified Flight Director for the B-727 in Windshear, GFC-183," (6 January 1978).

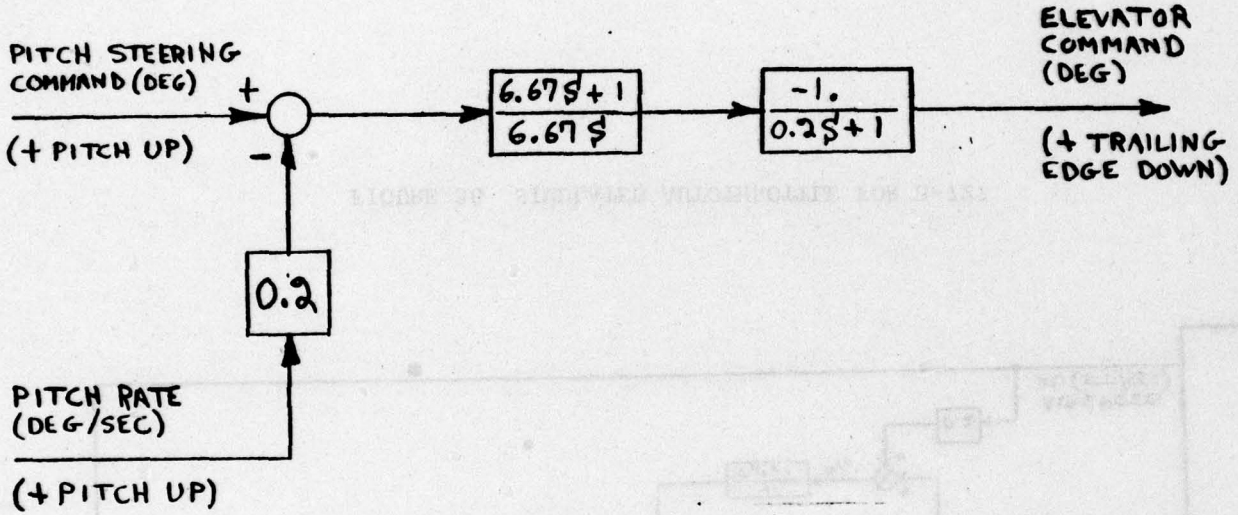

FIGURE 35 SIMULATED PITCH PILOT FOR B-727

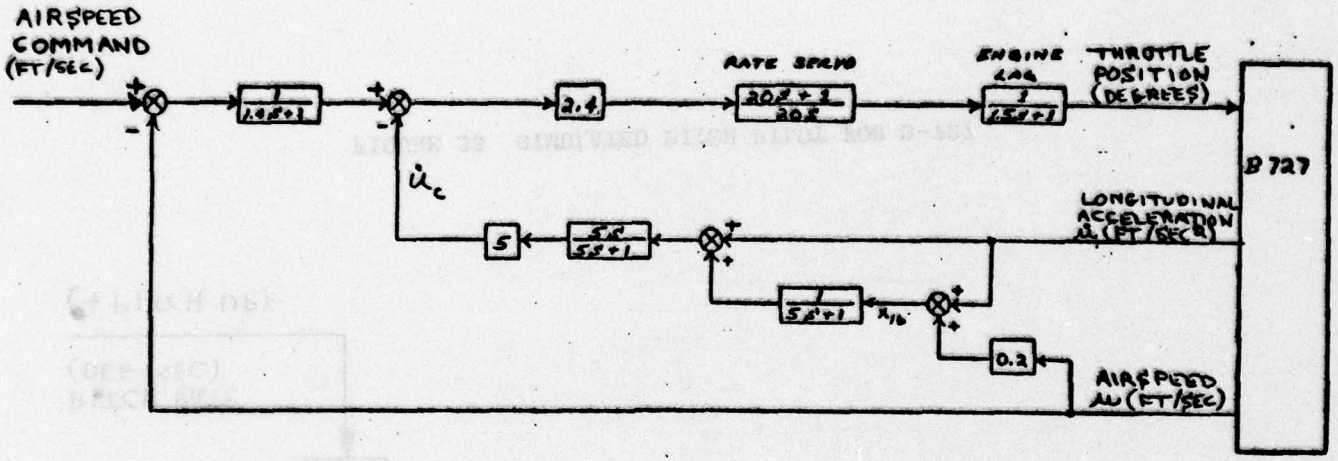

FIGURE 36 SIMULATED AUTOTHROTTLE FOR B-727

2. Baseline Flight Director System

A standard flight director design was used as a baseline to measure the performance of the modified flight director in a windshear environment. The baseline flight director algorithm structure for this study was representative of that employed on a majority of today's air-carrier aircraft. Figures 37 and 38 are block diagrams of the baseline longitudinal and lateral track laws, respectively. While the gains, time constants, and gain programming vary for different aircraft types (as well as for different users of the same aircraft type), these diagrams typified the guidance and steering laws employed in the current B-727 fleet.

In Figure 37, the pitch steering signal was merely the sum of gain-programmed glideslope deviation and high-passed pitch. The gain programmer was used to adjust the gain within the glideslope signal path to account for the increased angular sensitivity of the beam that occurs closer to the runway.

In considering the response of this algorithm to windshears, we note two inadequacies:

- The response of the aircraft required to remain on glideslope in a ramping headwind is a constant pitch rate. The output of the high-passed pitch filter will then be a constant nonzero value and a steady-state glideslope deviation will be required to null the pitch command.
- There is no vertical rate or, better yet, normal acceleration information in this algorithm. In the presence of vertical shears, no corrective pitch command will occur until a glideslope error accrues. Hence, there are no anticipatory corrective commands and large vertical deviations from the glidepath can be expected in the presence of vertical shears.

The lateral steering command depicted in Figure 38 was the sum of localizer deviation and complemented lateral rate. No gain programming was employed on localizer deviation. A complementary filter was used to derive beam rate error for damping. The input signal to this filter was comprised of localizer deviation, roll attitude, and heading.

Similar to the pitch axis, inadequacies are noted in this algorithm in the presence of a lateral windshear. The existence of the high-passed heading signal in the derived rate term will result in a steady-state output of the complementary filter. A localizer deviation will be required to null the roll command. Also the lack of lateral acceleration information means no anticipatory roll command will result from shear-generated side forces, and corrective roll commands will occur only after a localizer track error has accrued.

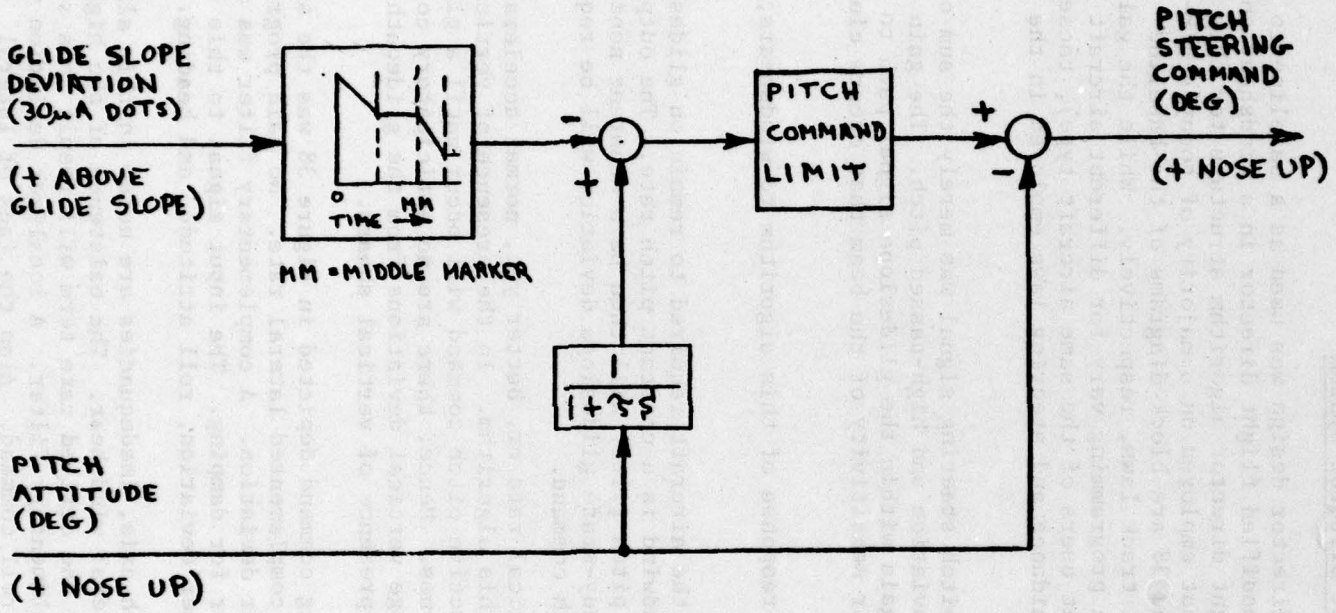

FIGURE 37 LONGITUDINAL TRACK LAW: BASELINE FLIGHT DIRECTOR

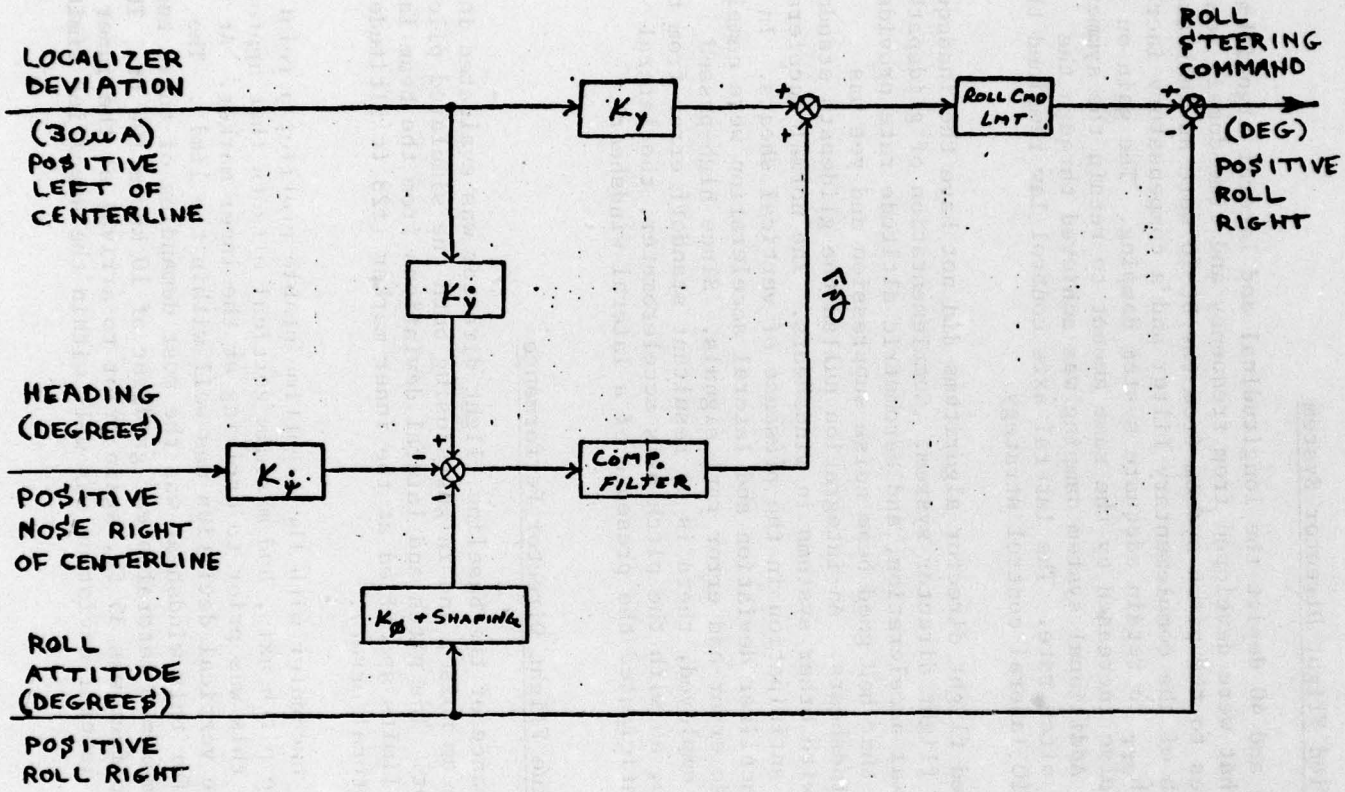

FIGURE 38 LATERAL TRACK LAW: BASELINE FLIGHT DIRECTOR

Frequency responses of the baseline longitudinal and lateral flight director systems with the simulated pilot models were obtained. Adequate stability margins were observed in both the longitudinal and lateral axes.

3. Modified Flight Director System

Figures 39 and 40 depict the longitudinal and lateral algorithms for the B-727 that were developed from frequency and time domain analyses. Principal changes to the pitch system from the DC-10 were an increase in the bandwidth of the complementary filter and a compensatory increase in the gain on $\dot{h}_{err}$ to retain adequate system damping. The gain on the beam error was also increased by the same amount to retain the symmetry of the filter. Additional system damping was achieved through the introduction of pitch rate. The lateral axis control law remained the same as the DC-10 lateral control strategy.

The modified flight director algorithms did not have the inadequacies of the baseline flight director system. Complementation of glidepath beam error, normal acceleration, and barometric altitude rate provided a filtered signal that had good beam noise suppression and yet was responsive to windshears. An integration nulled the glidepath standoff error observed with other systems in windshears. The normal acceleration signal provided anticipation in the presence of vertical shears. In the lateral axis, localizer deviation and lateral acceleration were complemented to provide error and error rate signals. Since high-passed heading was not employed, there is no resultant standoff error from the localizer. Also, as with the pitch axis accelerometer, the lateral accelerometer anticipated the presence of a lateral windshear.

4. Baseline Flight Director Performance

The performance of the baseline flight director was evaluated in calm air, with beam noise, and in gusts using both the simulated pilot and a human pilot. The pitch and lateral deviations from the beam lay well within the limits specified at the inner marker (±28 ft altitude error, ±75 ft lateral error).

A simulated encounter with the nighttime stable profile, a relatively mild shear in the pitch axis, had maximum vertical offsets that approached 20 ft. However, this was prior to arriving at the inner marker. At the inner marker, the vertical deviation was well within the limit. The lateral profile for this windshear was the most demanding of those tested and exhibited a maximum lateral shear gradient of 10 knots/100 ft. The maximum lateral offset was 35 ft, again prior to arrival at the inner marker where the lateral deviation was well within the specified limits.

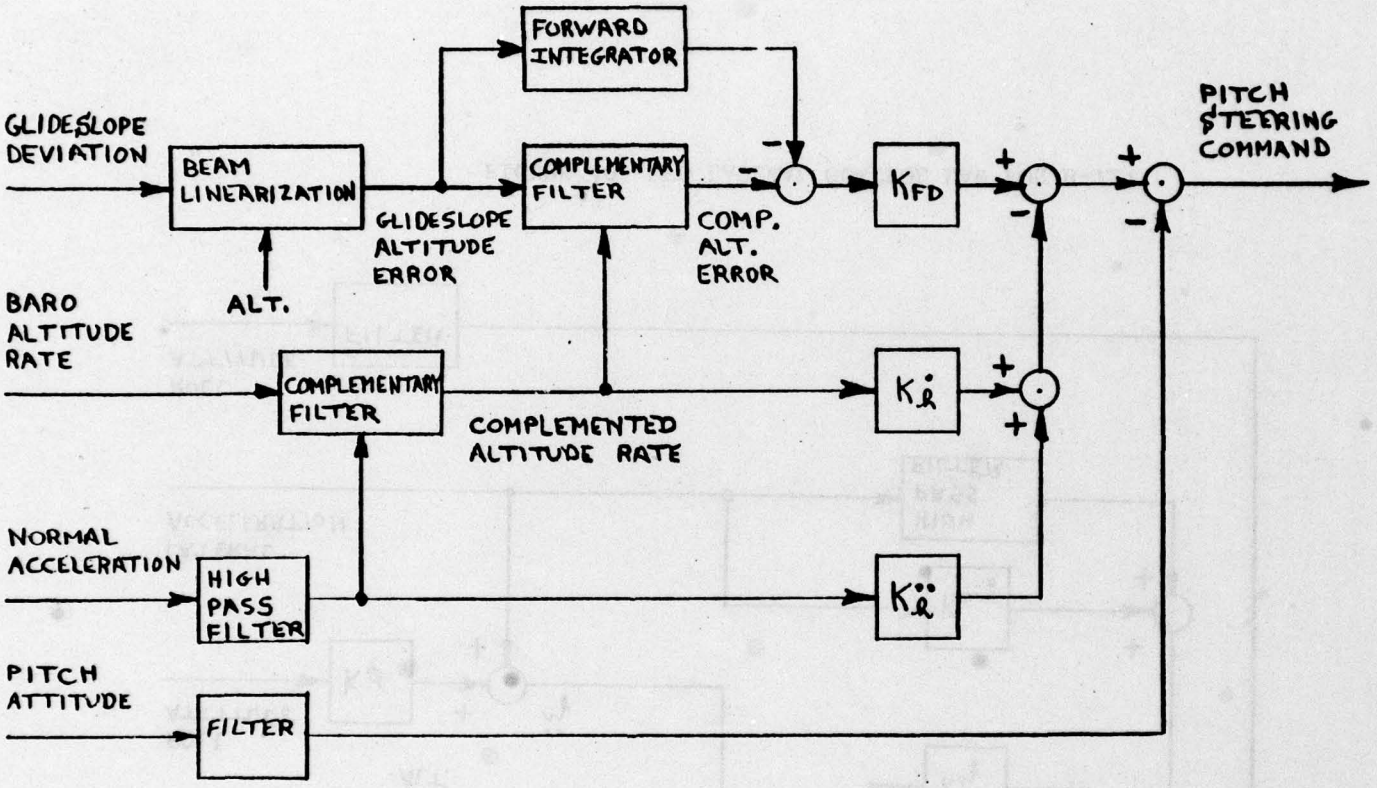

FIGURE 39 LONGITUDINAL CONTROL LAW FOR B-727

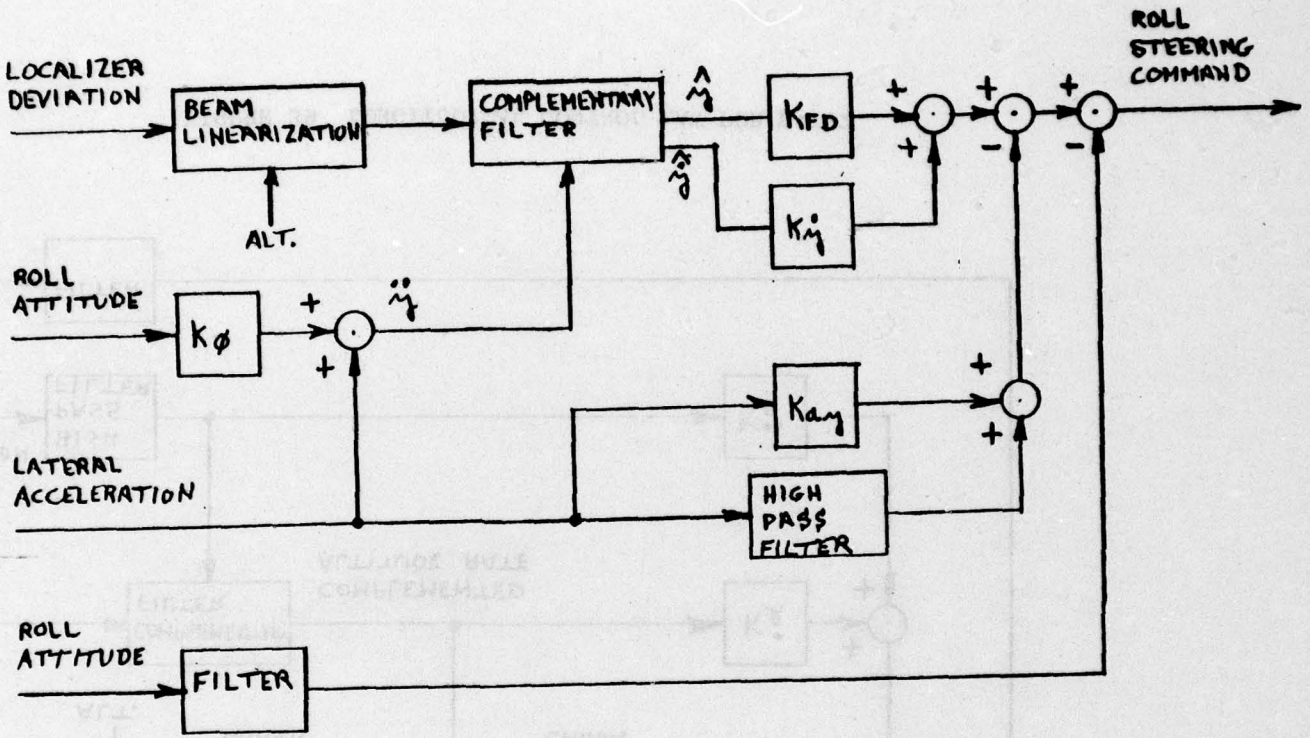

FIGURE 40 MFD LATERAL CONTROL LAW FOR B-727

A simulated encounter with the frontal shear induced marginal performance with the simulated pilot model where vertical offsets reached 40 ft, very close to the inner marker. Surprisingly, the human pilot was able to perform better on this particular trial. However, if taken over an ensemble of pilots and trials, marginal results would be anticipated. The lateral deviation was also significant, but was not outside the limits.

The thunderstorm windshear profile presented a severe challenge to the baseline flight director system. While the lateral deviation was within limits, the vertical deviation from the beam approached or exceeded 100 ft inside the middle marker for both the simulated as well as the human pilot. This was unacceptable.

The combination of beam radio noise, wind gusts, or turbulence, and an encounter with the thunderstorm windshear profile is depicted in Figures 41a and 41b, which shows the catastrophic results.

5. Modified Flight Director Performance

The performance of the modified flight director was also evaluated in calm air, with beam noise, and in gusts using both the simulated pilot model and a human pilot. The pitch and lateral deviations from the beam in all cases lay well within the approach gate limits of the inner marker, and were smaller for the modified flight director than for the baseline flight director.

In an encounter with the nighttime stable boundary-layer shear offsets from the beam in both the lateral and pitch axes with both simulated and human pilots were not only well within the limits of the approach gate at the inner marker, but also were significantly less than with the baseline flight director.

The performance of the modified flight director system in a frontal shear encounter was better in both axes with both the pilot model and the human pilot when compared to the results obtained with the baseline flight director. Although the vertical offset approached the limit with a beam deviation of about -25 ft, it was within the specified limit, as opposed to the -40 ft of vertical deviation observed with the baseline system.

In a simulated encounter with the thunderstorm windshear for the modified flight director system, performance was within limits with either pilot. The combination of beam radio noise, turbulence, and an encounter with the thunderstorm windshear profile is depicted in Figures 42a and 42b. Note that even in this extreme environment, the maximum vertical offset from the beam inside the middle marker was less than 30 ft for both the simulated and the human pilots.

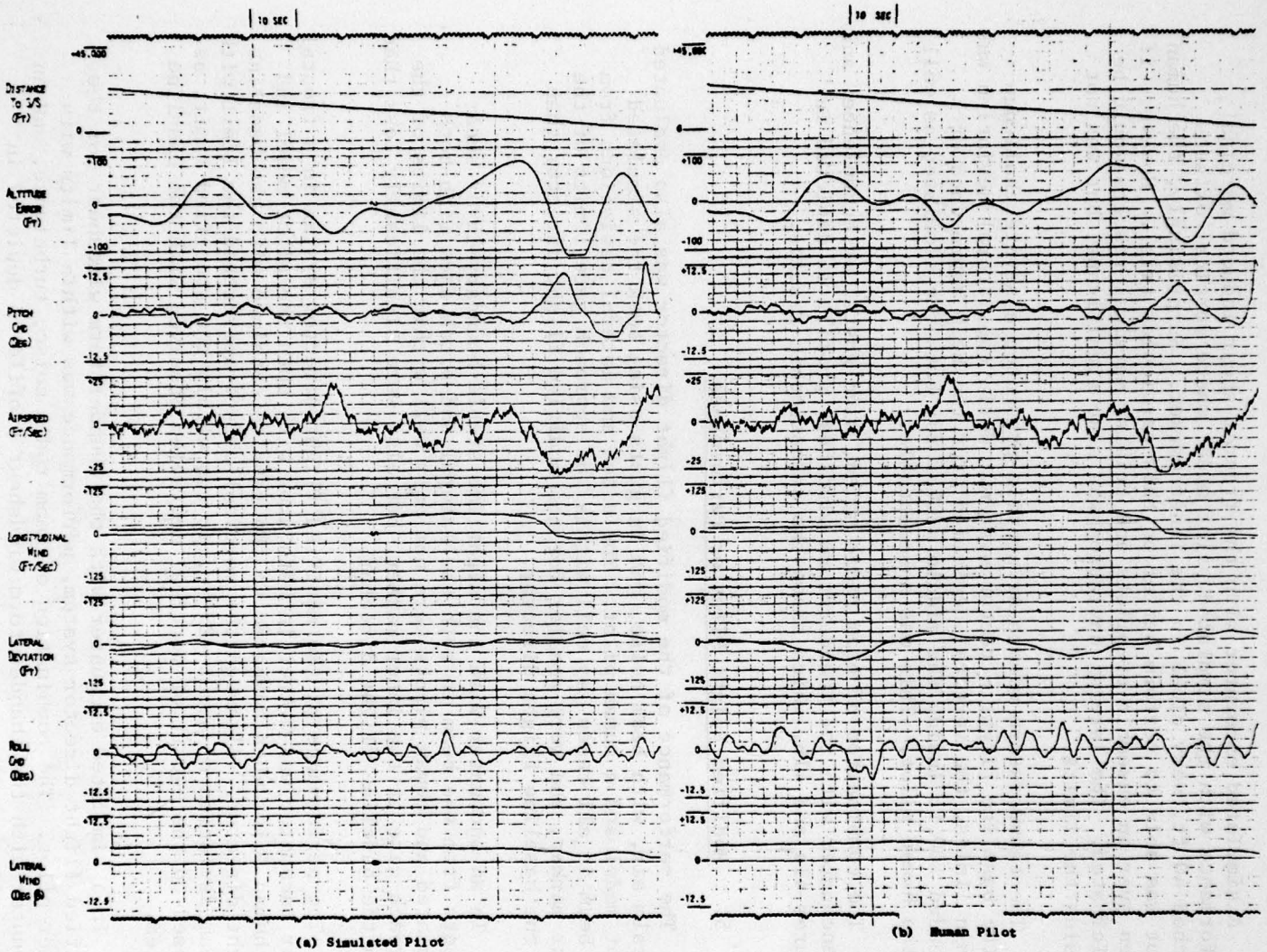

FIGURE 41 BASELINE F/D COMBINATION

(a) Simulated Pilot

(b) Human Pilot

FIGURE 42 MODIFIED F/D - COMBINATION

Table 3 compares the performances of the baseline and modified flight director systems. Unlike the baseline flight director results, deviation from the beam in frontal and thunderstorm profiles (as well as the combination of a thunderstorm profile, beam noise, and turbulence) resided well within the specified limits with the modified flight director system.

It was concluded that the modified flight director considerably improved the performance in windshear and beam noise environments when compared with the baseline flight director.

6. Flight Director Checkout at NASA Ames

Tests of several windshear aiding concepts as they apply to the B-727 were conducted on the Flight Simulator for Advanced Aircraft (FSAA) at NASA-Ames during July 1977. Among these concepts were the baseline and the modified flight director systems. A detailed report has been written by SRI International.[9]

The FSAA consists of a full six-degree-of-freedom motion base cab and a Sigma 8 digital computer on which the B-727 and both flight director algorithms were programmed. The cab was configured to resemble a B-727 flight deck. A Rockwell-Collins 329B-8G attitude director indicator was used to display attitude and command information to the pilot. The visual was provided by a Redifon display system. The flight director algorithms were simulated by implementing them in a standard difference equation format in Fortran language on the Sigma 8 and sampling at an adequate rate.

Considerable effort was expended to assure that the flight director algorithms were implemented properly on the FSAA simulator. Open-loop frequency responses showed the frequency response from each sensor input to steering command output for each algorithm; these were compared with ones generated at Rockwell-Collins. The results of these comparisons were very good, indicating that the algorithms were implemented properly. The response of each system to a step in position of aircraft center of gravity (in altitude and lateral position) compared closely with step responses recorded at Cedar Rapids. These step responses, performed with a simulated pilot to assure objective results, confirmed that the algorithms had been correctly programmed.

THIS PAGE IS BEST QUALITY PRACTICABLE
FROM COPY FURNISHED TO DDC

Table 3

PERFORMANCE OF BASELINE AND MFD SYSTEMS

Wind Condition	Vertical Offset From 3° Glideslope (ft)			Pitch Command (Deg)	
	Max Above	Max Below	100 ft D.H.	Max Nose Up	Max Nose Down
Turbulence					
Baseline	26	26	20	2.5	2.5
Modified	16	12	4	2.5	4.0
Frontal shear					
Baseline	40	40	-38	4.5	∿
Modified	10	20	-20	2.0	2.0
Thunderstorm shear					
Baseline	68	120	34	12.5	5.5
Modified	16	30	15	3.8	2.3

VI MFD IMPLEMENTATION IN GULFSTREAM I

The last subtask undertaken by Collins was the design, fabrication, installation, and checkout of the modifications required to implement the MFD algorithms in the flight director of a test airplane. The aircraft selected was the FAA Grumman Gulfstream I, based at the National Aviation Facility and Experiment Center; the modifications were installed in the Collins model FGC-80 flight director of the Grumman.

Longitudinal and lateral MFD control laws were installed by Collins under another FAA contract. The work on this AWLS Task 5 subtask, then, was concerned with the provision of the MFD thrust command, which was displayed on the Fast/Slow indicator of the flight director. In carrying out the job, Collins performed a simulation and analysis to adapt the acceleration-augmented algorithms to the Gulfstream I.

The localizer control law was modified to lower the course error washout time constant from 4 seconds to 1 second in the track mode. A lateral accelerometer was added to partly offset the reduced damping supplied by the faster course error washout and to provide a further reduction in beam standoff during shears. Glideslope tracking performance in the presence of severe windshears was improved slightly with a 25% increase in glideslope deviation gain. In addition, command activity due to beam noise was reduced by using a 2 second complementary filter on the beam deviation.

Either of two speed-control modes--IAS or windshear--may be selected. For the IAS mode, a conventional airspeed control law is used. In the windshear mode, computed headwind (TAS-GNS) minus a bias is added to airspeed error, resulting in a commanded ground speed equal to the desired airspeed minus the bias. If the pilot sets the bias equal to the reported ground headwind, this control scheme will maintain a constant inertial speed in a decreasing headwind. Longitudinal acceleration is used for damping. Pitch attitude is retained in the computations. It is important that the lags on IAS error, TAS, and ground speed be identical.

Based on the simulation results, the modified flight director should provide very good glideslope and localizer tracking performance even in severe windshears. The simple airspeed control system will provide adequate performance, but the windshear mode of the speed command gives slightly better glideslope tracking while significantly reducing pitch attitude and throttle excursions.

The modifications were checked out in the Collins test facility. Collins began work on this subtask in November 1978 and completed it 15 June 1979, after which the airplane and its modified flight director were returned to the FAA for test.

VII CONCLUSIONS

Task 5 of the AWLS project was a complex job, involving the application of new control techniques to solve especially difficult problems presented by environmental conditions such as severe windshear. Collins engineers carried the work from initial design studies through detailed analysis of the candidate algorithms, simulation on an analog computer, and tests with both human pilots and simulated autopilots. Designs were developed for fully automatic control, for flight director coupled to a full ILS, and for flight director for nonprecision approaches. Detailed control laws were designed for a four-engine jet (the CV-880), a wide-body jet (the DC-10), a medium jet airliner (the B-727), and a two-engine turboprop test airplane (the Gulfstream I). The designs were tested and, in the case of the Gulfstream, carried to implementation in flight hardware. Collins engineers also put these MFD algorithms on the large piloted flight simulators used in Task 2 for windshear tests.

When compared to conventional autopilots and flight directors in current use, the acceleration-augmented algorithms showed considerable quickening. They responded much more quickly to wind changes. On the other hand, the complementary filters enabled them to "ride through" guidance beam dropouts and other disturbances. With even experienced pilots, on first exposure to the quickened commands of the MFD, there was some indication that the MFD was too responsive. However, the tests at Collins and the windshear flight simulation tests showed that, with proper pilot training, these control laws provided significantly better performance in a wind shear environment than conventional systems. Also, somewhat surprisingly, the pilots' subjective estimates of their workload on approach and landing in windshear and turbulence were not any higher with the MFD than with the conventional. In short, the Collins acceleration-augmented (MFD) controls were both flyable and acceptable to airline pilots.

The emphasis throughout the task was on relatively inexpensive methods for improving the performance of conventional airplane controls. Therefore, the investigations centered on augmentation of the standard sensor set with body-mounted accelerometers. In the tests at Collins, the new-design (MFD) control laws were subjected to noise, gusts, beam disturbances and four windshear profiles of different degrees of severity. The CV-880 study showed that the system design with body-mounted accelerometers performed as well as that based on a full inertial navigation system, which would be much more expensive. The new controls demonstrated in simulation their ability to provide a Category-III level of airplane control on ILS beams rated to only Category I or II standards. All the Collins studies showed that the new MFD control algorithms could provide performance in severe wind shear superior to

that of conventional controls. This conclusion was confirmed for the flight directors in the large-scale piloted simulation tests of Task 2, which had as many as 12 different wind shear profiles and included test sets with enough subject pilots to be significant. It was apparent that the Collins Modified Flight Director can provide an aircraft with more protection against the effects of windshear then is available with a conventional system.

Appendix A

WIND, TURBULENCE, BEAM NOISE AND BEAM DISTURBANCE MODELS

A. Wind Profiles with Shear

Four test wind models were defined by the FAA.

Shear 1: Logarithmic Profile (Neutral Boundary Layer). Total wind magnitude for this shear was

$$V(Z) = \frac{V(20)\ \ln\ (Z/1.5)}{\ln\ (20/1.5)} \text{ knots}$$

where

Z = wing height above ground level (ft)

V(Z) = wind speed at height Z (knots)

V(20) = reference windspeed at Z = 20 ft (knots)

The reference windspeed was 23 knots. Figure A-1 shows the wind velocity/gear altitude profile as simulated for the longitudinal axis and the lateral axis in the CV-880 and B-727 studies.

For DR-10 simulations, the wind direction on profile 1 was assumed to be 30° off runway centerline; consequently, the longitudinal and lateral profiles were attentuated 87 and 50%, respectively.

Shear 2: Nighttime Stable Boundary Layer. This profile had the following specified magnitude between 30 and 1500 ft:

Wing Altitude (ft)	V(Z) (knots)
30	7.7
75	11.7
150	19.7
300	23.7
450	32.5
600	29.9
750	26.2
900	23.4
1050	22.8
1200	22.5
1300	22.2
1500	22.2

Below 30 ft the following equation was used:

$$V(Z) = 7.7\left(\frac{Z}{30}\right)^{0.45} \text{ knots}$$

Figure A-2 shows the profile as simulated for the B-727 study. In the CV-880 work in the longitudinal axis, the total wind was taken as headwind, and in the lateral axis the total wind was used in crosstrack.

For DC-10 simulations, the wind direction on profile 2 was assumed to be 30° off runway centerline; consequently, the longitudinal and lateral profiles were attenuated 87 and 50%, respectively.

Shear 3: Frontal Winds. This wind model was based on a reconstruction of the conditions of the Iberia Airlines DC-10-10 flight 933 at Logan Airport, Boston, on 17 December 1973. The total wind magnitude was modeled as:

$$V(Z) = 7\left(\frac{Z}{30}\right)^{0.43} \text{ knots} \qquad 0 \leq Z \leq 1500 \text{ ft}$$

This shear had a characteristic change of direction specified as follows:

$$\theta = 120 + \theta_0 \qquad 400 \leq Z \leq 1500 \text{ ft}$$

$$\theta = 0.4(Z - 100) + \theta_1 \qquad 100 \leq Z \leq 400 \text{ ft}$$

$$\theta = \theta_0 \qquad 0 < Z < 100 \text{ ft}$$

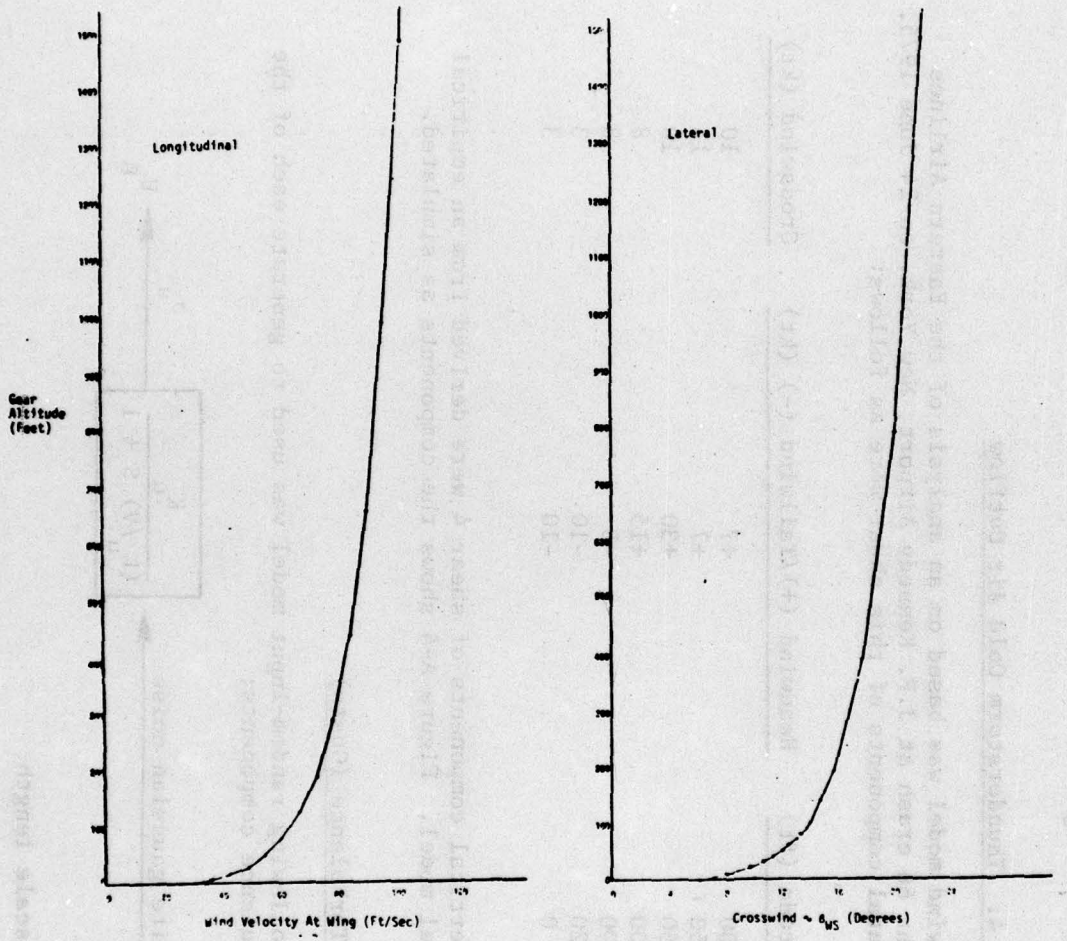

FIGURE A-1 SHEAR 1 - LOGARITHMIC PROFILE

where

θ = wind direction (deg)

θ_0 = wind direction at touchdown (deg)

Figure A-3 shows the shears for the longitudinal and lateral axis simulations with θ_0 equal to zero.

Shear 4: Thunderstorm Cold Air Outflow

This wind model was based on an analysis of the Eastern Airlines B-727 flight 66 crash at J.F. Kennedy Airport, New York, on 24 June 1975. The horizontal components of this shear were as follows:

Wing Altitude (ft)	Headwind (+)/Tailwind (-) (kt)	Crosswind (kt)
1500	+7	10
750	+7	13
450	+30	10
300	+15	8
200	-5	8
20	-10	3
0	-10	3

The vertical components of shear 4 were derived from an empirical mathematical model. Figure A-4 shows the components as simulated.

B. Wind Turbulence (Gusts)

The following random-input model was used to generate each of the three turbulence components:

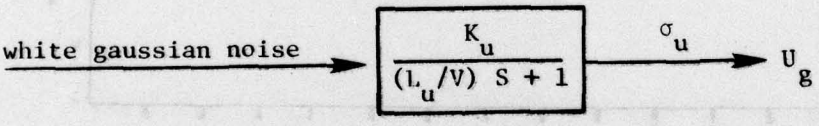

L_u = scale length

V = approach velocity (airspeed)

σ_u = rms intensity

K_u = gain constant

K is adjusted to obtain the correct output intensity (σ_u).
U_g is longitudinal gust, the component of wind over the ground.

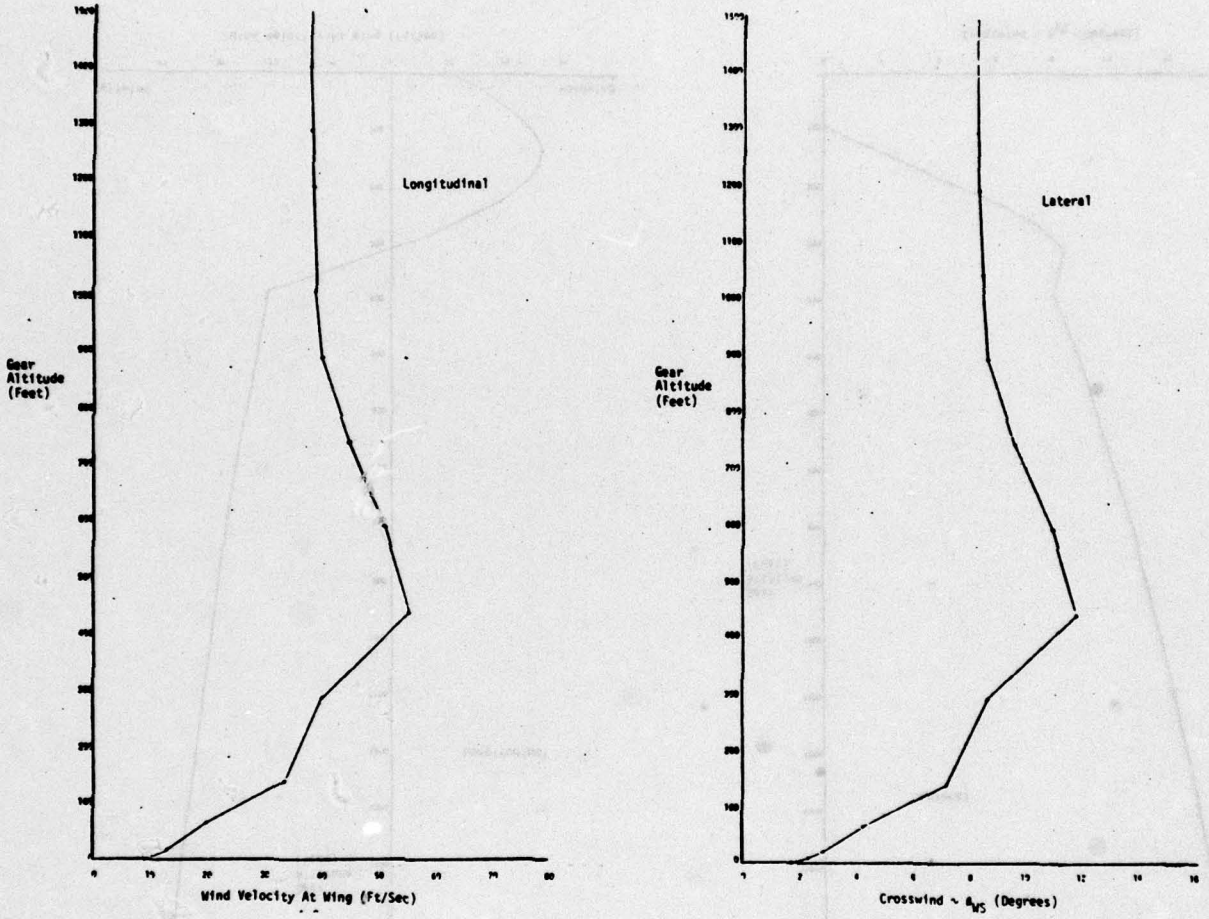

FIGURE A-2 SHEAR 2 - NIGHTTIME STABLE

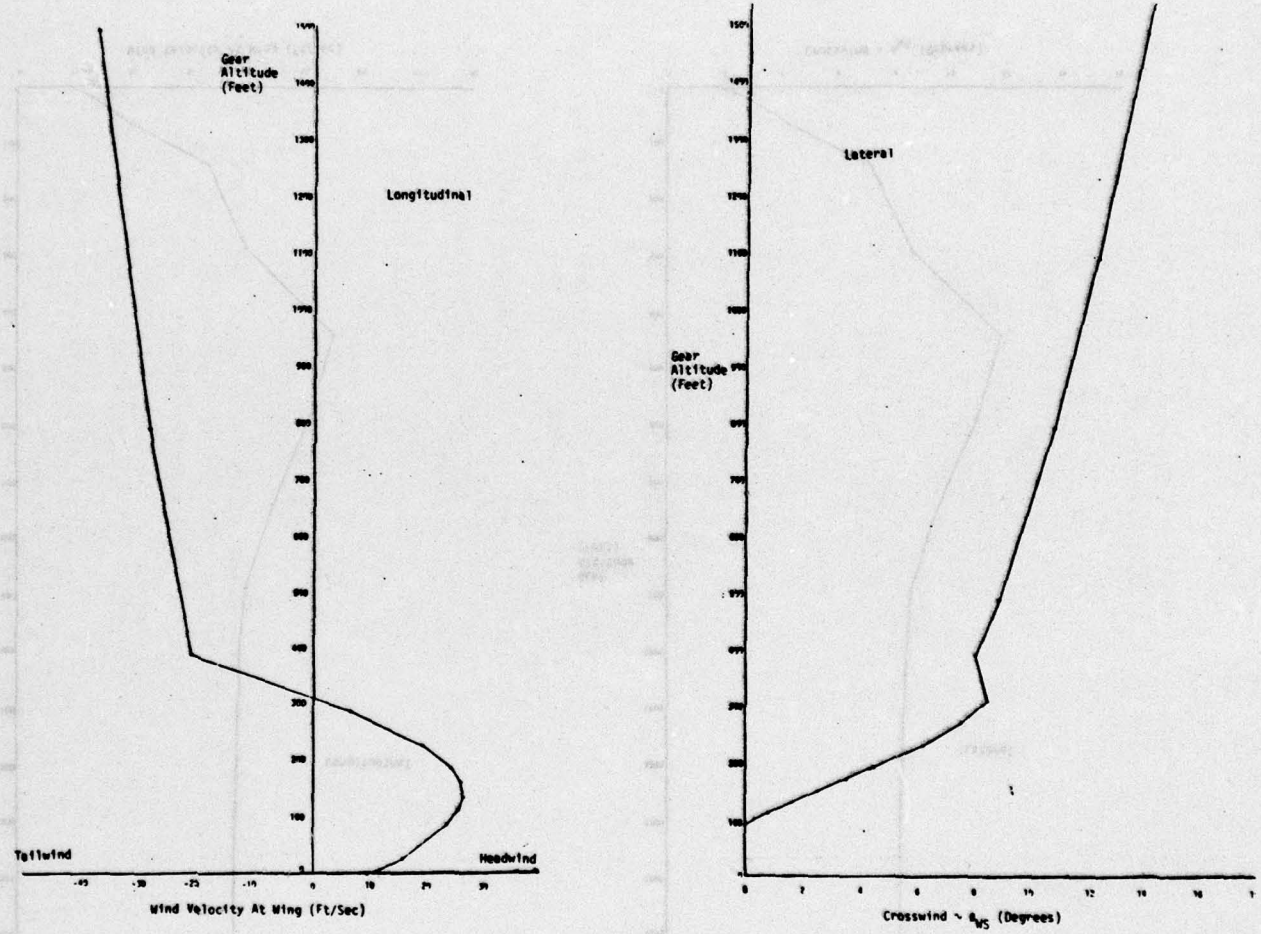

FIGURE A-3 SHEAR 3 - FRONTAL PROFILE

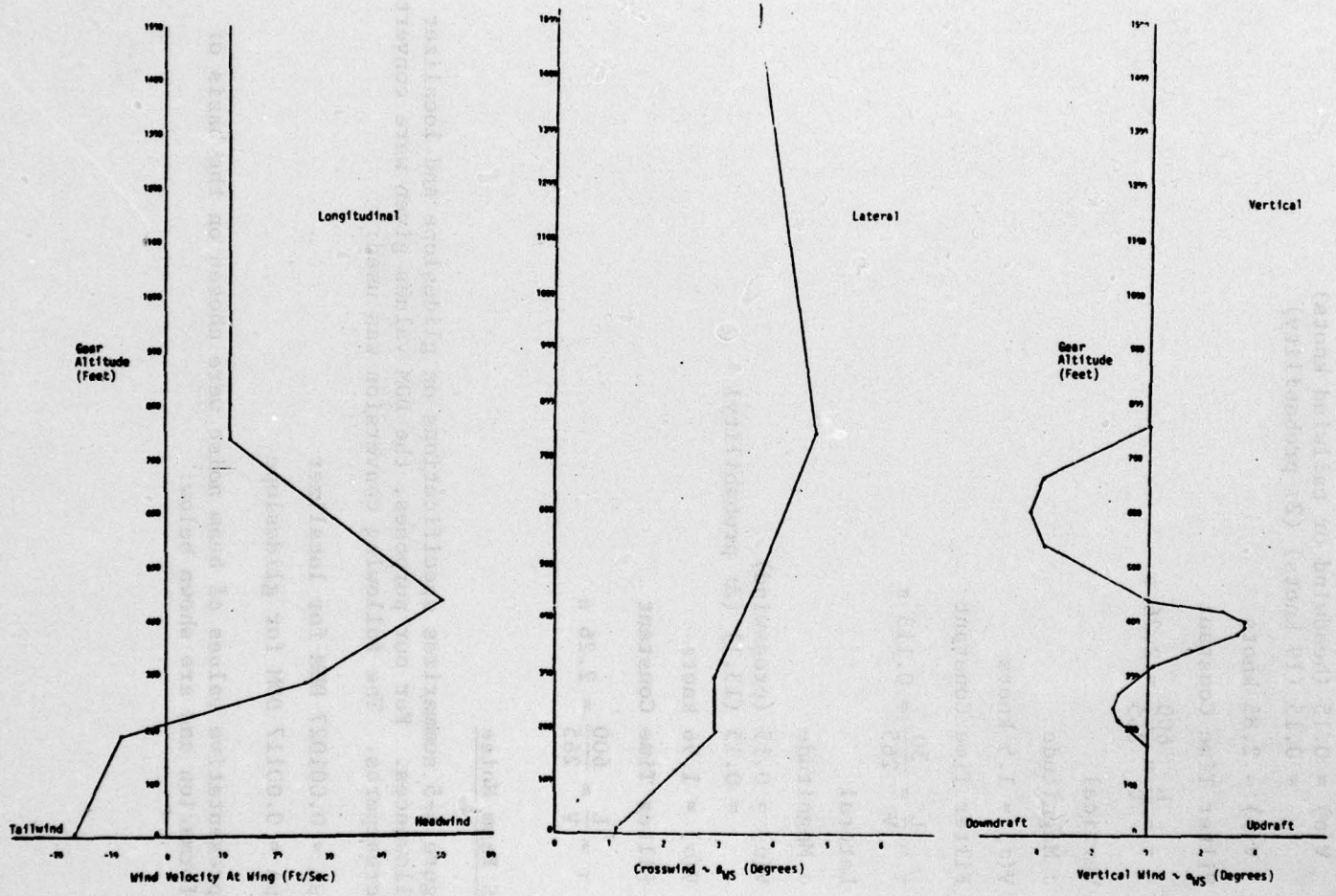

FIGURE A-4 SHEAR 4 - THUNDERSTORM COLD AIR OUTFLOW

The specifications for wind turbulence parameters were:

- Longitudinal

  σ Magnitude

  $V(\sigma)$ = 0.15 (headwind or tailwind knots)
  = 0.15 (19 knots) (2σ probability)

  $V(\sigma)$ = 2.85 knots

  Filter Time Constant

  $$\tau = \frac{L}{V} = \frac{600}{265} = 2.26 \text{ s}$$

- Vertical

  σ Magnitude

  $V(\sigma)$ = 1.5 knots

  Filter Time Constant

  $$\tau = \frac{L}{V} = \frac{30}{265} = 0.113 \text{ s}$$

- Lateral

  σ Magnitude

  $V(\sigma)$ = 0.15 (crosswind)
  = 0.15 (13.1) (2σ probability)

  $V(\sigma)$ = 1.96 knots

  Filter Time Constant

  $$\tau = \frac{L}{V} = \frac{600}{265} = 2.26 \text{ s}$$

C. ILS Beam Noise

Figure A-5 summarizes specifications on glideslope and localizer noise allowances. For our purposes, the DDM values given were converted into microamperes. The following conversion was used:

1 μA = 0.001027 DDM for localizer

1 μA = 0.00117 DDM for glideslope

Representative values of beam noise were chosen on the basis of this information and are shown below:

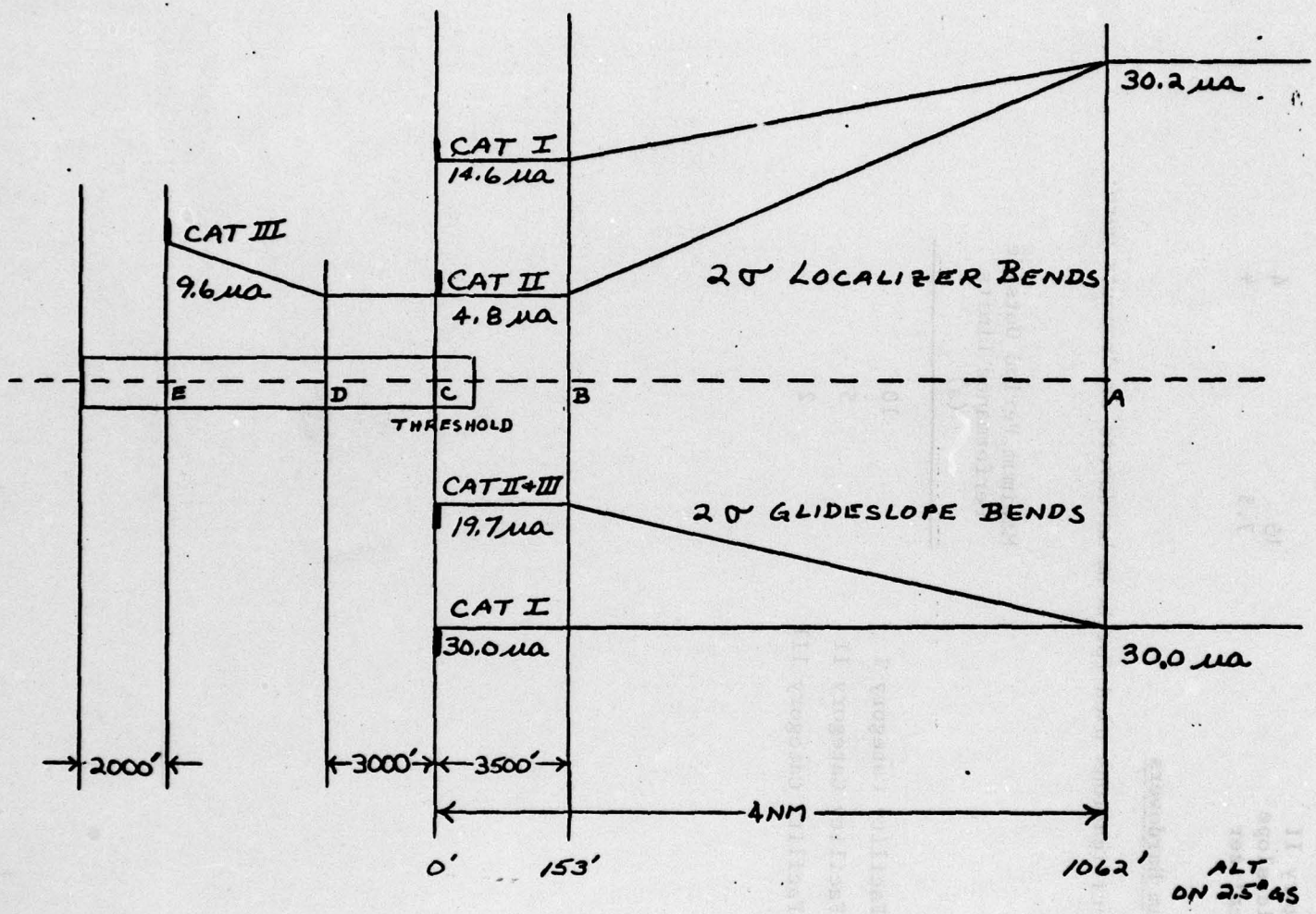

FIGURE A-5 ICAO ILS BEAM BEND LIMITS (BASED ON 2.5 DEG GS)

	3σ Magnitude (μA)	Correlation Time Constant (s)
Facility Category I	30	10
Category II		
Glideslope	15	4
Localizer	7.5	4

D. ILS Beam Hardovers

The specifications used for beam hardovers or dropouts were:

	Maximum Period Outside Performance Limits (s)
Facility Category I	10
Facility Category II	5
Facility Category III	2

Appendix B

COMPLEMENTARY FILTER TECHNIQUE

The complementary filter is used in modern control algorithms to combine information from two sensor sources to provide an estimate of a specific parameter while utilizing the most favorable frequency spectrum of each sensor's output. The filter can be of any order and can use many of the sensors found on current aircraft. To present the technique in this text we will use a second-order filter on localizer deviation complemented with lateral acceleration derived from a body-mounted accelerometer. Figure B-1 shows the block diagram of this filter. Localizer deviation can be written:

$$\eta = y + \eta_e \tag{B.1}$$

where

η = localizer receiver output

y = true lateral position

η_e = localizer errors

Lateral acceleration can be written:

$$\ddot{y}_a = \ddot{y} + a_{ye}$$

where

$\ddot{y}_a$ = roll and distance corrected accelerometer output

$\ddot{y}$ = true lateral acceleration

a_{ye} = accelerometer error

We can extend this to:

$$\ddot{y}_a = S^2 y + a_{ye} \quad . \tag{B.2}$$

Now, if we write the total equation for the complemented output

$$y_c = \frac{1}{S + k_3}\left[k_2\eta + \frac{1}{S}\left(k_1\eta - k_4 y_c + y_a\right)\right]$$

substituting from Eqs. B.1 and B.2:

$$y_c = \frac{1}{S + k_3}\left[k_2 y + k_2\eta_e + \frac{1}{S}\left(k_1 y + k_1\eta_e - k_4 y_c + S^2 y + a_{ye}\right)\right]$$

and

$$y_c = \left(\frac{S^2 + k_2 S + k_1}{S^2 + k_4 S + k_3}\right)y + \left(\frac{k_2 S + k_1}{S^2 + k_4 S + k_3}\right)\eta_e + \left(\frac{1}{S^2 + k_4 S + k_3}\right)a_{ye} \qquad \text{(B.3)}$$

We specify $y_c = y$ when $\eta_e = 0$ and $a_{ye} = 0$.

For true complementation we must choose $k_2 = k_4$ and $k_1 = k_3$ and Eq. (B.3) becomes

$$y_c = y + \left(\frac{k_2 S + k_1}{S^2 + k_2 S + k_1}\right)\eta_e + \left(\frac{1}{S^2 + k_2 S + k_1}\right)a_{ye} \quad .$$

Our goal has been to reduce control activity due to radio noise (η_e) by filtering localizer. The bandpass of the filter on radio will be proportional to the square root of k_1. We therefore desire to decrease k_1 as far as possible. However, the gain on the essentially steady-state accelerometer error (a_{ye}) increases by the inverse of k_1. A steady-state error in $\ddot{y}_a$ will result in a position error (localizer standoff). We therefore increase the steady-state position error by the square of any reduction in the filter bandpass. The tradeoff between steady-state position error and high-frequency control activity is the basis for the final optimum filter constants. Single-order complementing filters can be analyzed with equivalent mathematical techniques.

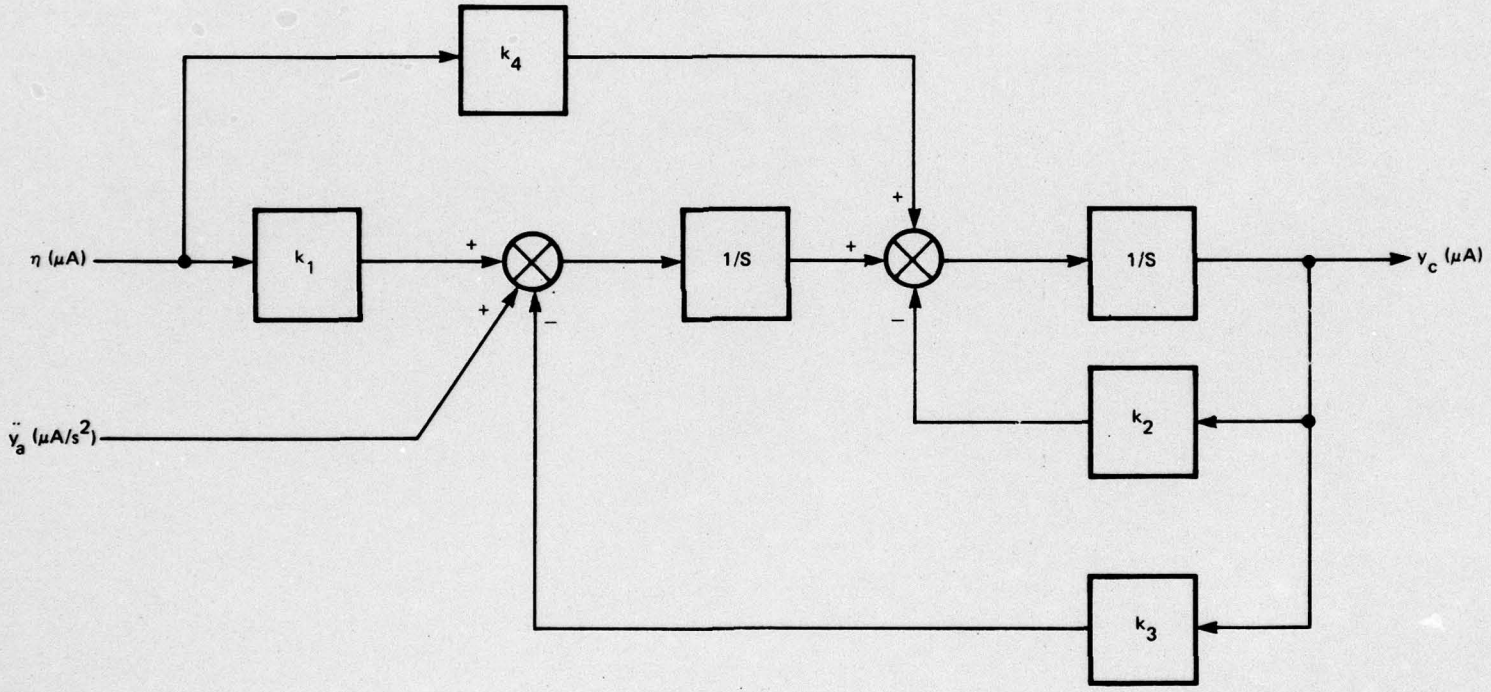

FIGURE B-1 SECOND-ORDER COMPLEMENTARY FILTER

REFERENCES

1. Advisory Circular 120-29, "Criteria for Approving Cat-I and Cat-II Landing Minima for FAR-121 Operators," Federal Aviation Administration, 25 September 1970.

2. Advisory Circular 20-57A, "Automatic Landing Systems," Federal Aviation Administration, 12 January 1971.

3. Gartner, W.B. et al., "Piloted Flight Simulation Study of Low-Level Wind Shear, Phase 2," Report No. FAA-RD-77-157, SRI International for U.S. DoT Federal Aviation Administration, March 1977.

4. Gartner, W.B. et al., "Piloted Flight Simulation Study of Low-Level Wind Shear, Phase 3," Interim Report, SRI International for U.S. DoT Federal Aviation Administration, March 1978.

5. Bleeg, R.J. et al., "Inertially Augmented Automatic Landing System: Autopilot Performance with Imperfect ILS Beams," The Boeing Company, Report No. FAA-RD-72-22, April 1972.

6. Broxmeyer, Charles et al., "Application of Inertial Navigation and Modern Control Theory to the All-Weather Landing Problem," Massachusetts Institute of Technology, Report R-613, June 1968.

7. "Design Development and Flight Evaluation of Inertially Augmented Automatic Landing Systems," Lear Siegler, Inc., Astronics Division, Report ADR-754, 23 April 1971.

8. Foy, W. H., and W. B. Gartner, "Piloted Flight Simulation Study of Low-Level Wind Shear, Phase 4," Report No. FAA-RD-79-84, SRI International for U.S. DoT Federal Aviation Administration, March 1979.

9. Gartner, W. B., et al., "B-727 Simulation Experiment on Techniques for Coping with Wind Shear," Report on Contract DoT-FA75WA-3650, for U.S. DoT Federal Aviation Administration, by SRI International, January 1978.